

SYNTHESIS OF PORPHYRINIC DERIVATIVES FROM CARDANOL
AS PETROLEUM FLUORESCENT MARKER

Miss Siriorn Puangmalee

A Thesis Submitted in Partial Fulfillment of the Requirements
for the Degree of Master of Science Program in Petrochemistry and Polymer Science
Faculty of Science
Chulalongkorn University
Academic Year 2007
Copyright of Chulalongkorn University

การสังเคราะห์อนุพันธ์ฟอรีไฟรินจากคาร์ดานอลเพื่อใช้เป็นสารทำเครื่องหมายเรืองแสง
ในน้ำมันปิโตรเลียม

นางสาวสิริอร พวงมาลี

วิทยานิพนธ์นี้เป็นส่วนหนึ่งของการศึกษาตามหลักสูตรปริญญาวิทยาศาสตรมหาบัณฑิต
สาขาวิชาปิโตรเคมีและวิทยาศาสตร์พอลิเมอร์
คณะวิทยาศาสตร์ จุฬาลงกรณ์มหาวิทยาลัย
ปีการศึกษา 2550
ลิขสิทธิ์ของจุฬาลงกรณ์มหาวิทยาลัย

Thesis Title SYNTHESIS OF PORPHYRINIC DERIVATIVES FROM
CARDANOL AS PETROLEUM FLUORESCENT MARKER
By Miss Siriorn Puangmalee
Field of Study Petrochemistry and Polymer Science
Thesis Advisor Assistant Professor Patchanita Vatakul, Ph.D.
Thesis Co-advisor Associate Professor Amorn Petsom, Ph.D.

Accepted by the Faculty of Science, Chulalongkorn University in Partial
Fulfillment of the Requirements for the Master 's Degree

..... Dean of the Faculty of Science
(Professor Supot Hannongbua, Ph.D.)

THESIS COMMITTEE

..... Chairman
(Associate Professor Supawan Tantayanon, Ph.D.)

..... Thesis Advisor
(Assistant Professor Patchanita Vatakul, Ph.D.)

..... Thesis Co-advisor
(Associate Professor Amorn Petsom, Ph.D.)

..... Member
(Associate Professor Warinthorn Chavasiri, Ph.D.)

..... Member
(Associate Professor Polkit Sangvanich, Ph.D.)

สิริอร พวงมาลี : การสังเคราะห์อนุพันธ์พอร์ไฟรินจากคาร์ดานอลเพื่อใช้เป็นสารทำเครื่องหมายเรืองแสงในน้ำมันปิโตรเลียม. (SYNTHESIS OF PORPHYRINIC DERIVATIVES FROM CARDANOL AS PETROLEUM FLUORESCENT MARKER) อ.ที่ปรึกษา : ผศ. ดร. พัชณิตา วาทะกุล, อ.ที่ปรึกษาร่วม : รศ. ดร. อมร เพชรสม, 110 หน้า.

ได้สังเคราะห์สารทำเครื่องหมายชนิดเรืองแสงสำหรับน้ำมันดีเซล จากอนุพันธ์ของคาร์ดานอล ซึ่งสกัดได้จากเปลือกเม็ดมะม่วงหิมพานต์ โดยทำการสังเคราะห์ meso-tetrakis(2-methoxyphenyl)porphyrin เพื่อใช้เป็นแบบจำลองในการสังเคราะห์พอร์ไฟรินจากคาร์ดานอล จากการสังเคราะห์ meso-tetrakis(2-methoxy-4-pentadecylphenyl)porphyrin (7) พบว่าสามารถละลายได้ดีในน้ำมันดีเซล และสารละลายอินทรีย์อื่นๆ และเมื่อนำไปเติมในน้ำมันดีเซลที่ระดับความเข้มข้น 2 ถึง 5 ส่วนในล้านส่วน จะไม่ทำให้สมบัติของน้ำมันดีเซลเปลี่ยนแปลงไป และเมื่อเปรียบเทียบกับน้ำมันที่ไม่ได้เติมสารทำเครื่องหมายนี้ลงไป พบว่า สมบัติทางกายภาพของน้ำมันดีเซลไม่เปลี่ยนแปลงไปจากเดิม ซึ่งทดสอบด้วยวิธีมาตรฐาน ASTM เมื่อทำการทดสอบความคงตัวของสารทำเครื่องหมายเรืองแสงที่สังเคราะห์ได้ พบว่า สามารถมีความคงตัวอยู่ในน้ำมันดีเซลเป็นระยะเวลาไม่ต่ำกว่า 3 เดือน

สาขาวิชา...ปิโตรเคมีและวิทยาศาสตร์พอลิเมอร์
ปีการศึกษา.....2550.....

ลายมือชื่อนิสิต.....
ลายมือชื่ออาจารย์ที่ปรึกษา.....
ลายมือชื่ออาจารย์ที่ปรึกษาร่วม.....

4873413423 : PETROCHEMISTRY AND POLYMER SCIENCE

KEY WORD: CARDANOL, PORPHYRIN, FUEL, PETROLEUM MARKER

FLUORESCENT, CASHEW NUT SHELL LIQUID

SIRIORN PUANGMALEE : SYNTHESIS OF PORPHYRINIC
DERIVATIVES FROM CARDANOL AS PETROLEUM FLUORESCENT
MARKER.

THESIS ADVISOR : ASST. PROF. PATCHANITA VATAKUL, Ph.D.,

THESIS COADVISOR : ASSOC. PROF. AMORN PETSOM, Ph.D., 103

PP.

A novel fluorescent marker for diesel fuels was synthesized from cardanol, which was obtained from cashew nut shell liquid (CNSL). The synthesis of *meso*-tetrakis(2-methoxyphenyl)porphyrin was performed as a model synthetic pathway in the synthesis of porphyrin from cardanol. The resulting *meso*-tetrakis(2-methoxy-4-pentadecylphenyl)porphyrin (**7**) exhibited high solubility in diesel fuel and common organic solvents. When added into diesel fuel at the concentration of 2-5 ppm, porphyrin **7** exhibits satisfactory optical properties in diesel fuel. Compared with those of unmarked diesel, the physical properties of porphyrin **7**-containing diesel fuel investigated by ASTM testing methods are not significantly altered. By monitoring its fluorescence intensity, stability of porphyrin **7** in diesel fuel was evaluated and found to be stable for 3 month.

Field of study: Petrochemistry and Polymer science Student's signature:.....

Academic year:2007..... Advisor's signature:.....

Co-advisor's signature:.....

ACKNOWLEDGEMENTS

I would like to begin by thanking Assistant Professor Dr. Patchanita Vatakul and my thesis co-advisor Associate Professor Dr. Amorm Petsom for being the best advisors anyone could ever ask for. There are no words that can express the depth of gratitude that I have towards them. They have supported me whole heartedly in everything that I set out to do improved the synthetic skills that I have right now, believed in me even at the moments of my life when I was down and helped me to get back on my feet.

I am also grateful to Associate Professor Dr. Supawan Tuntayanon, for serving as the chairman, and Associate Professor Dr. Warintorn Chavasiri and Associate Professor Dr. Polkit Sangvanich for serving as the members of my thesis committee, respectively, for their valuable suggestion and comments.

I am indebted to staffs at PTT for their assistance in determining physical properties of fuel for the ASTM test methods. I also thank Graduate School, Chulalongkorn University and Research Centre for Bioorganic Chemistry (RCBC) for warm welcome me into their family, great experience and opportunity laboratory facilities, chemicals and equipments. I feel blessed and very privileged to have joined a group with great members who supported me throughout this course.

I sincerely thank Mr. Jatupol Leangsakul, Miss Jamreang Tummatorn and Miss. Sunisa Suwancharoen for their tireless efforts in helping me with the NMR, suggestions, and comments. Special appreciation is also extended to Miss Saowanaporn Choksakulporn for her advice, helpfulness and kind gratitude of providing me the valuable information.

I would also like to thank all my friends at the RCBC group who have made my life here enjoyable and worth-living, you all know who you are. Furthermore, I would like to express special thank to Miss Pattanaporn phonpiboon for her share of happiness and troubles throughout my entire education.

Finally I am grateful to my family for their love, understanding, and great encouragement throughout the entire course of my study.

CONTENTS

	Page
ABSTRACT (THAI)	iv
ABSTRACT (ENGLISH)	v
ACKNOWLEDGEMENTS	vi
CONTENTS	vii
LIST OF TABLES	x
LIST OF FIGURES	xi
LIST OF SCHEMES	xiii
LIST OF ABBREVIATIONS	xiv
CHAPTER I INTRODUCTION	1
1.1 The objectives of this research.....	2
1.2 The scope of this research.....	2
CHAPTER II THEORY AND LITERATURE REVIEWS	3
2.1 Fluorescence.....	3
2.2 Chemical structure and fluorescence.....	5
2.3 Phosphorescence.....	6
2.4 Porphyrins.....	7
2.4.1 Porphyrin synthesis.....	9
2.4.1.1 Adler-Longo condensation.....	10
2.4.1.2 Lindsey condensation.....	13
2.4.1.3 2+2 Porphyrin synthesis.....	15
2.4.1.4 3+1 Porphyrin synthesis.....	16
2.4.1.5 Porphyrins from linear tetrapyrroles.....	16
2.4.2 Uses and applications of porphyrin derivatives.....	18
2.5 Diesel fuel and its chemical composition	19
2.6 Marker.....	20
2.7 Cashew Nut Shell Liquid (CNSL).....	21
2.7.1 Extracting process of CNSL.....	22
2.7.2 Use and application of CNSL.....	23
2.8 Literature reviews.....	24

	Page
CHAPTER III EXPERIMENTAL	32
3.1 Chemicals.....	32
3.2 Analytical instruments.....	33
3.3 Experimental procedure.....	34
3.3.1 Synthesis of 2-methoxybenzaldehyde(2).....	34
3.3.2 Synthesis of <i>meso</i> -tetrakis(methoxyphenyl)porphyrin(3).....	35
3.3.3 Synthesis of 2- hydroxy-4-pentadecylbenzaldehyde(5).....	36
3.3.3.1 Formylation of hydrogenated cardanol(4) using Reimer-Tiemann reaction.....	36
3.3.3.2 Condensation of hydrogenated cardanol(4) with paraformaldehyde.....	36
3.3.4 Synthesis of 2-methoxy-4-pentadecylbenzaldehyde(6).....	37
3.3.5 Synthesis of <i>meso</i> -tetrakis(2-methoxy-4- pentadecylphenyl)porphyrin(7).....	38
3.3.5.1 Effect of acid-catalyst on the porphyrin formation	38
3.3.5.2 Effect of time on the formation of porphyrin.....	39
3.3.5.3 Synthesis of compound 5 under optimized condition..	39
3.3.6 Synthesis of 2-hydroxy-4-alkenylbenzaldehyde(5-1).....	40
3.3.6.1 Formylation of non hydrogenated cardanol using Reimer-Tiemann reaction.....	40
3.3.6.2 Condensation of cardanol with paraformaldehyde...	40
3.3.7 Synthesis of 2-methoxy-4-alkenylbenzaldehyde(6-1).....	41
3.3.8 Synthesis of <i>meso</i> -tetrakis(2-methoxy-4- alkenylphenyl)porphyrin(7-1).....	42
3.3.9 Synthesis of <i>meso</i> -tetrakis(2-methoxyphenyl) porphyrinatozinc(II) (Zn-3).....	43
3.3.10 Use of fluorescent marker in varied oil refinery.....	44
3.3.11 Preparation of stock solution of fluorescent Marker 7	44
3.3.12 Quantitative determination of fluorescent markers in diesel fuel.....	45
3.3.13 Stability test of fluorescent marker in diesel fuel.....	45

	Page
3.3.14 Effect of fluorescent marker on the physical properties of diesel fuel.....	45
CHAPTER IV RESULTS AND DISCUSSION.....	47
4.1 Porphyrin model.....	47
4.2 Porphyrinic derivative 7 from hydrogenated cardanol.....	49
4.2.1 Synthesis of 2- hydroxy-4-pentadecylbenzaldehyde(5).....	49
4.2.1.1 Reimer-Tiemann Reaction.....	49
4.2.1.2 <i>Ortho</i> -formylation of hydrogenated cardanol with parformaldehyde.....	51
4.2.2 Synthesis of 2-methoxy-4-pentadecylbenzaldehyde(6).....	52
4.2.3 Synthesis of <i>meso</i> -tetrakis(2-methoxy-4-pentadecylphenyl)porphyrin(7).....	53
4.2.3.1 Optimization of reaction condensation for porphyrin formylation.....	53
4.3 Porphyrinic derivatives from non-hydrogenated cardanol.....	56
4.4 Synthesis of <i>meso</i> -tetrakis(2-methoxyphenyl)porphyrinatozinc(II)(Zn-3).....	57
4.5 Fluorescent properties of porphyrin model and porphyrin derivatives....	58
4.5.1 Quantitative determination of fluorescent markers in diesel.....	60
4.5.2 Stability test of fluorescent marker in diesel	60
4.5.3 Effect of fluorescent marker on the physical properties of diesel.....	61
CHAPTER V CONCLUSION.....	63
REFFERENCES.....	65
APPENDICES.....	71
Appendix A.....	72
Appendix B.....	101
VITA.....	110

LIST OF TABLES

Table		Page
2-1	ASTM specifications for high speed diesel.....	20
2-2	Characteristics of cardanol.....	21
3-1	Condition for the synthesis of compound 7	38
3-2	The volume of the stock solution (500 ppm) used to prepare 0-10 ppm fluorescent marker in diesel.....	45
3-3	The ASTM testing methods of diesel.....	46
4-1	Condition for the synthesis of compound 7	54
4-2	The summarized excitation wavelength ($\lambda_{ex};nm$) and emission wavelength ($\lambda_{em};nm$) of porphyrin model and porphyrin derivative in dichloromethane.....	59
4-3	The stability of compound 7 (2 and 5 ppm) in diesel.....	60
4-4	Physical properties of marked and unmarked diesel.....	61

LIST OF FIGURES

Figure		Page
2-1	Transition giving rise to absorption and fluorescence emission spectra....	3
2-2	Idealised absorption and emission spectra.....	4
2-3	Transition from the excited singlet state (S_1) to the triplet state (intersystem crossing).....	7
2-4	Porphyrin macrocycle.....	8
2-5	Typical UV-Visible absorption spectrum of porphyrin.....	8
2-6	Examples of porphyrin derivatives that occur in nature.....	10
4-1	Intramolecular hydrogen bond of <i>ortho</i> -hydroxy aromatic aldehyde.....	52
4-2	Effect of acid catalyst on the time-course of porphyrin 7 formation.....	54
A-1	^1H -NMR spectrum of 2-methoxybenzaldehyde (Compound 2).....	73
A-2	^{13}C -NMR spectrum of 2-methoxybenzaldehyde (Compound 2).....	74
A-3	IR spectrum of 2-methoxybenzaldehyde (Compound 2).....	75
A-4	Mass spectrum of 2-methoxybenzaldehyde (Compound 2).....	76
A-5	^1H -NMR spectrum of porphyrin model (Compound 3).....	77
A-6	^{13}C -NMR spectrum of porphyrin model (Compound 3).....	78
A-7	IR spectrum of porphyrin model (Compound 3).....	79
A-8	Mass spectrum of porphyrin model (Compound 3).....	80
A-9	^1H -NMR spectrum of 2-hydroxy-4-pentadecylbenzaldehyde (Compound 5).....	81
A-10	^{13}C -NMR spectrum of 2-hydroxy-4-pentadecylbenzaldehyde (Compound 5).....	82
A-11	IR spectrum of 2-hydroxy-4-pentadecylbenzaldehyde (Compound 5).....	83
A-12	Mass spectrum of 2-hydroxy-4-pentadecylbenzaldehyde (Compound 5).....	84
A-13	^1H -NMR spectrum of 2-hydroxy-6-pentadecylbenzaldehyde (Compound 5a).....	85
A-14	^1H -NMR spectrum of 2-methoxy-4-pentadecylbenzaldehyde (Compound 6).....	86
A-15	^{13}C -NMR spectrum of 2-methoxy-4-pentadecylbenzaldehyde (Compound 6).....	87
A-16	IR spectrum of 2-methoxy-4-pentadecylbenzaldehyde (Compound 6).....	88

Figure	Page
A-17 Mass spectrum of 2-methoxy-4-pentadecylbenzaldehyde (Compound 6).....	89
A-18 ¹ H-NMR spectrum of porphyrinic derivative (Compound 7).....	90
A-19 ¹³ C-NMR spectrum of porphyrinic derivative (Compound 7).....	91
A-20 IR spectrum of porphyrinic derivative (Compound 7).....	92
A-21 Mass spectrum of porphyrinic derivative (Compound 7).....	93
A-22 ¹ H-NMR spectrum of 2-hydroxy-4-alkenylbenzaldehyde and 2- hydroxy-6-alkenylbenzaldehyde.....	94
A-23 ¹ H-NMR spectrum of 2-hydroxy-4-alkenylbenzaldehyde.....	95
A-24 ¹ H-NMR spectrum of 2-methoxy-4-alkenylbenzaldehyde.....	96
A-25 ¹ H-NMR spectrum of porphyrinic derivatives from cardanol.....	97
A-26 ¹ H-NMR spectrum of Zn(II) porphyrin model(Compound Zn-3).....	98
A-27 IR spectrum of Zn(II) porphyrin model(Compound Zn-3).....	99
A-28 Mass spectrum of Zn(II) porphyrin model(Compound Zn-3).....	100
B-1 Absorption spectrum of Compound 3 in CH ₂ Cl ₂	102
B-2 Absorption spectrum of Compound 7 in CH ₂ Cl ₂	102
B-3 Absorption spectrum of Zn-3	103
B-4 Fluorescent spectrum of Zn-3	103
B-5 Fluorescent spectra of Compound 3 in CH ₂ Cl ₂	104
B-6 Fluorescent spectra of Compound 7 in CH ₂ Cl ₂	104
B-7 Fluorescent spectra of diesel fuel in CH ₂ Cl ₂	105
B-8 The excitation wavelength (λ_{ex} = 420 nm) and emission wavelength (λ_{em} = 652 nm and 719 nm) of Compound 7 (1 ppm) in diesel oil(PTT).....	106
B-9 The excitation wavelength (λ_{ex} = 420 nm) and emission wavelength (λ_{em} = 652 nm and 719 nm) of Compound 7 (1 ppm) in diesel oil(Petronas).....	106
B-10 The excitation wavelength (λ_{ex} = 420 nm) and emission wavelength (λ_{em} = 652 nm and 719 nm) of Compound 7 (1 ppm) in diesel oil(Esso).....	107
B-11 The excitation wavelength (λ_{ex} = 420 nm) and emission wavelength (λ_{em} = 652 nm and 719 nm) of Compound 7 (1 ppm) in diesel oil(Caltex).....	107

Figure		Page
B-12	The excitation wavelength ($\lambda_{\text{ex}}= 420 \text{ nm}$) and emission wavelength ($\lambda_{\text{em}}= 652 \text{ nm}$ and 719 nm) of Compound 7 (1 ppm) in diesel oil(Bangchak).....	108
B-13	The excitation wavelength ($\lambda_{\text{ex}}= 420 \text{ nm}$) and emission wavelength ($\lambda_{\text{em}}= 652 \text{ nm}$ and 719 nm) of Compound 7 (1 ppm) in diesel oil(Veerasuwan).....	108
B-14	The fluorescent spectrum of Compound 7 in diesel oil at 2, 4, 6, 8 and 10 ppm ($\lambda_{\text{ex}}= 512 \text{ nm}$ and $\lambda_{\text{em}} 652 \text{ nm}$ and 719 nm).....	109
B-15	The calibration curve for the quantitative determinations of Compound 7 in diesel oil ($\lambda_{\text{ex}}= 512 \text{ nm}$ and $\lambda_{\text{em}} 652 \text{ nm}$).....	109

LIST OF SCHEMES

Scheme	Page
2-1 Formation of tetraphenylporphyrin under Rothmund condition	10
2-2 Reaction conditions: (i) Propionic acid; (ii) Pyridine hydrochloride, 220°C, 2.5 h; (iii) (A), Cs ₂ CO ₃ , NaH, DMF, 65°C, 42–36 h; (iv) CH ₃ I/CH ₃ NO ₂ (4:3), 70°C, 12 h.....	11
2-3 Reaction conditions: (i) DiBAL-H, CH ₂ Cl ₂ , 08C, then 45°C, 4 h, 60%; (ii) Potassium phthalimide, DMF, reflux, 4 h, 90%; (iii) Pyrrole, acid; (iv) NaOH, heat, then 70% H ₂ SO ₄ , heat.....	12
2-4 Formation of porphyrin from porphyrinogen.....	13
2-5 Formation of <i>meso</i> -tetramesitylporphyrin.....	14
2-6 2+2 Porphyrin synthesis.....	15
2-7 Differentially substituted porphyrin.....	16
2-8 Formation of porphyrin containing two acrylic acid units on the same pyrrole.....	16
2-9 Porphyrin formation from β -bilanes.....	17
2-10 New route to ABCD-porphyrins via bilanes.....	18
2-11 Chemical structure of major compounds in natural CNSL.....	22
2-12 Synthesis novel cardanol-based porphyrins.....	27
2-13 Preparation of phthalocyanine derivatives.....	28
2-14 Synthesis the novel cardanol-based porphyrins.....	29
2-15 Synthesis of a new hybrid <i>meso</i> -tetrarylporphyrin-cardanol with the cardanol bearing an unsaturated chain.....	30
2-16 The synthesis of cyclic cardanol-based porphyrin derivative.....	31
4-1 Synthesis of <i>meso</i> -tetrakis(2-hydroxyphenyl)porphyrin.....	47
4-2 The synthesis of <i>meso</i> -tetrakis(2-methoxyphenyl)porphyrin.....	48
4-3 The total synthesis of Compound 7.....	49
4-4 Propose mechanism of formylation of Reimer-Tiemann formation.....	50
4-5 The mechanism pathway of the tin(IV)tetrachloride and triethylamine catalysed condensation of cardanol and paraformaldehyde.....	51
4-6 Proposed the mechanism of the porphyrin and N-confused formation.....	55

LIST OF ABBREVIATIONS

$^{13}\text{C-NMR}$:	carbon-13 nuclear magnetic resonance spectroscopy
$^1\text{H-NMR}$:	proton nuclear magnetic resonance spectroscopy
<i>br</i>	:	broad
CDCl_3	:	deuterated chloroform
CH_2Cl_2	:	methylene chloride
CHCl_3	:	chloroform
cm^{-1}	:	unit of wavenumber (IR)
CNSL	:	cashew nut shell liquid
cP	:	centipoise
d	:	doublet (NMR)
dd	:	doublet of doublet (NMR)
eq	:	equivalent (s)
EtOAc	:	ethyl acetate
EtOH	:	ethanol
g	:	gram (s)
h	:	hour (s)
Hz	:	hertz (s)
IR	:	Infrared resonance spectroscopy
<i>J</i>	:	coupling constant
M	:	molar (s)
m	:	multiplet (NMR)
m.p.	:	melting point
max	:	maximum
m/z	:	mass per charge ratio
MeOH	:	methanol
min	:	minute

mg	:	milligram (s)
mL	:	milliliter (s)
mM	:	millimolar (s)
mmol	:	millimole (s)
MS	:	mass spectroscopy
NMR	:	nuclear magnetic resonance spectroscopy
nm	:	nanometer
°C	:	degree Celcius
ppm	:	parts per million
rt	:	room temperature
s	:	singlet (NMR)
st	:	stretching vibration (IR)
t	:	triplet (NMR)
TLC	:	thin layer chromatography
UV/Vis	:	ultraviolet visible spectrometry
δ	:	chemical shift
λ_{em}	:	emission wavelength
λ_{ex}	:	excitation wavelength
λ_{max}	:	maximum wavelength

CHAPTER I

INTRODUCTION

At present the large demand petroleum fuel oils are consumed in many countries. Petroleum fuel oils are taxed according to the government rates, which are dependent on the types of petroleum fuel oils as well as their application purposes. This causes the government many problems such as smuggling diesel from abroad into the country, adulteration of the higher-priced product with lower-priced material, for example an addition of low-taxed light heating oil to high-taxed diesel fuel, leading to loss of fuel revenues and low-quality petroleum fuel oils in the markets.

One of the solutions to these problems is the addition of a marker into fuel in order to differentiate specific brands of fuel and classifying the type of fuel and petroleum products for taxing purposes, and detect its characteristic by a particular technique, such as absorption spectroscopy, depending on its properties.

Fuel markers are chemical compounds that may be added to a wide variety of petroleum products such as gasoline, diesel fuel, jet fuel, kerosene, gas oil, etc. The compounds must be miscible in the petroleum product, impart no color and exhibit high stability under the using condition. They are used to guarantee product integrity, protect against counterfeiting, adulteration, and tax fraud.

Fluorescent material are used herein is defined as a substance which, when irradiated with light of specific wavelength, generates light with a different wavelength from that of the applied light by forming an electronic resonance structure. It may be detected with ease by irradiating visible light or ultraviolet thereto, even though it is present in a small amount in the petroleum product. However, most fluorescent materials have poor solubility in the petroleum products such as in gasoline or in diesel fuel.

Porphyrins are tetrapyrrolic macrocycles that have a special structure with big p-orbital on the carbon nitrogen framework. Because of the large conjugational effect of the tetrapyrrolic macrocycle, porphyrins have special photophysical properties and have been used in many fields. In recent years, dyads and triads containing porphyrins as electron acceptor or donor have proven to be of interest as photosynthetic model compounds [1]; metal porphyrins have also been widely used in photocatalysis [2],

light-energy conversion [3] and various medical applications [4]. However, the major concern of the use of porphyrins in such applications is their low solubility due to high tendency of molecular aggregation.

According to the solubility enhancement resulting from its solubility group, cardanol is introduced into the porphyrin and other macrocycle frameworks, such as phthalocyanine and fullerene. Cardanol is a natural alkyl phenol obtained by vacuum distillation cashew nut shell liquid (CNSL). Cardanol derivatives represent a simple point for the preparation of additives for lubricants, diesel engine fuels, pour point depressant, flame retardants, resin, inks hydrorepellents, stabilizers and antioxidants.

This research involves the synthesis of a highly soluble porphyrin as fluorescent markers for diesel fuel from the naturally occurring cardanol derivatives.

The physical properties of the diesel fuel marked by this compound are investigated, as well as the stability of the marker in the diesel fuel is examined.

1.1 The objective of this research

The objectives of this research are synthesizing porphyrinic derivatives from cardanol as petroleum fluorescent marker and evaluate its performance as a fluorescent marker when added in diesel fuel.

1.2 The scope of this research

The scope of this research covers the synthesis of porphyrinic derivatives from cardanol as petroleum fluorescent marker. These markers are fully characterized by spectroscopic techniques such as mass spectrometry, and FT-IR, $^1\text{H-NMR}$, $^{13}\text{C-NMR}$, UV-Visible and Fluorescence spectroscopy, In addition, the physical properties of the diesel fuel marked by this compound are investigated, and the stability of markers in petroleum fuel were studied.

CHAPTER II

THEORY AND LITERATURE REVIEWS

2.1 Fluorescence [5,6,7]

At room temperature most molecules occupy the lowest vibrational level of the ground electronic state, and on absorption of light they are elevated to produce excited states. The simplified diagram below shows absorption by molecules to produce either the first, S₁, or second, S₂ excited state (Figure 2-1).

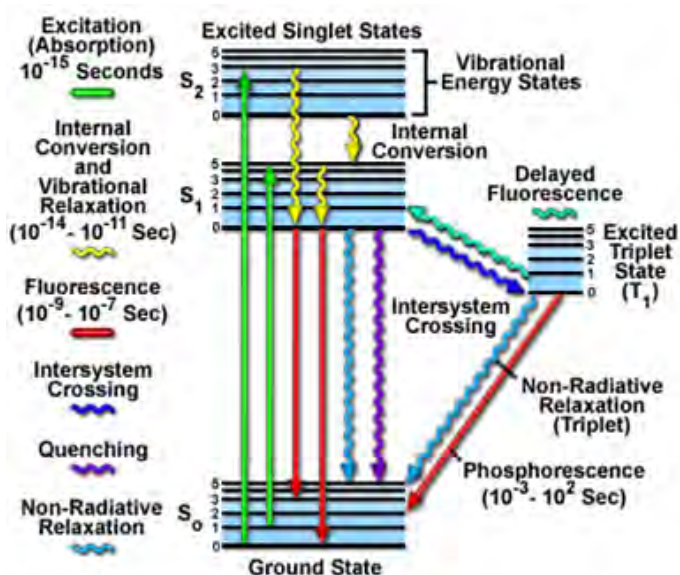


Figure 2-1 Transition giving rise to absorption and fluorescence emission spectra

Excitation can result in the molecule reaching any of the vibrational sub-levels associated with each electronic state. Since the energy is absorbed as discrete quanta, this should result in a series of distinct absorption bands. However, the simple diagram above neglects the rotational levels associated with each vibrational level and which normally increase the number of possible absorption bands to such an extent that it becomes impossible to resolve individual transitions.

Therefore, most compounds have broad absorption spectra except for those where rotational levels are restricted (for example, planar, aromatic compounds).

Having absorbed energy and reached one of the higher vibrational levels of an excited state, the molecule rapidly loses its excess of vibrational energy by collision and falls to the lowest vibrational level of the excited state. In addition, almost all molecules occupying an electronic state higher than the second undergo internal conversion and pass from the lowest vibrational level of the upper state to a higher vibrational level of a lower excited state which has the same energy. From there the molecules again lose energy until the lowest vibrational level of the first excited state is reached.

From this level, the molecule can return to any of the vibrational levels of the ground state, emitting its energy in the form of fluorescence. If this process takes place for all the molecules that absorbed light, then the quantum efficiency of the solution will be a maximum and unity. However, other route is followed the quantum efficiency will be less than one and may even be almost zero.

One transition, that is from the lowest vibrational level in the ground electronic state to the lowest vibrational level in the first excited state, the 0 - 0 transitions, is common to both the absorption and emission phenomena, whereas all other absorption transitions require more energy than any transition in the fluorescence emission. Therefore we can expect the emission spectrum to overlap the absorption spectrum at the wavelength corresponding to the 0 - 0 transitions and the rest of the emission spectrum to be of lower energy, or longer wavelength (Figure 2-2).

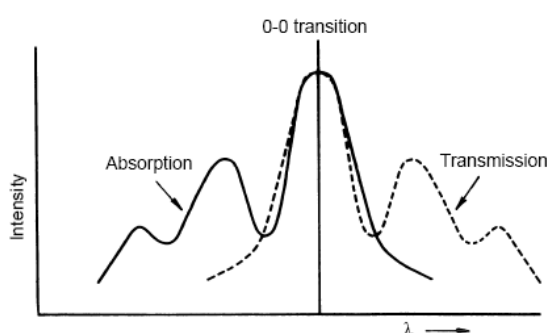


Figure 2-2 Idealised absorption and emission spectra

In practice, the 0-0 transitions in the absorption and emission spectra rarely coincide exactly. The absorption of energy to produce the first excited state does not perturb the shape of the molecule greatly and this means that the distribution of vibrational levels is very similar in both the ground and first excited states. The

energy differences between the bands in the emission spectrum will be similar to those in the absorption spectrum and frequently the emission spectrum will be approximate to a mirror image of the absorption spectrum. Since the emission of fluorescence always takes place from the lowest vibrational level of the first excited state, the shape of the emission spectrum is always the same, despite changing the wavelength of exciting light. A plot of emission against wavelength for any given excitation wavelength is known as the emission spectrum. If the wavelength of the exciting light is changed and the emission from the sample is plotted against the wavelength of exciting light, the result is known as the excitation spectrum. Furthermore, if the intensity of exciting light is kept constant as its wavelength is changed, the plot of emission against exciting wavelength is known as the corrected excitation spectrum. The quantum efficiency of most complex molecules is independent of the wavelength of exciting light and the emission will be directly related to the molecular extinction coefficient of the compound; in other words, the corrected excitation spectrum of a substance will be the same as its absorption spectrum.

2.2 Chemical structure and fluorescence [8]

In principle, any molecule that absorbs ultraviolet radiation could fluoresce. There are many reasons why they do not; but we will not go into these, other than to point out, in general, what types of substances may be expected to fluoresce. Many aromatic and heterocyclic compounds fluoresce, particularly if they contain certain substituted group. Compounds with multiple conjugated double bonds are favorable to fluorescence. One or more electron-donating groups such as $-\text{OH}$, $-\text{NH}_2$, and $-\text{OCH}_3$ enhances the fluorescence. Polycyclic compounds such as vitamin K, purines, and nucleosides and conjugated polyenes such as vitamin A are fluorescent. Groups such as $-\text{NO}_2$, $-\text{COOH}$, $-\text{CH}_2\text{COOH}$, $-\text{Br}$, $-\text{I}$, and azo groups tend to *inhibit* fluorescence. The fluorescence of many molecules is greatly pH dependent because only the ionized or un-ionized form may be fluorescent. For example, phenol ($\text{C}_6\text{H}_5\text{OH}$) is fluorescent but its anion ($\text{C}_6\text{H}_5\text{O}^-$) is not.

If a compound is nonfluorescent, it may be converted to a fluorescent derivative. For example, nonfluorescent steroids may be converting to fluorescent

compounds by dehydration with concentrated sulfuric acid. These cyclic alcohols are converted to phenols. Similarly, dibasic acid, such as malic acid, may be reacted with β -naphthol in concentrated sulfuric acid to form a fluorescein derivative. Antibodies may be made fluorescence by condensing them with fluorescein isocyanate, which reacts with the free amino groups of the proteins. And the reduced form of nicotinamide adenine dinucleotide (NADH) can also fluorescence which is fluoresces. It is a product or reactant (cofactor) in many enzyme reactions. Its fluorescence serves as the basis of the sensitive assay of enzymes and their substrates. Most amino acids do not fluoresce but fluorescent derivatives are formed by reaction with dansyl chloride.

2.3 Phosphorescence [9]

In the production of excited states by promotion of an electron into a higher orbital, the direction of the spin of the electron is preserved. Since most molecules have an even number of electrons and these are normally arranged in pairs of opposite spin, the promotion of an electron does not disturb this parity. However, it is possible for the spin of the promoted electron to be reversed so that it is no longer paired and the molecule has two independent electrons of the same spin in different orbitals. Quantum theory predicts that such a molecule can exist in three forms of very slightly differing, but normally indistinguishable energy, and the molecule is existing in a triplet state. The indirect process of conversion from the excited state produced by absorption of energy from singlet state, to triplet state, is known as intersystem crossing (Figure 2-3) and can occur in many substances when the lowest vibrational level of the excited singlet state, S1, has the same energy level as an upper vibrational level of the triplet state.

Direct transition from the ground state, usually a singlet state, for a molecule with an even number of electrons, to an excited triplet state is theoretically forbidden, which means that the reverse transition from triplet to ground state will be difficult. Thus, while the transition from an excited singlet state, for example, S1 to the ground state with the emission of fluorescence can take place easily and within 10^{-9} - 10^{-6} seconds, the transition from an excited triplet state to the ground state with the emission of phosphorescence requires at least 10^{-4} seconds and may take as long as 102 seconds. This delay was once used as the characterization of phosphorescence,

but a more precise definition requires that phosphorescence be derived from transitions directly from the triplet state to the ground state.

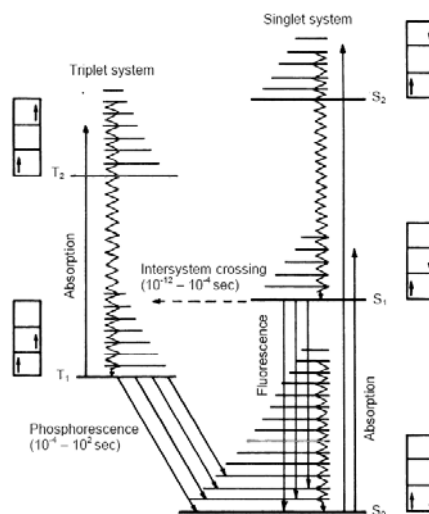


Figure 2-3 Transition from the excited singlet state (S_1) to the triplet state (intersystem crossing)

The triplet state of a molecule has a lower energy than its associated singlet state so that transitions back to the ground state are accompanied with the emission of light of lower energy than from the singlet state.

2.4 Porphyrins

Porphyrins are biochemically important, medically useful, and synthetically interesting compounds. Porphyrins that occur naturally play a major role in the life sustaining biochemical reactions. They are an ubiquitous class of compounds with many important biological representatives including chlorophylls, myoglobins, hemes, cytochromes, catalases, peroxidases, and several others. Used by nature in the most important processes of photosynthesis and solving transport and other problems in living systems, these compounds have been described as “pigments of life” [10]. Their aromatic character, inner chelating pocket and varying peripheral carbon chains have allowed scientists to discover new and unique chemical reactions. Porphyrins and their metal complexes have also stirred interdisciplinary interest due to a multitude of their intriguing physical, chemical and biological properties [11].

The porphyrin macrocycle consists of four pyrrole rings joined by four interpyrrolic methinebridges to give a highly conjugated macrocycle (Figure 2-4). The aromaticity of porphyrins has been well established both by its chemical and physical

properties. These tetrapyrrolic systems have a closed loop of edgewise overlapping p-orbitals which interact favorably to stabilize the olefins : the 22 π electrons available porphyrins make up six different 18e-delocalization pathway which follows Hückel's $4n+2$ rule for aromaticity. A lower number of delocalization pathways result in less aromatic character that produces differences in spectroscopic properties.

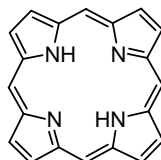


Figure 2-4 Porphyrin macrocycle

Porphyrin and their derivatives are highly colored absorbing strongly in the visible region near 400 nm (molar extinction coefficients are about $10^3 \text{ Mol}^{-1}\text{L}$) characteristic of the macrocyclic conjugation and several weaker absorption bands known as Q band between 450-700 nm (Figure 2-5). The main intense absorption band is known as the Soret band, named after the biochemist who first observed it in hemoglobin. A variation in the peripheral substituents of the porphyrin ring normally results in a slight change in the intensity and wavelength of the absorption bands. A disrupted porphyrin macrocycle results in the disappearance of the *Soret band*. Each tetrapyrrolic system can be unique and therefore different in color. Naturally occurring porphyrins are dark, red while chlorin that are reduced tetrapyrrolic systems are dark green or blue green.

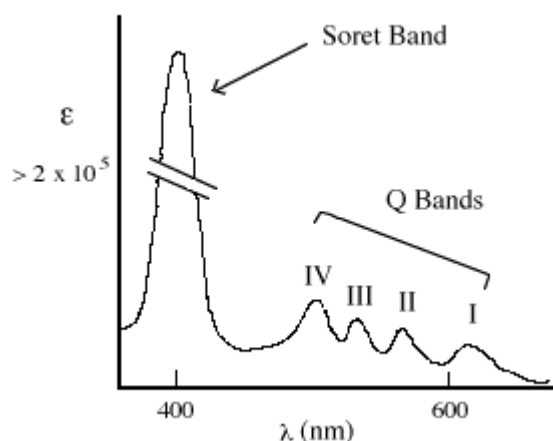


Figure 2-5 Typical UV-Visible absorption spectrum of porphyrin

The absorbance energy intensities vary with chelation, pH, and differences in the structure of peripheral substituents. However, as long as a cyclic 18 π e-path exists, the intense Soret band is really a major characteristic of their optical spectra.

The porphyrin macrocycle and its derivatives are amphoteric, behaving both as acids and bases. Pyrrolic nitrogen atoms at the centre of the porphyrin core are responsible for this interesting characteristic. The NHs can be deprotonated with strong bases, while the two-imine nitrogens can be protonated with acid. However, metallated porphyrins lack this amphoteric quality because the nitrogens are chelated to the metal with both covalent and dative bonds. The NMR spectrum of the aromatic tetrapyrrole shows anisotropic effect. The ring current generated by the applied field induces a local magnetic field similar to that in benzene. The NH protons inside the porphyrin ring system are therefore shifted upfield to as high as -5 ppm in porphyrins, whereas the deshielded *meso*-protons appear at very low field ($\delta \sim 10$ ppm). The pyrrolic protons are also deshielded and tend to resonate at δ 8 to 9, versus $\delta \sim 6$ ppm in pyrrole. These porphyrin systems make their NMR spectra challenge spectra.

2.4.1 Porphyrin synthesis

A wareness of porphyrin importance to life has stimulated large amounts of research into purification, structure determination, synthetic manipulation, and total synthesis of these macrocycles.

The porphyrin field began with the synthesis of the large class of pyrroles. Most of this early work was accomplished by Fischer H. [12] in munich, and was followed by the synthesis of a variety of porphyrins. Known as the grandfather of porphyrin chemistry, Fischer has inspired a large number of research groups throughout the world to improve upon his methodologies. In general, there are several routes that can be followed to afford porphyrins. The first route entails the functionalization of an intact ring system obtained from natural sources such as chlorophylls *a* or *b*, bacterio-chlorophylls and hemin (Figure 2-6) which are modified to give the desired porphyrin. The second route is the formal total synthesis beginning with monopyrrolic subunits. Regardless of the method of synthesis, porphyrins make up a selected class of compounds which are an important part of chemistry and possess some very important applications that are yet to be completely explored. Most of the synthetic methodologies that will be discussed in detail henceforth are important because some will be utilized throughout this dissertation.

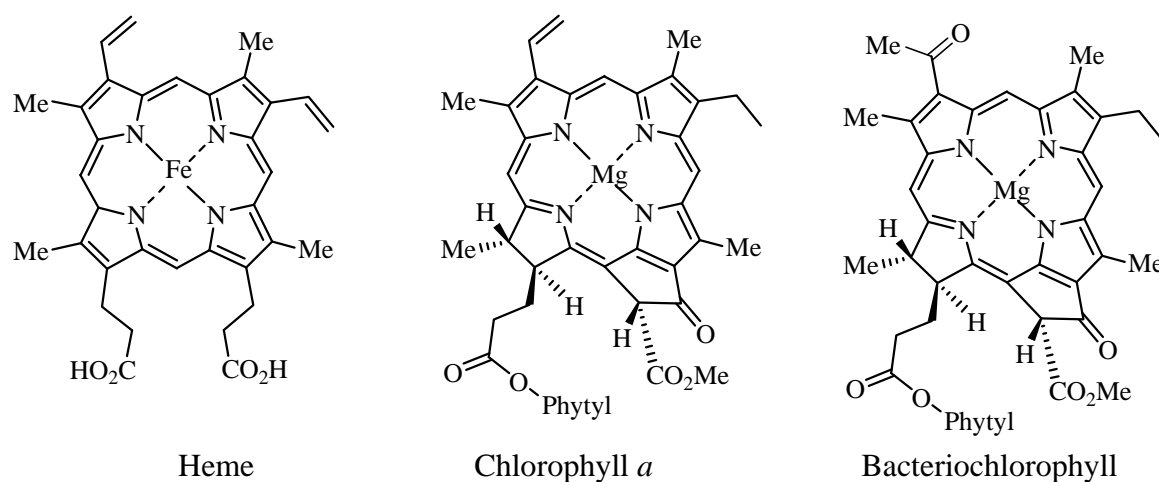
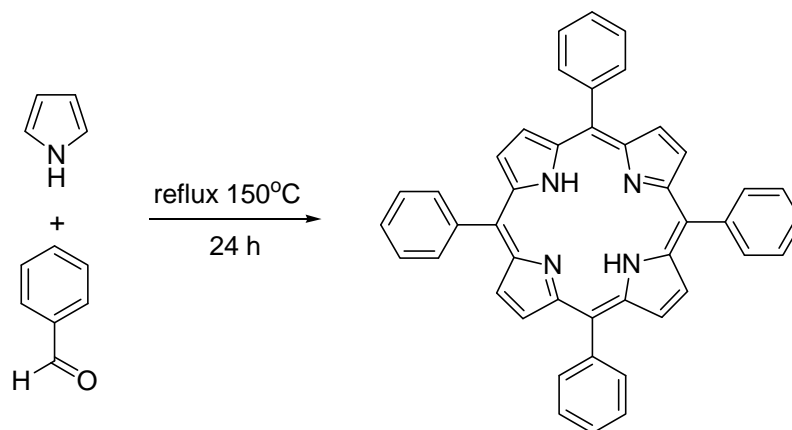


Figure 2-6 Examples of porphyrin derivatives that occur in nature

2.4.1.1 Adler–Longo condensation

Tetraphenylporphyrin (TPP) was first synthesised using benzaldehyde and pyrrole in 1936 by Rothmund, P. (Scheme 2-1) [13]. The reaction was carried out in a sealed tube at 150°C for 24 h. However, the yields were low and the harsh conditions meaning that only a limited number of aromatic aldehydes survived the procedure.



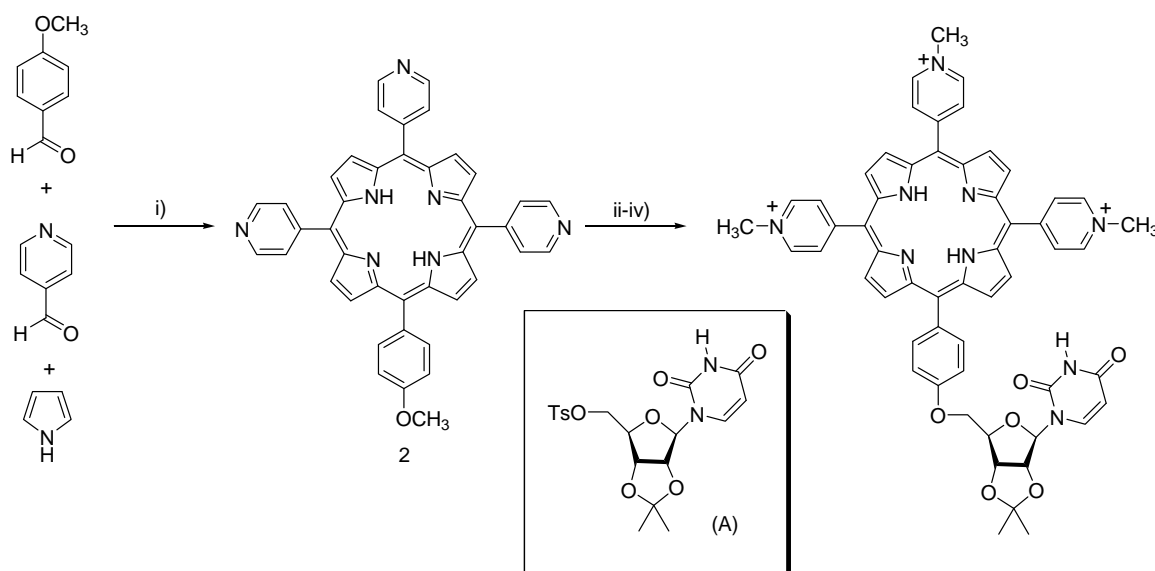
Scheme 2-1 Formation of tetraphenylporphyrin under Rothmund condition.

Improvements to this method were made by Adler and Longo in 1967. Benzaldehyde was reacted with pyrrole in refluxing propionic acid for 30 min, in air [14]. Using this conditions, a greater variety of substituted benzaldehydes were converted into the corresponding 5,10,15,20-tetraphenylporphyrins. The reactions could also be scaled up to give multi-gram quantities of porphyrin, and in some cases

yields of up to 20% were obtained. This method is still widely used when large quantities of porphyrin are needed and where the aldehydes are capable of withstanding acidic conditions. Examples of this method include the synthesis of basket handle porphyrins by Chandrashekar *et al.* using a preformed dialdehyde and pyrrole in propionic acid [15].

Differentially functionalized porphyrins can also be prepared by using two different aldehydes under essentially the same conditions. This type of reaction is often used for the preparation of porphyrins containing three substituted phenyl rings derived from one aldehyde and one substituted phenyl ring derived from the other. The obvious problem is the separation of the mixture of products, which can include up to six different compounds. However, by varying the stoichiometry of the reagents, yields of the desired product can be maximized.

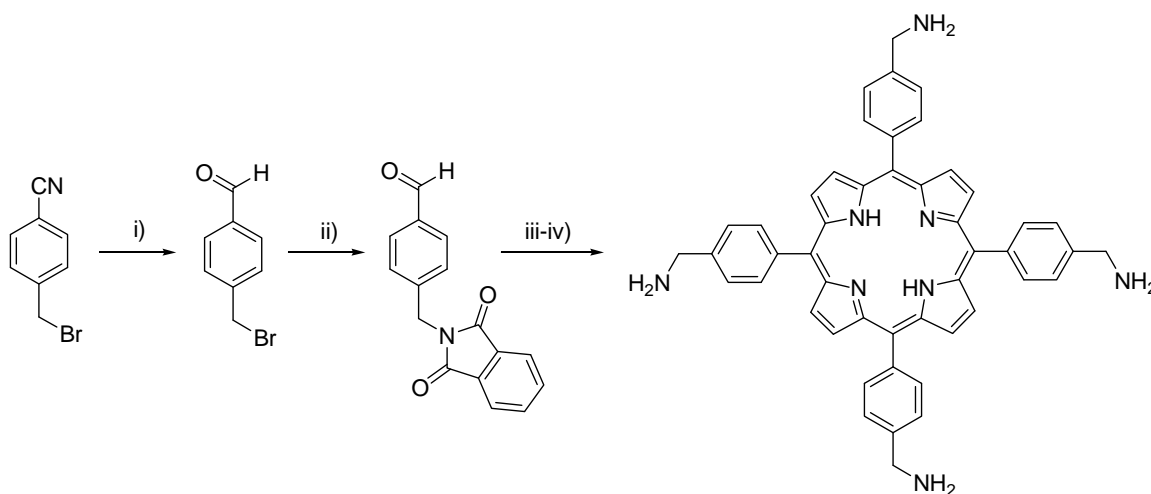
The Adler–Longo method is often used to obtain unsymmetrically substituted tetraphenylporphyrins with groups suitable for further modification. An elegant example of this is the recent synthesis of water soluble porphyrinyl nucleosides by Czuchajowski and co-workers [16]. In this synthesis 4-methoxybenzaldehyde and 4-pyridinecarboxaldehyde were condensed with pyrrole under Adler–Longo conditions. (Scheme 2-2).



Scheme 2-2 Reaction conditions: (i) Propionic acid; (ii) Pyridine hydrochloride, 220°C, 2.5 h; (iii) (A), Cs₂CO₃, NaH, DMF, 65°C, 42–36 h; (iv) CH₃I/CH₃NO₂ (4:3), 70°C, 12 h.

The mixture of products contained porphyrins with up to three kind of 4-methoxyphenyl groups at the *meso*-positions, the remaining *meso*-positions being occupied by 4-pyridyl rings. These products were separated by silica gel chromatography. The three compounds were further functionalized on the 4-methoxyphenyl rings to give the porphyrinyl nucleosides only the porphyrin containing one 4-methoxyphenyl group is shown for clarity).

Other porphyrins made using the propionic acid procedure include *meso*-tetra(4-methoxynaphthyl)porphyrin which was subsequently demethylated and investigated as a potential tumour localizer [17]. Lavalle *et al.* have used the Adler–Longo method to synthesise cationic porphyrins which could be used for DNA binding studies [8]. In this case, a protected amino aldehyde was prepared and used to form the porphyrin, before removal of the protecting group to reveal a tetraaminomethylporphyrin (Scheme 2-3). The latter was protonated in the pH range suitable for DNA binding.

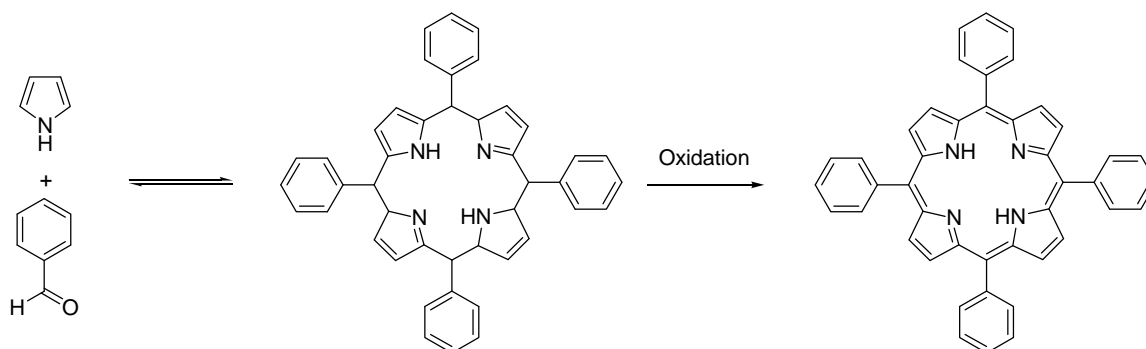


Scheme 2-3 Reaction conditions: (i) DiBAL-H, CH_2Cl_2 , 0°C , then 45°C , 4 h, 60%; (ii) Potassium phthalimide, DMF, reflux, 4 h, 90%; (iii) Pyrrole, acid; (iv) NaOH, heat, then 70% H_2SO_4 , heat.

While the above methods show the utility of the propionic acid method, there are several drawbacks. The formation of the reduced porphyrin (chlorin) invariably contaminates the product and a high percentage of tarry by-products are also formed. Another problem is the failure of the reaction with aldehydes containing acid sensitive functional groups.

2.4.1.2 Lindsey condensation

The Lindsey method relies on the formation of porphyrinogen as an intermediate in porphyrin synthesis [18]. The existence of this intermediate has previously been shown by Dolphin, that isolated β -octamethyl-*meso*-tetraphenylporphyrinogen under Adler–Longo conditions [8]. The advantage of this method is allows the formation of porphyrins from sensitive aldehydes in higher yields with more facile purification. The methodology relies on the fact that pyrrole and benzaldehyde under acid catalysis will establish equilibrium with tetraphenylporphyrinogen. The dilution conditions are important to optimize formation of the porphyrinogen at the expense of open chain polypyrrylmethanes. After the equilibrium has been established, an oxidant is added which irreversibly converts the porphyrinogen to the corresponding porphyrin (Scheme 2-4).

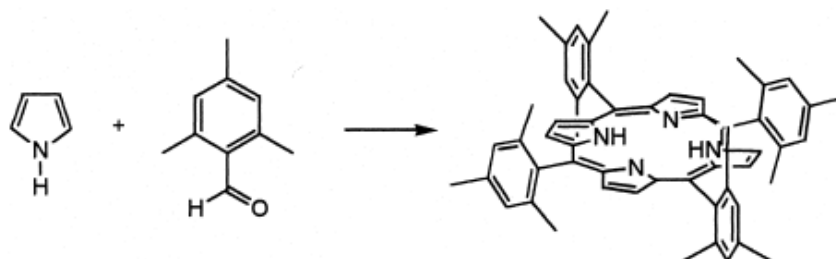


Scheme 2-4 Formation of porphyrin from porphyrinogen.

It was found using TPP as a model that equimolar concentrations of pyrrole, benzaldehyde and triethylorthoacetate (water scavenger), with boron trifluoride at room temperature produced optimal results. The reaction is carried out under inert conditions in dichloromethane for 1 h and followed by addition of 2,3,5,6-tetrachlorobenzoquinone (*p*-chloranil) and a further hour at reflux. Lindsey and co-workers have used this method to synthesize over 30 porphyrins with average yields around 30–40% using boron trifluoride or trifluoroacetic acid as the catalyst [18].

The Lindsey conditions were later modified to allow the formation of *o*-substituted tetraphenylporphyrins due to their sterically hindered nature are difficult to prepare [19]. Sterically hindered porphyrins are useful as crowding around the

macrocycle, leading to a non-planar conformation, which in turn can result in modified optical properties [20]. Using tetramesitylporphyrin as an example which had previously been prepared in yields of 1–6%. It was found that adding ethanol as a co-catalyst in the presence of BF_3 , resulted in the formation of *meso*-tetramesitylporphyrin in 30% yield (Scheme 2-5). The need for ethanol was attributed to its ability to dissociate the mesitaldehyde– BF_3 complex [21].



Scheme 2-5 Formation of *meso*-tetramesitylporphyrin.

The general utility of these optimized conditions was explored using various *o*-substituted benzaldehydes. The results showed that 2-alkoxy, 2-alkyl and 2,6-dialkoxybenzaldehydes gave improved yields with the addition of ethanol but *o*-substituted halogens showed no improvement [19]. Other examples of sterically hindered porphyrins which have been prepared using this methodology include dodecaphenylporphyrin, which was prepared using 3,4-diphenylpyrrole and benzaldehyde in 5.7% yield [22]. The Lindsey group has also prepared hindered porphyrins using derivatized benzaldehydes and pyrrole [23]. Octa- and dodecabenzoyloxyporphyrins have also been synthesized in 9–52% yield in this way. The use of diversely functionalized aldehydes for building porphyrin-based model systems has been described by Lindsey *et al.* [24]. The effects of the addition of salts such as NaCl or benzyltributylammonium chloride on the Lindsey procedure has been studied recently and it has been shown that, depending on the salt, porphyrin yield can be increased by up to two-fold [25].

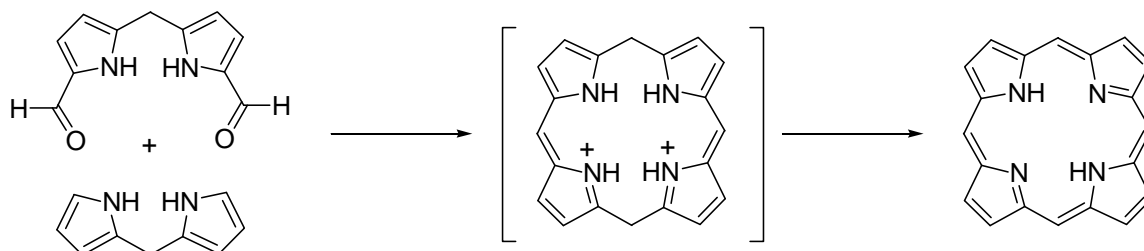
A noteworthy modification of the Lindsey procedure is the use of clays for porphyrin synthesis. Initial work in this area by Pinnavaia showed that TPP formed on the surface of montmorillonites [26]. Using this concept for the synthesis of *meso*-tetraalkylporphyrins, Onaka and co-workers used various acidic clays in place of BF_3 [27]. It was found that montmorillonite K10 catalysis gave the highest yield of

porphyrin (46% yield for *meso*-tetrapentylporphyrin, compared to 20% in the case of BF_3 catalysis).

Another method for *meso*-tetraarylporphyrin synthesis involves the use of transition metal salts. Llama *et al.* have used vanadium (V), titanium (IV) and manganese (III) salts to synthesize a variety of porphyrins in good yields (68% yield of TPP with VOCl_3) and at higher concentrations than the Lindsey method [28]. It was reported that the high valent metal salt, acting as an oxidant, converts the porphyrinogen to the porphyrin *via* a radical process.

2.4.1.3 2 + 2 Porphyrin synthesis

Porphyrins can also be prepared from dipyrromethanes using what are commonly called 2+2 syntheses. The term 2+2 arises because the porphyrin is formed by the condensation of two dipyrromethanes (fragments containing two pyrrole units). Early work in this area was pioneered by MacDonald *et al.* [29] and the basic synthetic route is shown in (Scheme 2-6). The original MacDonald method involves the use of one dipyrromethane bearing two formyl groups alpha to the pyrrolic nitrogen and another dipyrromethane with no α -substitution.

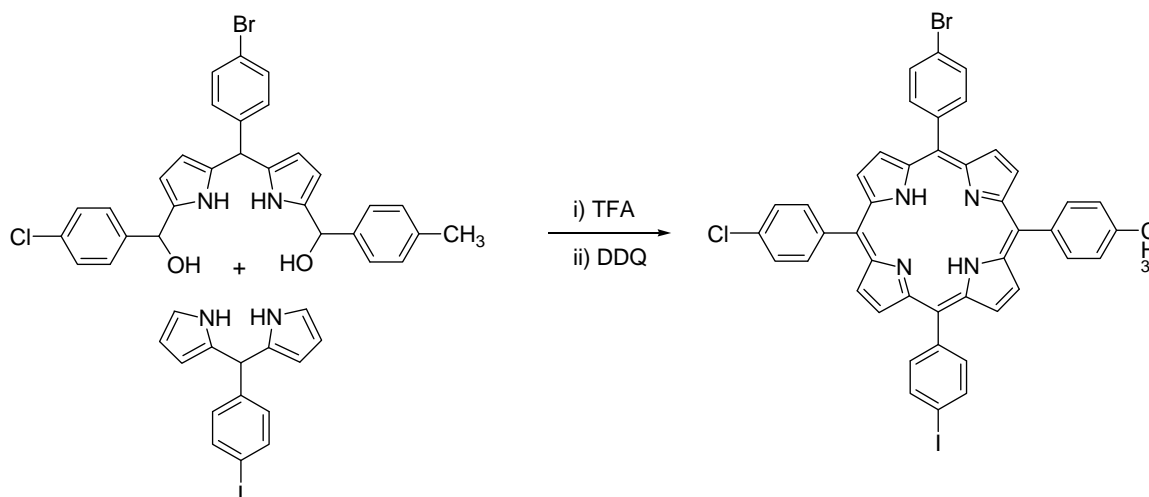


Scheme 2-6 2+2 Porphyrin synthesis.

There is an obvious scope for the preparation of a large variety of functionalized porphyrins using this route and a greater degree of regioselectivity can be attained relatively to the Adler and Lindsey methods. The β -positions can be differentially functionalized on the pyrrole rings and the bridging carbon in the dipyrromethane can also be substituted. Honeybourne *et al.* used a modified MacDonald synthesis for the preparation of models of naturally occurring porphyrins for studying the enzyme ferrochelatase [30]. They prepared dipyrromethanes

containing differentially substituted β -positions and formyl groups at the terminal α -positions. The coupling resulted in the formation of porphyrins in 10% yield

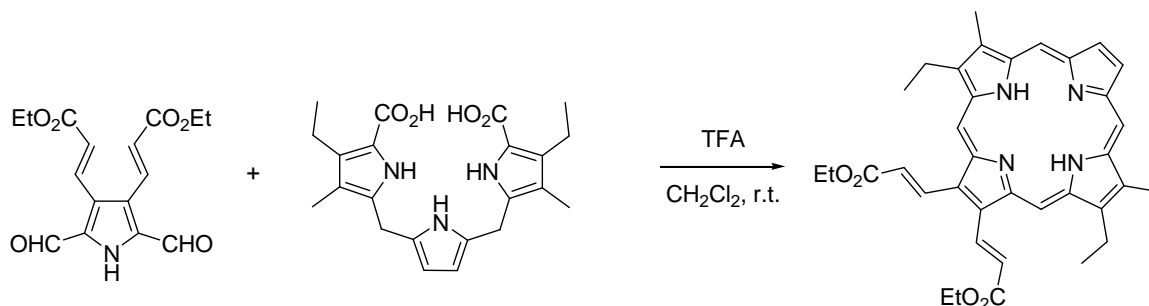
Lindsey *et al.* have also synthesized porphyrins containing four different *meso* substituents [31]. One of these compounds contains three different halogens attached to the phenyl rings and was prepared in 14% yield (Scheme 2-7)



Scheme 2-7 Differentially substituted porphyrin.

2.4.1.4 3+1 Porphyrin synthesis

The 3+1 synthetic route involves the condensation of a tripyrrane (compound containing three pyrrole groups linked alpha to the ring nitrogens by two saturated carbons) with a diformyl pyrrole. This area has seen much activity in the last five years, although the methodology has been used previously for the synthesis of expanded porphyrins and oxa- and thiaporphyrins. Momenteau *et al.* have used this procedure to prepare a porphyrin containing two acrylic acid units on the same pyrrole, in 33% yield as shown in Scheme 2-8 [32].



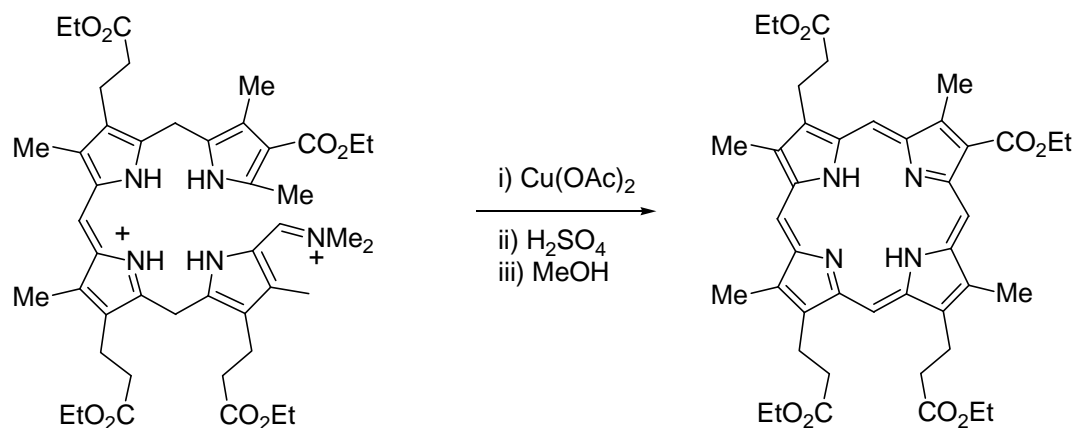
Scheme 2-8 Formation of porphyrin containing two acrylic acid units on the same pyrrole.

Lash has used pyrrole dialdehyde and tripyrrane to prepare an octaalkylporphyrin in 60% yield. More complex porphyrins such as acenaphthoporphyrins and phenanthrolineporphyrins containing fused 1,10-phenanthroline subunits have also been synthesized by Lash *et al.* while Sessler and co-workers have used this approach to produce mono functionalised alkylporphyrins. The 3+1 route has been used to create many exotic porphyrinoid structures such as oxybenzaporphyrins and carbachlorins. Other work includes the synthesis of porphyrin analogues containing cycloheptatriene and pyridine subunits.

2.4.1.5 Porphyrins from linear tetrapyrroles

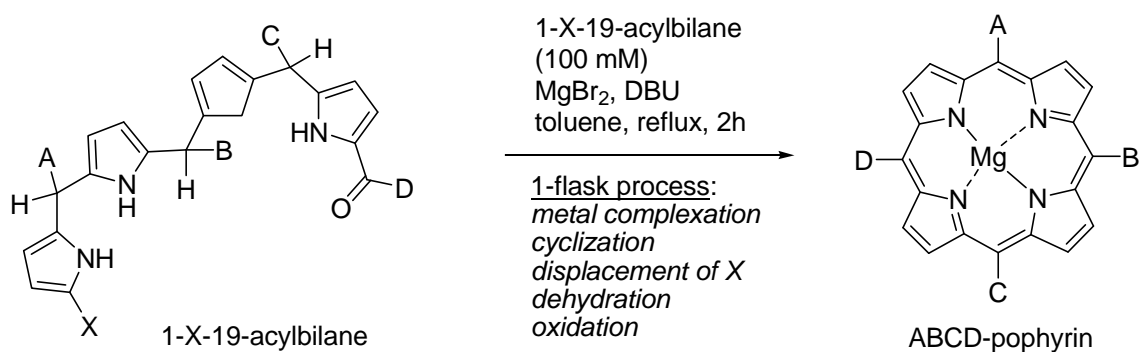
Linear tetrapyrroles or bilanes can be cyclized to produce porphyrins. This strategy is used when there is a need to synthesize porphyrins which are unsymmetrical and contain a variety of substituents at the β -position. *b*-Bilenes bearing an iminium group at the 1-position and a methyl at the 19-position have been used via an oxidative cyclisation strategy, to prepare porphyrins. Clezy *et al.* have used ^{13}C -labelled *b*-bilenes to show that the final carbon required to complete the ring system originates from the methyl group (Scheme 2-9) [33].

The most common tetrapyrroles used for porphyrin synthesis are *a,c*-biladienes. The use of 1-bromo-19-*a,c*-methylbiladienes as porphyrin precursors has been reviewed by Dolphin *et al.* [34]. It has been shown that vinylporphyrins can be prepared from 1-bromo-19-methyl-*a,c*-biladienes. Using this intermediate, Dolphin *et al.* carried out the cyclization step using DMSO–pyridine at room temperature. The bisacetate was then converted to the corresponding chloro compound in two steps, which in turn was dehydrochlorinated.



Scheme 2-9 Porphyrin formation from β -bilanes.

In 2007 Lindsey *et al.* have proposed a new strategy for preparing porphyrin that bear up to four different *meso*-substituent (ABCD-porphyrins) via bilane [35]. This method relies on two key reactions; one entails a directed synthesis of a 1-protected 19-acylbilane by acid-catalyzed condensation at high concentration (0.5 M) of a 1-acyldipyrromethane and a 9-protected dipyrromethane-1-carbinol (derived from a 9-protected-1-acyldipyrromethane). The bilanes were obtained in 72-80% yield. The other entails a one-flask transformation of the 1-protected-19-acylbilane under basic, metal-templating conditions to give the corresponding metaloporphyrin (Scheme 2-10).



Scheme 2-10 New route to ABCD-porphyrins via bilanes.

2.4.2 Uses and applications of porphyrin derivatives

There are a lot of interesting applications of porphyrins and other tetrapyrroles (chlorins and bacteriochlorins) in chemical and biomedical research. For example:

1. Photodynamic Therapy (PDT)
2. Modellsystems of photochemical reaction centres
3. Biomimetic models of several enzymes (Catalases, Cytochromes etc.)
4. Catalysis (especially with Mn, Fe and Pd metalloporphyrins)
5. Sensors and biosensors
6. Solar energy conversion and catalysis.

2.5 Diesel fuel [36]

Diesel fuel is obtained from fractional distillation of crude oil, which is a mixture of hydrocarbon such as benzene, pentane, hexane, heptane and toluene. The boiling range of distillate diesel fuel is approximately 150 - 370 °C (300-700 °F). It is a general property of hydrocarbons that the more volatile they are the higher temperatures for spontaneous ignition. It is for this reason that the less volatile middle distillate fractions of petroleum crude and even residues are more readily applicable to diesel engines than gasoline or lighter fractions. diesel fuel has two types namely:

1. High speed diesel (Automotive Diesel Oil (ADO)), gas oil or solar oil, used in buses, pickups and trucks.
2. Low speed diesel (Industrial Diesel Oil (IDO)), use in water crafts and submarines.

2.5.1 Chemical composition [37]

Petroleum derived diesel is composed of about 75% saturated hydrocarbons (primarily paraffins including *n*, *iso* and cycloparaffins) and 25% aromatic hydrocarbons (including naphthalene and alkylbenzenes). The average chemical formula for common diesel is $C_{12}H_{26}$, ranging from approximately $C_{10}H_{22}$ to $C_{15}H_{32}$. ASTM specifications for high speed diesel are summarized in Table 2-1 [38].

Table 2-1 ASTM specifications for high speed diesel

Test Items	ASTM method	Limit	Unit
Specific gravity at 15.6/15.6 °C	D 1298	0.81-0.87	
Cetane number/Calculated cetane index	D 613	Min 47	
Viscosity at 40 °C	D 445	1.8-4.1	cSt
Pour point	D 97	Max 10	°C
Sulfur content	D 4294	Max 0.035	% wt.
Copper strip corrosion	D 130	Max no.1	
Oxidation stability	D 2274	25	g/m ³
Carbon residue	D 189	Max 0.05	% wt.
Water and sediment, % vol	D 2709	Max 0.05	% vol.
Ash	D 482	Max 0.01	% wt.
Flash point	D 93-02a	Min 52	°C
Distillation : Initial Boiling Point (IBP)	D 86	Report	°C
Distillation : 10% vol., recovery	D 86	Report	°C
Distillation : 50% vol., recovery	D 86	Report	°C
Distillation : 90% vol., recovery	D 86	Max 357	°C
Colour : Hue Dye	D 1500	Blue Min 0.7	mg/l
Methyl ester of fatty acid	EN 14078	4-5	% vol.
Lubricity	CEC F-06-A-96	Max 460	µm

2.6 Marker [39]

Markers are also becoming particularly important for protecting brand integrity for consumers. Such markers must be readily detectable at relatively low concentrations in the product. In the petroleum industry, markers are also useful for ensuring compliance with governmental regulations. For example, products such as diesel fuel, gasoline and heating oils often contain visible dyes or colorless fluorescent compounds that identify the intended use, tax status, or brand name of the product.

A marker is defined as a substance, which can be used to tag petroleum products for subsequent detection and is invisible in the petroleum products. The

marker is dissolved in a liquid to be identified and then subsequently detected by performing a simple chemical or physical test on the tagged liquid.

2.7 Cashew Nut Shell Liquid (CNSL) [40]

Cashew nut shell liquid (CNSL) is the international name of the alkylphenolic oil that present in nearly 25–30% of the total cashew nut weight inside the spongy mesocarp of the shell (*Anacardium occidentale* L.). It occurs as a reddish brown viscous liquid in the soft honeycomb structure of the shell of cashew nut. CNSL is obtained as a by-product from mechanical processing for edible use of the cashew kernel. Since worldwide cashew nut production is presently estimated to be 1,200,000 tons per annum, the availability of CNSL ranges between 300,000–360,000 tons per annum.

CNSL is essentially a mixture of phenolics extracted from the shells of the cashew nut and is good natural alternatives to petrochemically derived phenol, a product whose price inherently linked to the fickle oil price and availability of fossil fuels. The major component of CNSL, depending slightly on the geographical location of the tree, is anacardic acid. It breaks down to give cardanol, which is essentially a phenol. Selected physical and chemical properties are shown in Table 2-2 [41].

Table 2-2 Characteristics of cardanol

Boiling point, °C	228-235 (3.4 mmHg)
Color (Livibond, 1 cm cell) (freshly distilled)	Red (1.0-3.0) Yellow (1.5-3.5)
Viscosity, 30°C (cP)	40-60
Specific gravity 30/30 °C	0.93-0.95
Volatile loss, % by wt (max)	2.0
Acid value	1.9-2.0
Iodine value (Wijs method)	210-220
Hydroxyl value	180-200

2.7.1 Extracting process of CNSL [42]

Traditionally, Indian processors of cashew nuts roast them in an open perforated drum. CNSL either leaks away or is burnt in the fire. With increase in the price of CNSL, many refined extraction techniques have come into vogue.

Hot oil bath method

This is the most common method for commercial extraction. The raw nuts are passed through a bath of hot CNSL (180 - 200°C) itself, when the outer part of the shell burst open and releases CNSL (50% recovery). Another 20% could be extracted by passing the spent shells through an expeller and the rest by solvent extraction techniques.

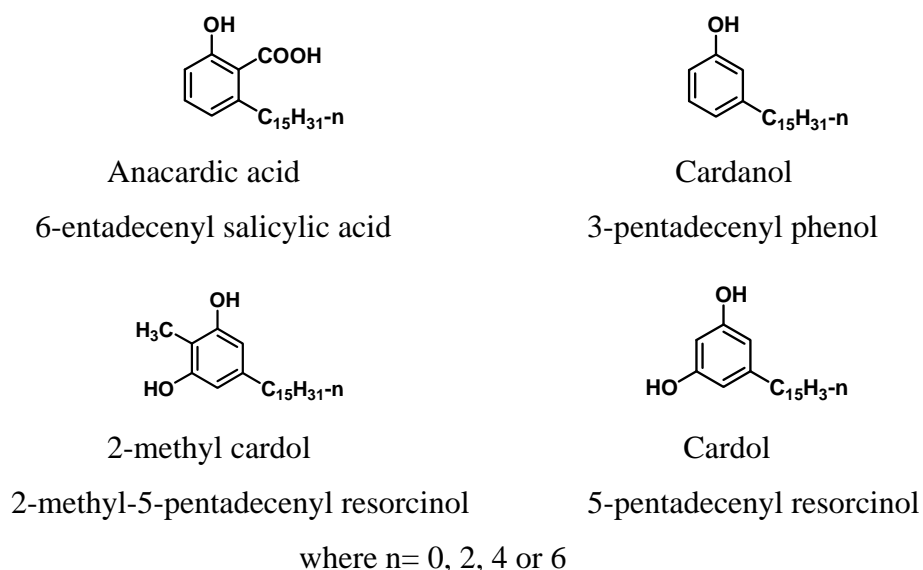
Expeller method

Some factories introduce manually operated cutting machines in which shell of lightly roasted nuts are cut, keeping the kernel intact. The shells are then fed to an expeller to recover 90% of the oil.

Klin method

The nuts are shelled after sun drying or after drum roasting. The liquid is obtained however, crude is contaminated.

CNSL, extracted with low boiling petroleum ether, contains about 90% anacardic acid and about 10% cardol. On distillation, CNSL gives the pale yellow phenolic derivative cardanol. The chemical structures of major compounds in natural CNSL are shown in Scheme 2-11. The side chain exists in saturated (n=0), monoene (n=2), diene (n=4), and triene (n=6) that form with *cis* configuration.



Scheme 2-11 Chemical structure of major compounds in natural CNSL.

2.7.2 Uses and applications

The CNSL is an undesirable by-product of the cashew kernel industry. This is an effective replacement of source and expensive petrochemicals. CNSL is described often a versatile industrial raw material. It has wide application in the manufacture of numerous industrial products.

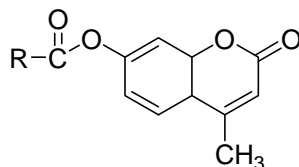
The CNSL of the cashew kernel or nutmeat is important in economic. In its natural state, it serves as a protection to the kernel against insect attack. If used in combination with kerosene or diesel oil, it is an effective insecticide against mosquito larvae [43]. Made into a varnish it is a preservation of wooden floors and fine carved wood, protecting from insect destruction [44]. For many years, fishermen have used the liquid to waterproof and preserve their fishnets, fishings lines and boats [45].

With recent advances in chemical technology, the CNSL is finding many new industrial applications. It is used commercially as a phenolic raw material for the manufacture of certain resin and plastics [46]. In particular, it is used as a friction modifier in the manufacture of brake linings and clutch facings. It has the property of absorbing the heat generated by friction in the braking action while retaining their braking efficiency longer [47]. It is also used in rubber compounds, where its acts as reinforcing fillers, which tensile strength, hardness and abrasion resistance are improved [48]. The resins from CNSL are used in laminating for papers, cloth and glass fibers, or impregnating materials where oil or acid resistance is required [49]. Other uses include the manufacture of lacquers, paints, printing inks, electrical insulation material, anti-corrosive for metals, water proofing compounds and adhesives [50].

2.8 Literature reviews

Michael R. Friswell *et al.* [51]

Synthesized markers for liquid petroleum products and industrial liquids having the following structure:

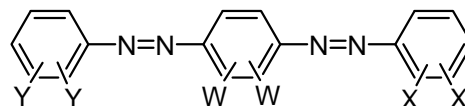


where the R is a linear or branched C₁-C₁₈ alkylcarboxy.

These compounds were conveniently synthesized by esterification of an appropriately selected linear or branched C₁-C₁₈ alkyl carboxylic acid or acid halide such as acid chloride with 7-hydroxy-4-methylcoumarin. These markers are used for tagging petroleum products at level of about 0.25 – 100 ppm. They may be detected in the products by extraction with an alkali aqueous solution which produces strongly fluorescence when examined under ultraviolet light at wavelength of 365 nm.

Michael J. Hallisy *et al.* [52]

Synthesized marker dyes for liquid petroleum products, having the following formula:

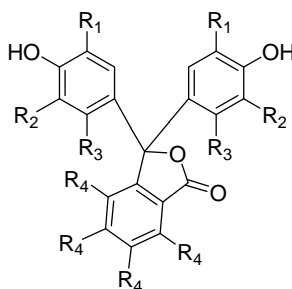


where Ws are O-(C₁-C₃alkyl) and hydrogen, provided that at least one W is O-(C₁-C₃alkyl), Xs and Ys are hydrogen, alkyl, substituted alkyl, alkenyl, substituted alkenyl, aryl, substituted aryl, fused aryl, substituted fused aryl, halogen, nitro, cyano, or alkoxy group.

These compounds were synthesized by azo coupling of an appropriately substituted aniline to a phenol, such as 2,6-di-*sec*-butyl phenol. Compounds of this general formula, generally pale red, are used at the concentration of 0.25-100 ppm in petroleum product and not readily observable by naked eyes. These markers can be detected by extraction of the tagged products with an alkali aqueous solution, e.g. 1-3% sodium hydroxide solution leading to blue solution.

Smith M.J. et al. [53]

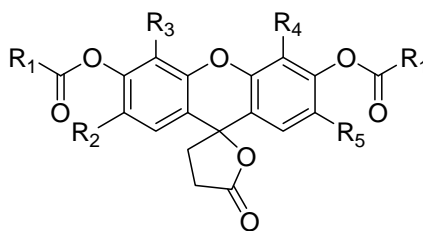
Disclosed the synthesis of isobenzofuranone derivatives as petroleum markers. The general structure is shown as follows:



where R_1 is C_1 - C_{18} alkyl or alkoxy group; R_2 and R_3 are hydrogen, alkyl group, alkoxy group, or part of naphthalene ring system; R_4 is any combination of bromine, chlorine or hydrogen.

These marker compounds were synthesized by condensation of phthalic acid or its anhydride with 2-alkylphenol or 1-naphthol. Because these markers are colorless in petroleum products, their presence was detected by the reaction with a basic developing reagent such as alkali metal hydroxide solution. The markers underwent chromaphoric reaction and produced color in an extracted phase.

Later on the same group reported the synthesis of fluorescein derivatives compounds which developed fluorescence when extracted with an appropriate basic solution for marking petroleum fuels [54]. These markers have the general formula:

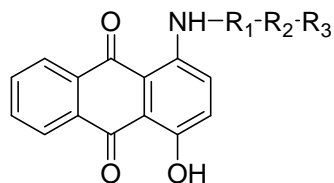


where R_1 is C_1 - C_{18} alkyl group or an aryl group; R_2 , R_3 , R_4 and R_5 are hydrogen, chlorine, bromine or C_1 - C_{12} alkyl group.

These markers were synthesized by converting fluorescein to an organic diester to eliminate any tendency to partition into water. The ester markers can be added to any liquid petroleum products and detected by the reaction with the developing agent. Examples of the developing agent are an aqueous solution of alkali metal hydroxide and aqueous solution of the quaternary ammonium hydroxide. These base hydrolyze the esters, and prompt formation of a highly fluorescent dianion which may be variously colored.

Friswell, M.R. *et al.* [55]

Reported the synthesis of tagging markers with the following formula:

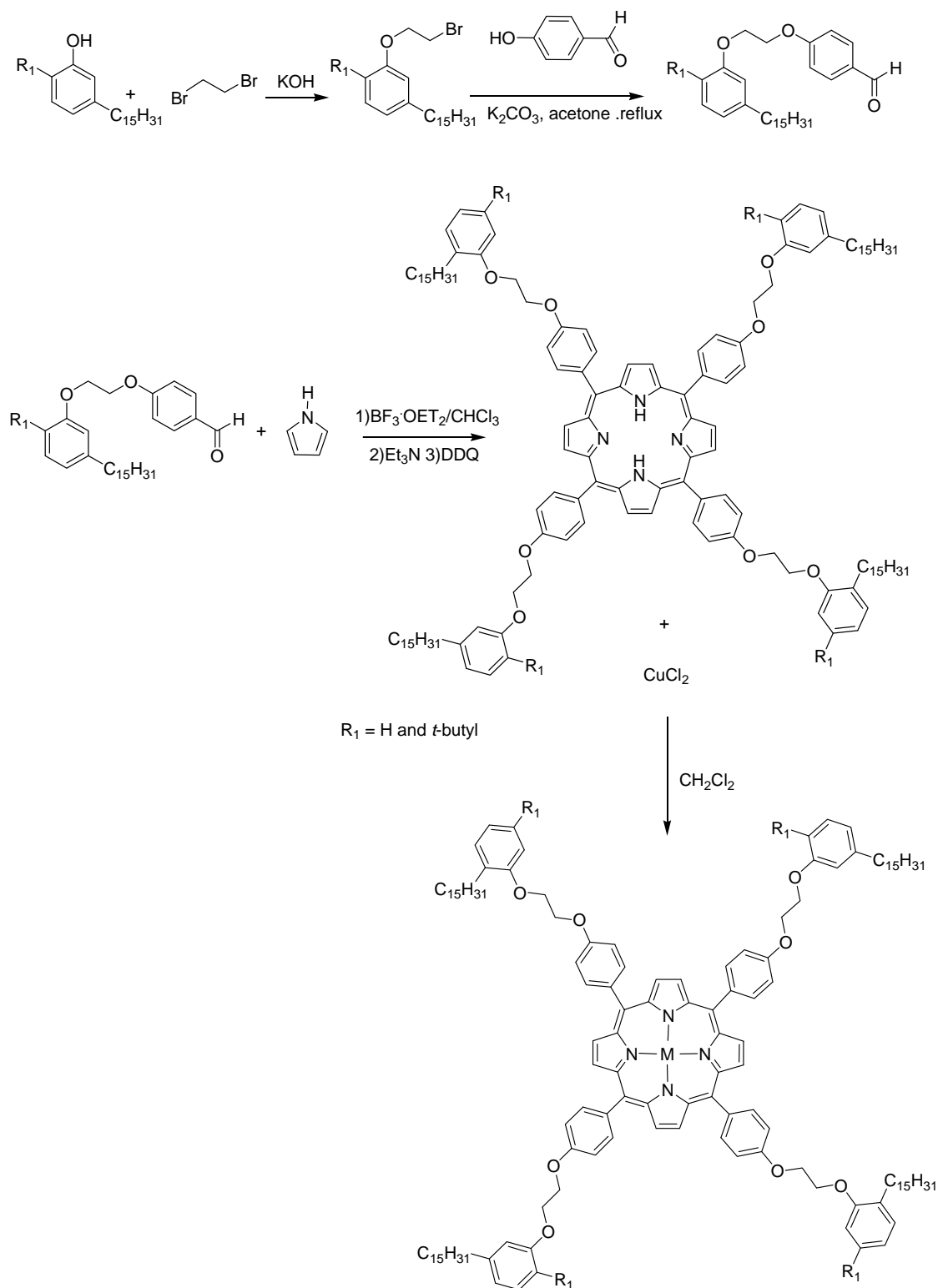


where R₁ is C₁-C₆ alkyl, and R₂ and R₃ are nothing or O-(C₁-C₃ alkyl)

These markers, which are known as “marker purple” were prepared by reaction of quinizarin, reduced quinizarin or mixture of quinizarin and reduced quinizarin with the amine formula, H₂N-R₁R₂R₃, wherein R₁, R₂ and R₃ are as define above. These compounds have purple colors but in the range from about 1-100 ppm, the markers impart little visible color to the petroluem products. The markers were detected in the petroleum products by the extraction with a reagent comprising water, a strong base and preferably a water soluble oxygenated cosolvent or a water-soluble amine cosolvent. This reagent causes the markers to react and produces a clearly defined color that allow the identification of petroleum products.

Mele G. et.al [56]

Described the synthesis and characterization of new metal-free and Cu-substituted *meso*-tetraarylporphyrins containing 3-*n*-pentadecylphenolic substituents (Scheme 2-12).

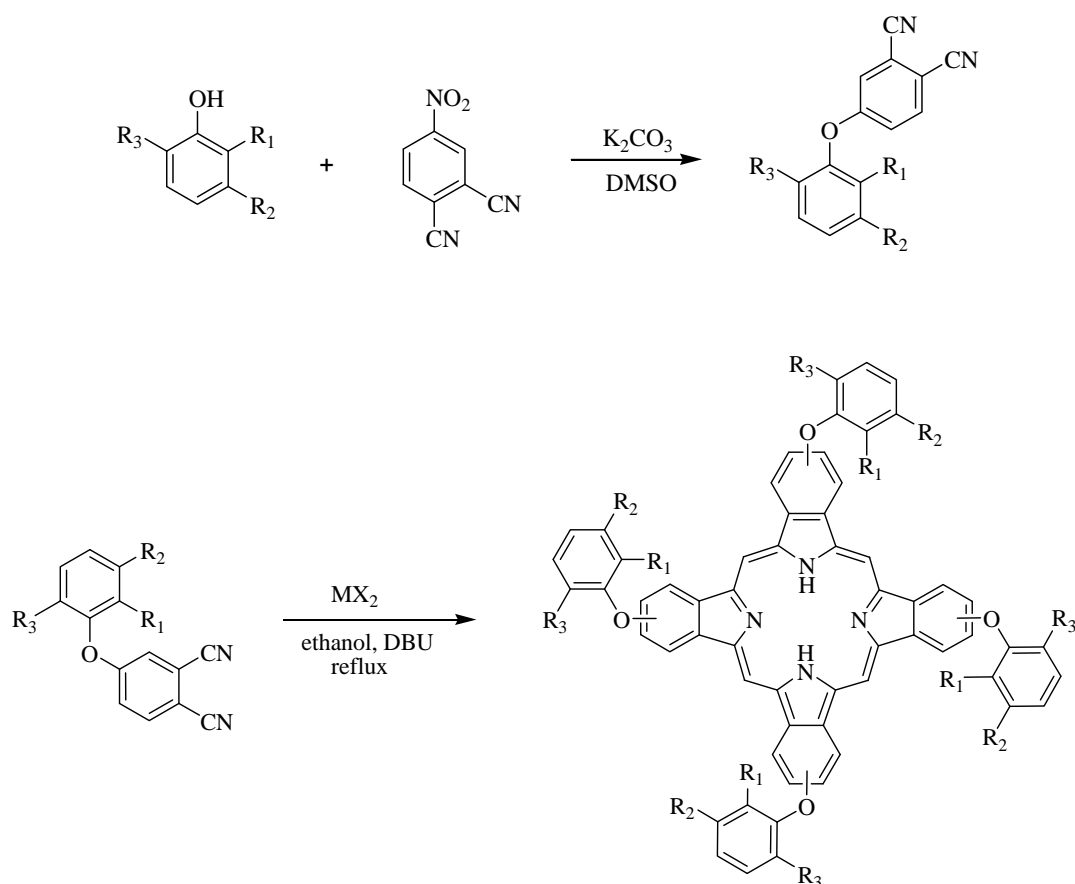


Scheme 2-12 Synthesis novel cardanol-based porphyrins.

The novel cardanol-based porphyrins showed high solubility in organic solvents and were used to impregnate TiO₂ in the crystalline phase of anatase. The photocatalytic activity of TiO₂ loaded with these novel porphyrins was investigated through the examination of the probe reaction of photodegradation of 4-nitrophenol in an aqueous suspension, indicating that the presence of the sensitizer increases the photoactivity and confirms the important role of Cu in this process.

Attanasi, O. A. *et al.* [57]

Reported the synthesis and characterization of phthalocyanine derivatives. Such phthalocyanine derivatives were obtained by a base-catalyzed nucleophilic aromatic nitro-displacement of 4-nitrothalonitrile with an alcohol or a phenol compound (Scheme 2-13).



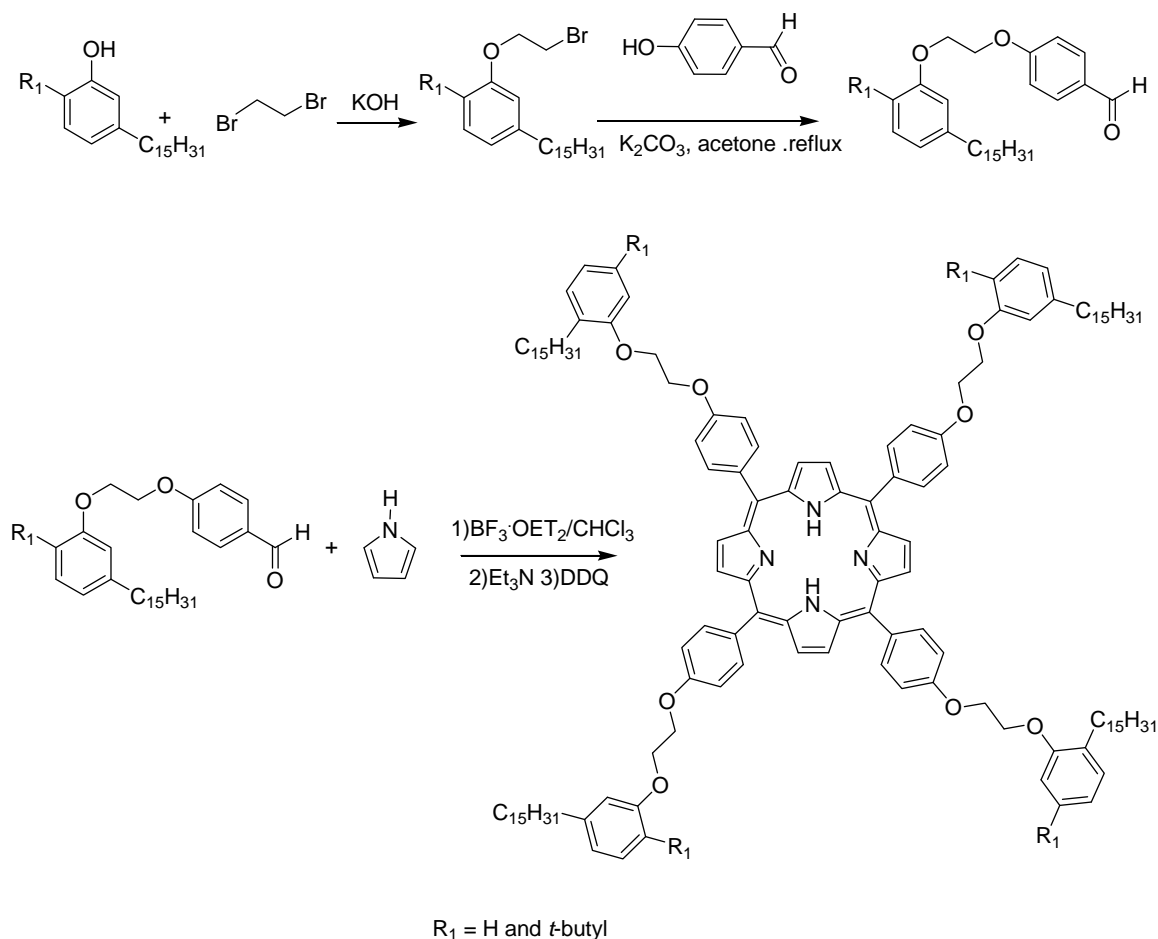
Scheme 2-13 Preparation of phthalocyanines derivatives.

where R_1 and R_3 are H or allyl, and R_2 is $C_{15}H_{31}$ and M are Cu, Pd, Zn or Ni, $X = Cl$

A mixture of the unsaturated compounds of the pentadecylphenol and cardanol underwent a similar reaction giving a mixture of phthalonitrile products having differently unsaturated chains. The phthalocyanine derivatives showed important properties, for example relatively low melting points (within 38 - 49°C) and relatively high solubility in organic solvents due to the long alkyl chains.

Orazio A. Attanasi *et al.* [58]

Reported the synthesis and characterization of new metal-free and metallo complexes (Cu, Zn, Co) of substituted *meso*-tetraarylporphyrins containing cardanol derivatives (3-*n*-pentadecylphenol and 2-*tert*-butyl-5-*n*-pentadecylphenol) (Scheme 2-14).

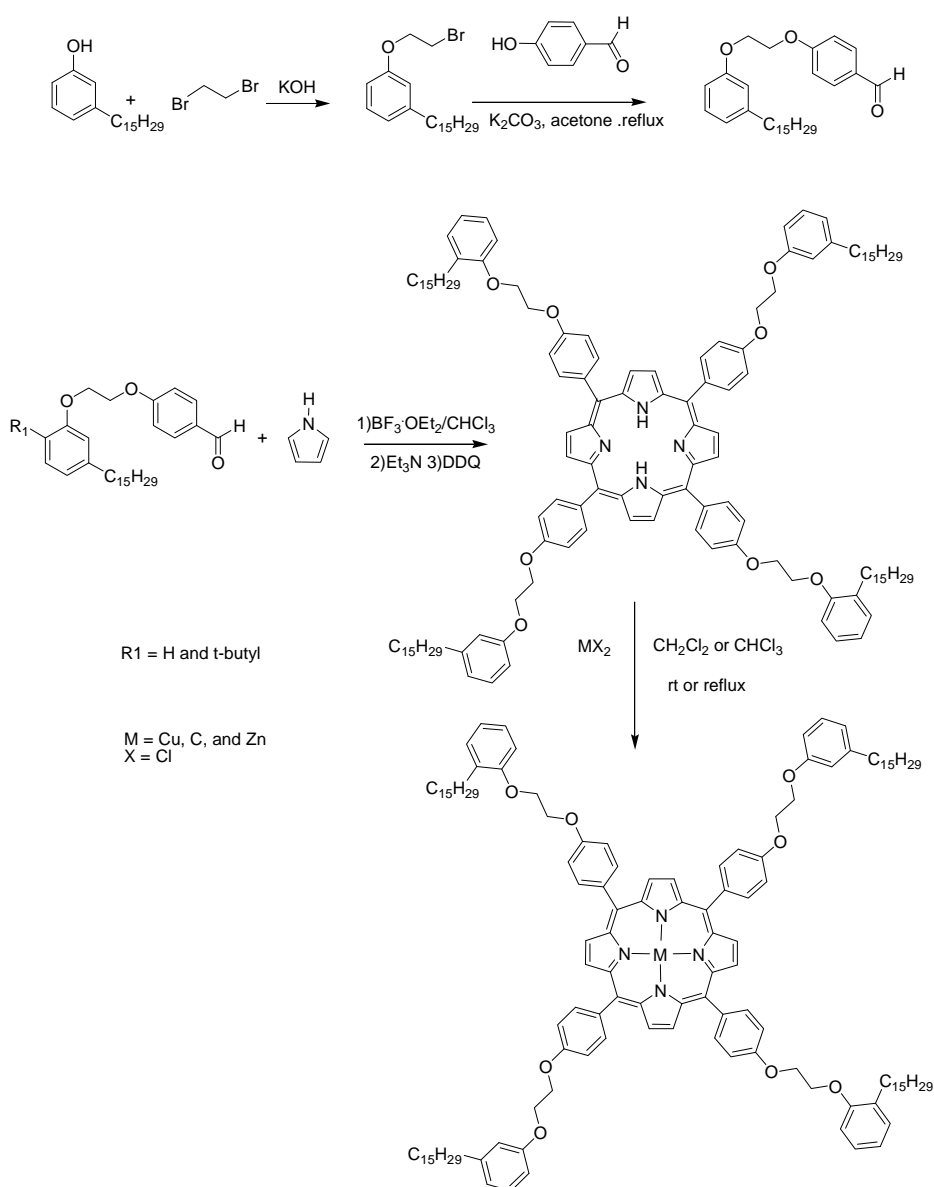


Scheme 2-14 Synthesis the novel cardanol-based porphyrins.

Due to the presence of the long alkyl side-chain on the aryl ring, the *meso*-tetraarylporphyrins exhibited solubility in organic solvents and relatively low melting points. Furthermore, the metalloporphyrin complexes prepared from 2-*tert*-butyl-5-*n*-pentadecylphenol showed melting points lower than those both of the corresponding free-base porphyrin and the metalloporphyrin complex obtained from 3-*n*-pentadecylphenol.

Guo .Y.-C. *et al.* [59]

presented a synthesis of a new hybrid *meso*-tetraarylporphyrin-cardanol with the cardanol bearing an unsaturated chain (Scheme 2-15).

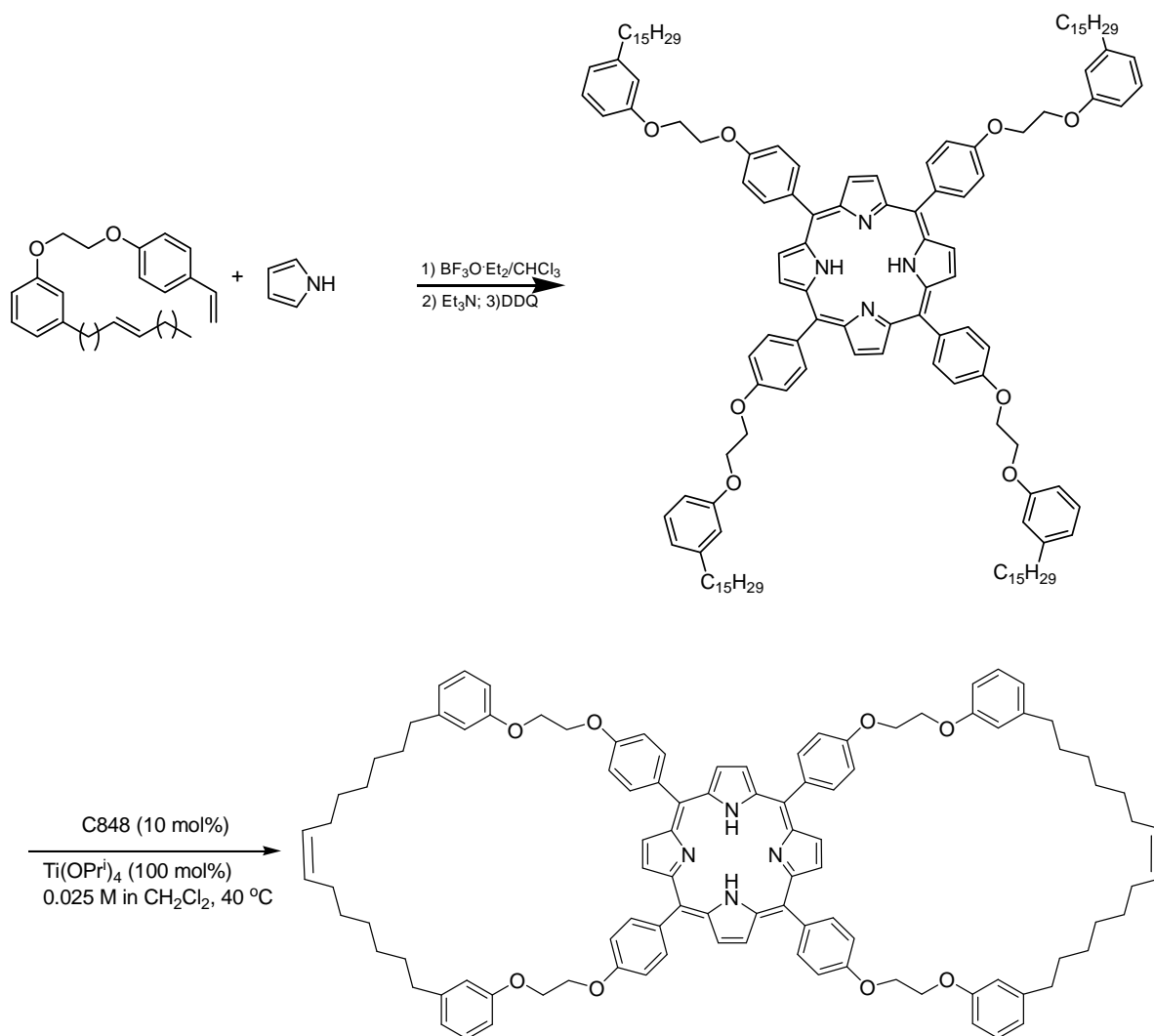


Scheme 2-15 Synthesis of a new hybrid *meso*-tetraarylporphyrin-cardanol with the cardanol bearing an unsaturated chain.

Due to the presence of the long alkyl side-chain on the aryl ring, the *meso*-tetraarylporphyrins exhibited solubility in organic solvents and relatively low melting points.

Some other quite interesting results have been obtained through self-metathesis reactions involving the double bonds of the cardanol derivative.

Later on the same group presented a novel procedure to synthesize bis-cardanol derivatives and cardanol-porphyrins starting from a cheap and renewable starting material through a home-cross-metathesis and ring-closing metathesis reactions using Grubb's catalysts (Scheme 2-16). This methodology provides a versatile approach for the efficient synthesis of various molecular hybrid systems [60].



Scheme 2-16 The synthesis of a cyclic cardanol-based porphyrin derivative.

CHAPTER III

EXPERIMENTAL

3.1 Chemical

1. Hydrogenated cardanol : Obtained locally
2. Sodium sulfate (anhydrous) : Merck
3. Triethylamine : Lab-scan
4. Sodium hydroxide : Merck
5. Chloroform : Lab-scan
6. Hydrochloric acid : Mallinckrodt Baker
7. Paraformaldehyde : Merck
8. Tin (IV) tetrachloride : Fluka
9. Methylene chloride : Distilled from commercial grade
10. Hexane : Distilled from commercial grade
11. Ethyl acetate : Distilled from commercial grade
12. Pyrrole : Fluka
13. Boron trifluoride diethyletherate ($\text{BF}_3 \cdot \text{OEt}_2$) : Fluka
14. 2,3-Dichloro-5,6-dicyano-*p*-benzoquinone (DDQ) : Fluka
15. Sodium chloride : Merck
16. Toluene : Carlo Erba
17. Salicylaldehyde : Fluka
18. Potassium carbonate : Merck
19. Iodomethane : Merck
20. Silica gel : Merck
21. Acetone : Fluka

3.2 Analytical instruments

Melting points were determined with a Stuart Scientific Melting Point SMP1 (Bibby Sterlin Ltd., Staffordshire, UK).

FT-IR spectra were recorded on a Nicolet Fourier Transform Infrared Spectrophotometer: Impact 410 (Nicolet Instruments Technologies, Inc. WI, USA). Infrared spectra were recorded between 400 cm^{-1} to $4,000\text{ cm}^{-1}$ in transmittance mode.

^1H -NMR and ^{13}C -NMR spectra were obtained in deuterated chloroform (CDCl_3) using Varian Mercury NMR spectrometer operated at 400.00 MHz for ^1H and 100.00 MHz for ^{13}C nuclei (Varian Company, CA, USA). The chemical shifts (δ) are reported in parts per million (ppm) relative to the residual CHCl_3 peak (7.26 ppm for ^1H -NMR and 77.0 ppm for ^{13}C -NMR). The coupling constants (J) are reported in Hertz (Hz).

Mass spectra were recorded on Mass Spectrometer: Waters Micromass Quattro micro API ESCi (Waters, MA, USA.). [Samples were dissolved in ethyl acetate and direct injected into Mass Spectrometer in 50 μL (Compound **2,5** and **6**)], and mass spectra of the porphyrin derivative were recorded by matrix-assisted laser desorption ionization mass spectrometry (MALDI-MS).

Fluorescence spectra were recorded on a Perkin Elmer LS 50 luminescence spectrophotometer. Wavelength is in the range of 400-800 nm and cell width is 1 cm.

The quantities of fluorescent marker in fuel oils were measured using a Perkin Elmer LS 50 luminescence spectrophotometer.

Kinematic viscosities of fluorescent and non-fluorescent diesel fuels were obtained with a Cannon automatic viscometer.

Flash point (pensky-Martens) of fluorescent and non-fluorescent diesel fuels were measured using a Perzoc ISL (PMFP93) automatic flash point tester.

Pour point of fluorescent and nonfluorescent diesel fuels were recorded on an ISL (CPP5GS) automatic pour point tester.

Sulfur contents in fluorescent and nonfluorescent diesel fuels were determined using Outokumpu (X-MET820) automatic sulfur content.

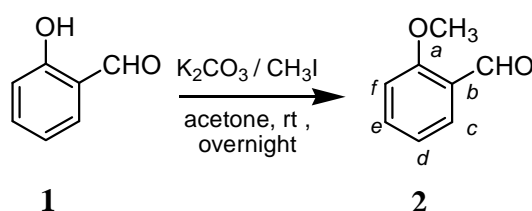
Distillation of fluorescent and nonfluorescent diesel fuels were carried out with a AD 865G (ISL) automatic distillation apparatus.

Colors of fluorescent and nonfluorescent diesel fuels were observed with a Lovibond (PFX990/P) petrochemical tintometer.

3.3 Experimental procedure

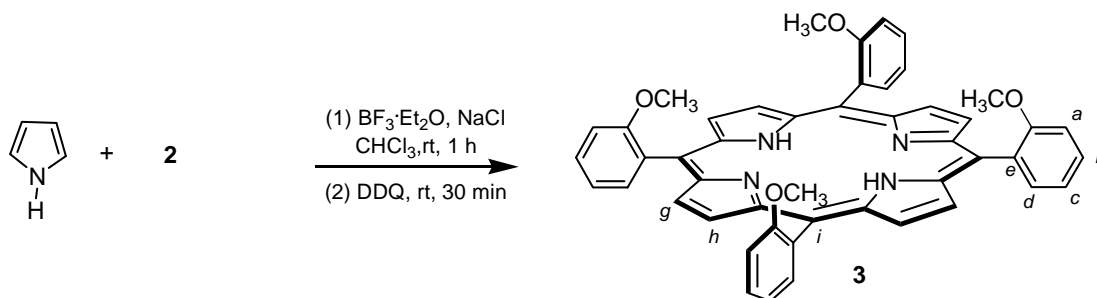
Part 1: Synthesis of porphyrin model

3.3.1 Synthesis of 2-methoxybenzaldehyde (**2**)



Following a previously published procedure [61], salicylaldehyde (**1**) (200.0 mg, 1.638 mmol) was dissolved in acetone (5 mL) and potassium carbonate (325.2 mg 1.968 mmol) was added. The reaction mixture was stirred at room temperature for 20 minutes and then, iodomethane (0.124 mL, 1.968 mmol) was added. The reaction mixture was stirred overnight at room temperature. The mixture was washed with distilled water (2x20 mL) and extracted with ethyl acetate (2x20 mL). The combined organic layer was dried over anhydrous sodium sulfate, filtered and concentrated to dryness. The resulting crude product was purified by column chromatography on a silica gel [hexane/dichloromethane (4:1)] to give **2** as pale yellow oil (63%, 140.3 mg); $^1\text{H-NMR}$: δ (ppm) 3.91 (s, 3H, $-\text{OCH}_3$), 7.02 – 6.96 (m, 2H, H_f , H_d), 7.53 (t, $J = 7.6$ Hz 1H, H_e), 7.80 (d, $J = 7.8$ Hz, 1H, H_c), 10.45 (s, 1H, $-\text{CHO}$) (**Figure A-1**); $^{13}\text{C-NMR}$ (CDCl_3): δ (ppm) 55.6 ($-\text{OCH}_3$), 111.6 (C_f), 120.6 (C_d), 124.7 (C_b), 128.4 (C_c), 135.9 (C_e), 161.8 (C_a), 189.8 ($\text{C}=\text{O}$) (**Figure A-2**); ν_{max} (cm^{-1}): 1725 ($\text{C}=\text{O}$ st), 1687 ($\text{C}=\text{C}$ st), 1247 ($\text{C}-\text{O}$ st) (**Figure A-3**); MS^{++}H^+ : $m/z = 136.9$ (**Figure A-4**).

3.3.2 Synthesis of *meso*-tetrakis(2-methoxyphenyl)porphyrin (**3**)

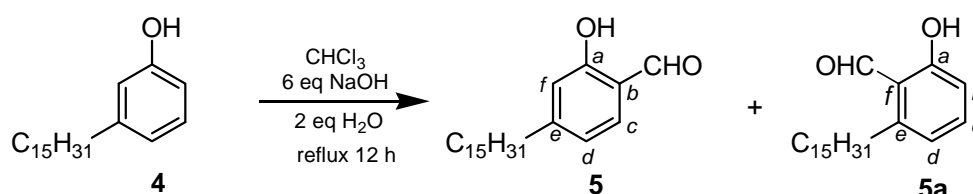


Following a general procedure [62], a solution of 2-methoxybenzaldehyde (100.0 mg, 0.734 mmol) in CHCl_3 (73 mL) was treated with pyrrole (49.86 μL , 0.734 mmol). The mixture was degassed with N_2 for 10 min, then $\text{BF}_3 \cdot \text{OEt}_2$ (34.40 μL , 0.242 mmol) was added and the resulting mixture was stirred for 60 min, the solution instantly darkened. DDQ (124.8 mg, 0.552 mmol) was added and stirred at room temperature for 60 min. The reaction mixture was filtered through a pad of silica and then chromatographed (silica, CH_2Cl_2), affording a purple solid (54.8 mg, 40%). m.p. > 300 °C; $^1\text{H-NMR}$: δ (ppm): δ (ppm) -2.63 (br. s, 2H, N-H), 3.61, 3.58, 3.55 (3s, 12H, -OCH₃), 7.33 (m, 8H, H_c, H_a), 7.74 (t, $J = 7.8$ Hz, 4H, H_b), 7.93, 7.99, 8.04 (3d, $J = 7.2$ Hz, 4H_d), 8.7 (s, 8H, H_g, H_h) (**Figure A-5**); $^{13}\text{C-NMR}$ (CDCl_3): δ (ppm) 55.9 (-OCH₃), 110.9 (C_a), 115.6 (C_i), 129.7 (C_c), 130.5 (C_g), 131.2 (C_e), 135.6 (C_d), 159.5 (C_f) (**Figure A-6**); ν_{max} (cm^{-1}) 3317 (N-H st), 1607 (C=C st), 1262 (C-O st) (**Figure A-7**) MALDI-MS: m/z 734.7 (**Figure A-8**); λ_{abs} 419, 514, 550, 589, 644 nm (**Figure B-1**); λ_{em} ($\lambda_{\text{ex}} = 550$ nm) 648, 713 nm (**Figure B-5**).

Part 2 Synthesis of porphyrin derivative from hydrogenated cardanol

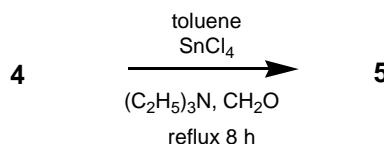
3.3.3 Synthesis of 2-hydroxy-4-pentadecylbenzaldehyde (5)

3.3.3.1 Formylation of hydrogenated cardanol (4) using Reimer-Tiemann reaction



Following a standard procedure [63], to a solution of hydrogenated cardanol (4) (3.045 g, 0.010 mol) in CHCl_3 (30 mL) was added sodium hydroxide (2.400 g 0.060 mol) and water (0.360 mL, 0.020 mol). The reaction was refluxed for 12 h under N_2 . After cooling to room temperature, the reaction mixture was then treated with water (20 mL). The aqueous layer was acidified to pH 1 with 1N HCl and the organic layer was collected. The aqueous layer was extracted with ethyl acetate (2x20 mL). The combined organic extracts were washed with brine, dried over anhydrous sodium sulfate and filtered. Then, ethyl acetate was removed by vacuum to obtain crude product that was purified by column chromatography (silica, hexane). The product from fraction 1 was characterized by $^1\text{H-NMR}$ showed very complicate signals that might arise from two isomers (**Figure A-13**).

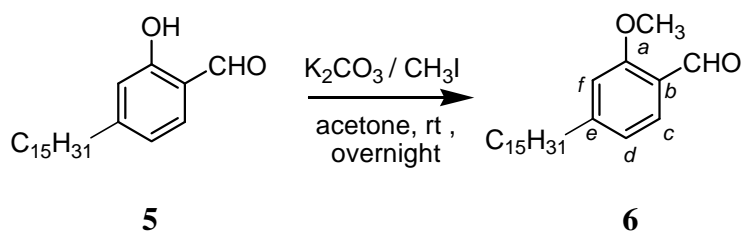
3.3.3.2 Condensation of hydrogenated cardanol with paraformaldehyde



Following a published procedure [64], to a solution of hydrogenated cardanol (3.045 g, 0.010 mol) in anhydrous toluene (20 mL) was added triethylamine (0.550 mL, 0.004 mol) and tin(IV)tetrachloride (115.0 μL , 0.001 mol). The mixture reaction was stirred for 20 min at room temperature under N_2 and then paraformaldehyde (0.658 g, 0.022 mol) was added. The mixture solution was heated at 100 $^\circ\text{C}$ for 8 h. After cooling down to room temperature, the reaction mixture was poured into water

and acidified to pH 2 with 10% HCl. The organic layer was collected and the aqueous layer was extracted with ethyl acetate. The organic phase was combined, dried over anhydrous sodium sulfate, filtered and concentrated to dryness. The resulting crude product was purified by chromatography (silica, hexane) to give white crystals, (2.99 g, 89%), m.p. 41-42 °C (lit. 52-54°C [51]); $^1\text{H-NMR}$: δ (ppm) 0.87 (t, 3H, $-\text{CH}_3$), 1.0 – 1.7 (m, 26H, $-\text{CH}_2-$), 2.60 (t, 2H, Ar- CH_2), 6.80 (s, 1H, H_f), 6.83 (d, $J = 7.8$ Hz, 1H, H_d), 7.44 (d, $J = 7.8$ Hz, 1H, H_c), 9.83 (s, 1H, $-\text{CHO}$), 11.04 (s, 1H, $-\text{OH}$) (**Figure A-9**); $^{13}\text{C-NMR}$: δ (ppm) 14.1 – 36.4 (sp^3 carbon), 109.7 (C_f), 117.1 (C_d), 120.5 (C_b), 133.5 (C_c), 153.8 (C_e), 161.8 (C_a), 195.8 ($-\text{C}=\text{O}$) (**Figure A-10**); ν_{max} (cm^{-1}) 3447 (O – H st) 2917 (C – H st) 1655 (C=O st) 1454 (C=C st) 1257 (C – O st) (**Figure A-11**); MS-H^+ : $m/z = 331.3$ (**Figure A-12**).

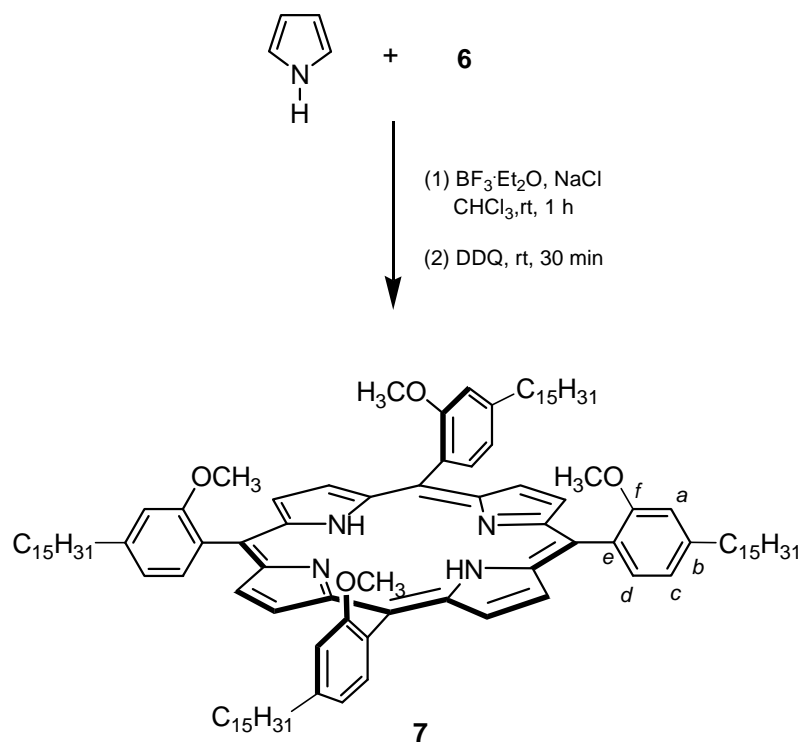
3.3.4 Synthesis of 2-methoxy-4-pentadecylbenzaldehyde (6)



Compound **5** (200.0 mg, 0.577 mmol) dissolved in acetone (5 mL) was treated with potassium carbonate (114.4 mg, 0.692 mmol) in a 50-mL round bottom flask. The mixture was stirred at room temperature for 10 minutes, and then iodomethane (43.07 μL , 0.692 mmol) was added. The reaction mixture was stirred until no more substrate was found by TLC monitoring (about 14 hours). The mixture was washed with distilled water (2x20 mL) and extracted with ethyl acetate (2x20 mL) in a separating funnel. The organic phase was separated, dried over anhydrous sodium sulfate and filtered. After the removal of solvent, the resulting crude product was purified by column chromatography (silica, hexane) to give white crystals (162 mg, 78%) m.p. 39-40°C; $^1\text{H-NMR}$: δ (ppm) 0.87 (t, 3H, $-\text{CH}_3$), 1.62 – 1.20 (m, 26H, $-\text{CH}_2-$), 2.62 (t, $J = 7.7$ Hz, 2H, Ar- CH_2-), 3.90 (s, $-\text{OCH}_3$), 6.76 (s, 1H, H_f), 6.82 (d, $J = 7.8$ Hz, 1H, H_d), 7.72 (d, 1H, $J = 7.8$ Hz, H_c), 10.3 (s, 1H, $-\text{CHO}$) (**Figure A-14**); $^{13}\text{C-NMR}$: δ (ppm) 14.1-36.7 (sp^3 carbons), 55.5 ($-\text{OCH}_3$), 111.5 (C_f), 120.9 (C_d), 122.7 (C_b) 128.6 (C_c), 152.4 (C_e), 161.9 (C_a), 189.5 ($-\text{C}=\text{O}$), (**Figure A-15**); ν_{max} (cm^{-1})

2911 (C-H st), 1674 (C=O st), 1564 (C=C st), 1186 (C-O st) (**Figure A-16**); $MS+H^+$: $m/z = 347.2$ (**Figure A-17**).

3.3.5 Synthesis of *meso*-tetrakis(2-methoxy-4-pentadecylphenyl)porphyrin (**7**)



3.3.5.1 Effect of acid-catalysis on the porphyrin formation

The reaction conditions for the synthesis **7** were varied by types and concentration of acid-catalysts (Table 3-1).

Table 3-1 Condition for the synthesis of Compound **7**

Entry	[pyrrole] (mM)	[ArCHO] (mM)	catalyst	concentraion (mM)	solvent	[DDQ] (mM)
1	10	10	$BF_3 \cdot OEt_2/NaCl/EtOH$	1.0/250	$CHCl_3$	7.5
2	10	10	$BF_3 \cdot OEt_2/TFA$	0.32/15	CH_2Cl_2	7.5
3	10	10	TFA	10	CH_2Cl_2	7.5

3.3.5.2 Effect of time on the formation of porphyrin

Following a published procedure [65], to monitor the progress of the reaction, aliquots were periodically removed from reaction bottom via syringe and injected into an oxidizing solution. The oxidation of porphyrinogen to porphyrin occurs almost instantaneously. The yield of porphyrinogen at any point in the condensation is taken to be equal to the yield of porphyrin formed upon oxidation. The particular 2 μ L aliquots were taken from a reaction vessel via syringe and injected into 300 μ L of a 10^{-2} M solution DDQ in toluene. This solution was diluted in 3 mL of $\text{CH}_2\text{Cl}_2/\text{EtOH}$ (3:1 mL) and visible spectra were recorded every 5 min for 45 min reaction time.

3.3.5.3 Synthesis of Compound 7 under optimized condition

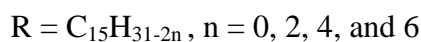
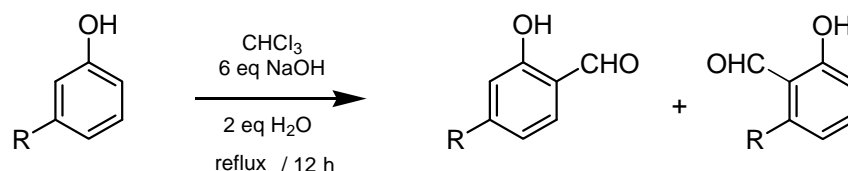
Compound **7** was synthesized under optimized condition following the procedure below:

A solution of **6** (200.0 mg, 0.577 mmol) in CHCl_3 (58 mL) was treated with pyrrole (38.71 μ L, 0.577 mmol). The mixture was degassed with N_2 for 10 min, then $\text{BF}_3 \cdot \text{OEt}_2$ (24.13 μ L, 0.190 mmol) was added and the resulting mixture was stirred for 10 min, when the solution instantly darkened. DDQ (98.52 mg, 0.434 mmol) was added and stirred at room temperature for 60 min. The reaction mixture was filtered through a pad of silica and then chromatographed (silica, CH_2Cl_2). Crystallization from hexane/ CHCl_3 furnished a purple solid. (80 mg, 35%); $^1\text{H-NMR}$: δ (ppm) -2.63 (br. s, 2H, N-H), 2.92 (t, $J = 7.7$ Hz, 8H, Ar- CH_2 -), 3.58, 3.55, 3.52 (3s, 12H, $-\text{OCH}_3$), 7.12 (m, 8H, H_c , H_a), 7.82, 7.86, 7.91 (3d, $J = 7.2$ Hz, 4 H_d), 8.7 (s, 8H, H_g , H_h) (**Figure A-18**); $^{13}\text{C-NMR}$: δ (ppm) 36.5-14.1 (sp^3 carbon), 55.8-53.4 ($-\text{OCH}_3$), 111.1 (C_a), 115.5 (C_i), 119.3 (C_c), 128.5 (C_g), 130.9 (C_e), 135.4 (C_d), 144.7 (C_f) (**Figure A-19**); ν_{max} (cm^{-1}) 3314 (N-H st), 2920 (C-H st) 1607 (C=C st), 1262 (C-O st) (**Figure A-20**); MALDI-MS: m/z 1576.4 (**Figure A-21**); λ_{abs} 420, 512, 546, 589, 645 nm (**Figure B-2**); λ_{em} ($\lambda_{\text{ex}} = 550$ nm) 652, 717 nm. (**Figure B-6**).

Part III: Synthesis of porphyrin derivatives from non-hydrogenated cardanol

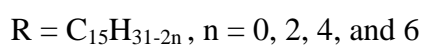
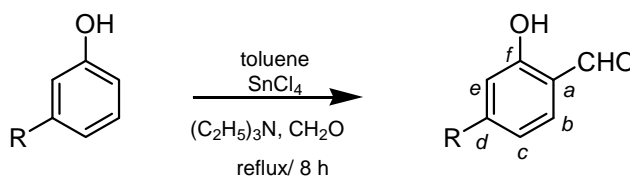
3.3.6 Synthesis of 2-hydroxy-4-alkenylbenzaldehyde (5-1)

3.3.6.1 Formylation of non-hydrogenated cardanol using Reimer-Tiemann reaction



Following a standard procedure [63], to a solution of cardanol (2.98 g, 0.01 mol) in $CHCl_3$ (30 ml) was added sodium hydroxide (2.40 g, 0.06 mol) and water (0.36 mL, 0.02 mol). The reaction was refluxed for 12 h under N_2 . After cooling to room temperature, the reaction mixture was then treated with water (20 mL). The aqueous layer was acidified to pH 1 with 1N HCl and the organic layer was collected. The aqueous layer was extracted with ethyl acetate (2x20 mL). The combined organic extracts were washed with brine, dried over anhydrous sodium sulfate and filtered. Then, ethyl acetate was removed by vacuum to obtain crude product that was purified by column chromatography (silica, hexane) to give pale yellow oil. The product from fraction 1 was characterized by 1H -NMR showed very complicate signals that might arise from two isomers (**Figure A-22**).

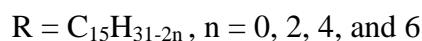
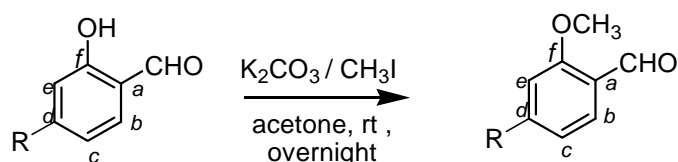
3.3.6.2 Condensation of non-hydrogenated cardanol with paraformaldehyde



Following a published procedure [64], to a solution of cardanol (2.98 g, 10.0 mol) in anhydrous toluene (20 mL) was added triethylamine (0.55 mL, 4.00 mmol)

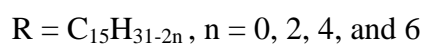
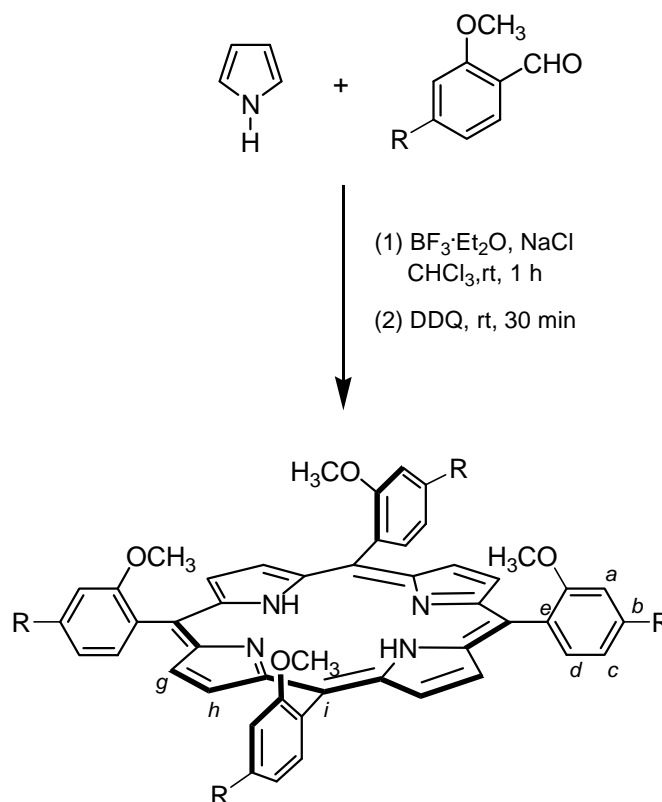
and tin(IV)tetrachloride (115 μ L, 1.00 mmol). The mixture reaction was stirred for 20 min at room temperature under N_2 and then paraformaldehyde (0.66 g, 0.022 mol) was added. The mixture solution was heated at 100 $^{\circ}$ C for 8 h. After cooling down to room temperature, the reaction mixture was poured into water and acidified to pH 2 with 10% HCl. The organic layer collected and the aqueous layer extracted with ethyl acetate. The organic phase was separated, dried over anhydrous sodium sulfate, filtered and concentrated to dryness. The resulting crude product was purified by chromatography (silica, hexane) to give a pale yellow oil; 1H -NMR: δ (ppm) 0.80 – 2.10 (m, $-CH_2$, $-CH_3$), 2.60 (t, $J= 7.7$ Hz, Ar- CH_2), 2.80 (m, $=C-CH_2$), 5.0, 5.4, 5.8 (m, $C=CH$), 6.79 (s, H_e) 6.82 (d, $J=7.9$ Hz, H_c), 7.43 (d, $J=7.9$ Hz, H_b) 9.81 (s, $-CHO$), 11.04 (s, $-OH$) (**Figure A-23**).

3.3.7 Synthesis of 2-methoxy-4-alkenylbenzaldehyde (6-1)



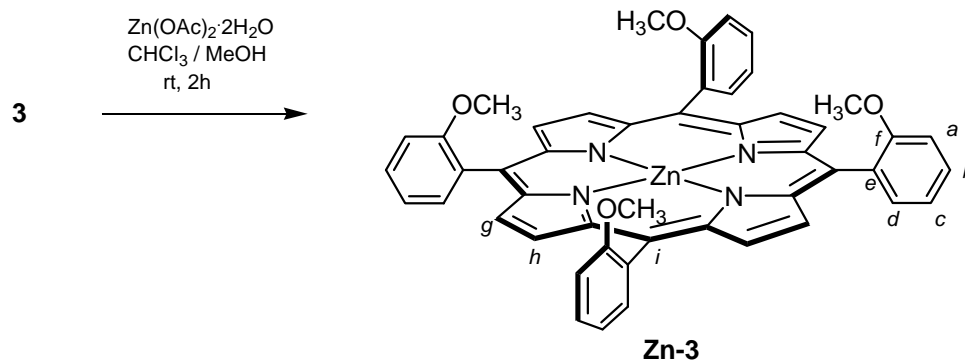
Compound **3-1** (200.0 mg, 0.612 mmol) dissolved in acetone (5 mL) was treated with potassium carbonate (121.5 mg, 0.734 mmol) in a 50-mL round bottom flask. The mixture was stirred at room temperature for 10 minutes, and then iodomethane (45.68 μ L, 0.734 mmol) was added. The reaction mixture was stirred until no more substrate was found by TLC monitoring (about 14 hours). The mixture was washed with distilled water (2x20 mL) and extracted with ethyl acetate (2x20 mL) in a separating funnel. The organic phase was separated, dried over anhydrous sodium sulfate and filtered. After the removal of solvent, the resulting crude product was purified by column chromatography (silica, hexane) to give a pale yellow oil; 1H -NMR: δ (ppm) 0.80 – 2.10 (m, $-CH_2$, $-CH_3$), 2.63 (t, $J= 7.7$ Hz, Ar- CH_2), 2.80 (m, $=C-CH_2$), 3.91 (s, OCH_3), 5.0, 5.4, 5.8 (m, $C=CH$), 6.77 (s, H_e), 6.83 (d, $J=7.8$ Hz, H_c), 7.73 (d, $J=7.8$ Hz, H_b), 10.40 (s, $-CHO$) (**Figure A-24**).

3.3.8 Synthesis of *meso*-tetrakis(2-methoxy-4-alkenylphenyl)porphyrin(7-1)



A solution of 2-methoxy-4-alkenylbenzaldehyde (100 mg, 0.29 mmol) in CHCl_3 (29 mL) was treated with pyrrole (20.3 μL , 0.29 mmol). The mixture was degassed with N_2 for 10 min, then $\text{BF}_3 \cdot \text{OEt}_2$ (13.8 μL , 0.09 mmol) was added and the resulting mixture was stirred for 60 min, the solution instantly darkened. DDQ (50.1 mg, 0.22 mmol) was added and stirred at room temperature for 60 min. The reaction mixture was filtered through a pad of silica and then chromatographed (silica, CH_2Cl_2), affording a purple solid; $^1\text{H-NMR}$: δ (ppm) -2.69 (br. s, N-H), 3.45, 3.48, 3.52 (3s, -OCH₃), 8.7 (s, 8H, H_g, H_h) (**Figure A-25**).

3.3.9 Synthesis of *meso*-tetrakis(2-methoxyphenyl)porphyrinatozinc(II)(Zn-3)



A solution of **3** (100.0 mg, 0.136 mmol) in CHCl_3 (60 mL) was treated with $\text{Zn(OAc)}_2 \cdot \text{H}_2\text{O}$ (149.3, 0.680 mmol) in methanol (3 mL) at room temperature for 2 h. The reaction mixture was washed with water, dried (Na_2SO_4) and concentrated to dryness. Chromatography (silica, CHCl_3) afforded a purple solid (102 mg, 93%). m.p $>300^\circ\text{C}$; $^1\text{H-NMR}$: δ (ppm) 3.60, (s, 12H, $-\text{OCH}_3$), 7.31, 7.32, 7.33, 7.35 (m, 8H, H_c , H_a), 7.73, 7.75, 7.77 (t, $J = 7.9$ Hz, 4H, H_b), 7.98 – 8.01 (m, 4 H_d), 8.81 (s, 8H, H_g , H_h) (**Figure A-26**); ν_{max} (cm^{-1}) 2932 and 2826 (C – H st), 1631 (C=C st), 1247 (C–O st), (**Figure A-27**); MALDI-MS: m/z 734.7 (**Figure A-28**); λ_{abs} 419, 547 nm (**Figure B-3**); λ_{em} ($\lambda_{\text{ex}} = 550$ nm) 645 nm (**Figure B-4**).

3.3.10 Use of fluorescent marker in varied oil refinery

The fluorescent property of a solution of compound **7** in 6 diesel samples from the following oil refineries was determined:

- PTT Public Company Limited
- Bangchak petroleum public company Limited
- Petroliam Nasional Berhad (Petronas)
- Exxon Mobil Corporation (Esso)
- Caltex Oil (Thailand) Limited
- Verasuwan oil refinery

Compound **7** was blended in diesels at the concentration of 1 ppm and the resulting marked diesels were taken into the fluorescence with the following parameters:

- The wavelength of the excitation monochromator (λ_{ex}) was set at 420 nm.
- The response was set for one second.
- The photomultiplier tube voltage level (PMT Grain) was set at medium level.
- The spectrum bandwidth of the emission monochromator (Em SBW) was set at 10.
- The spectrum bandwidth of the excitation monochromator (Ex SBW) was set at 10.

3.3.11 Preparation of stock solution of fluorescent marker **7**

Each 500 ppm stock fluorescent marker solution was prepared by dissolving 25 mg of compound **7** in diesel and made up to 50 mL in a volumetric flask.

3.3.12 Quantitative determination of fluorescent markers in diesel fuels

Quantitative determination of fluorescent marker **7** in diesel was carried out by a spectrofluorometer. A standard calibration curve of **7** in diesel was prepared at concentration from 0 - 10 ppm by pipetting the stock solution into a 50 mL volumetric flask and made up the volume with diesel. The volume of the stock solution used to prepare each calibration solution is shown in Table 3-2.

Table 3-2 The volume of the stock solution (500 ppm) used to prepare 0-10 ppm fluorescent marker in diesel

Concentration (ppm)	Volume of 500 ppm stock solution (mL)
0	0
2	0.2
4	0.4
6	0.6
8	0.8
10	1.0

The quantitative determination of fluorescent markers in diesel was recorded in a spectrofluorometer (**Figure B-9**). The calibration curve was plotted between intensity (y-axis) and the concentration (x-axis) of fluorescent markers in diesel (**Figure B-10**).

3.3.13 Stability test of fluorescent marker in diesel fuel

To evaluate the stability of marker **7**, the quantity of **7** blend in diesel was determined monthly for 3 months by the following procedure:

Compound **7** in diesel stock solution with the concentration of 2 and 5 ppm was placed into a 5 mL vial and stored for 3 months in ambient environment. The solution from the vials was directly taken into the measurement after 1, 2 and 3 months. The quantity of fluorescent marker contained in diesel was measured by spectrofluorometer with the same measuring parameters as mentioned in section 3.3.6 with an exception that was set as 512 nm.

3.3.14 Effect of fluorescent markers on the physical properties of diesel fuel

A diesel sample employed in this study was obtained from PTT Public Company Limited. Physical properties of marked and unmarked diesel were investigated according to the ASTM method described in Table 3-3.

Table 3-3 The ASTM testing methods of diesel

Test items	Test method ASTM
API gravity @ 60 °C	D 4052
Specific gravity @ 15.6°C	D 4052
Density	D 5002
Calculated Cetane Index	D 976
Kinematic viscosity @ 40°C	D 445
Pour point , °C	D 97
Flash point, °C	D 93
Sulfur content, %wt	D 4294
Distillation	D 86
Color	D 1500

Cetane Index (CI)

Cetane Index is an estimated value, generally calculated from fuel density and volatility. According to the method D 976 by ASTM however, the Cetane Index is calculated by using density and three distillation points as shown below:

$$CI = 454.74 - 1641.146 D + 774.74 D^2 - 0.554 B + 97.803 (\log B)^2$$

D = Density at 15 °C, g/mL

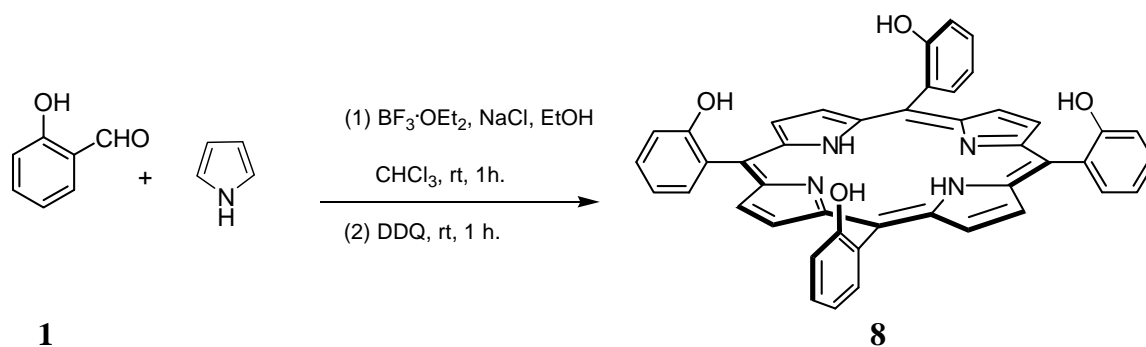
B = 50% vol. Distillation, °C

CHAPTER IV

RESULTS AND DISCUSSION

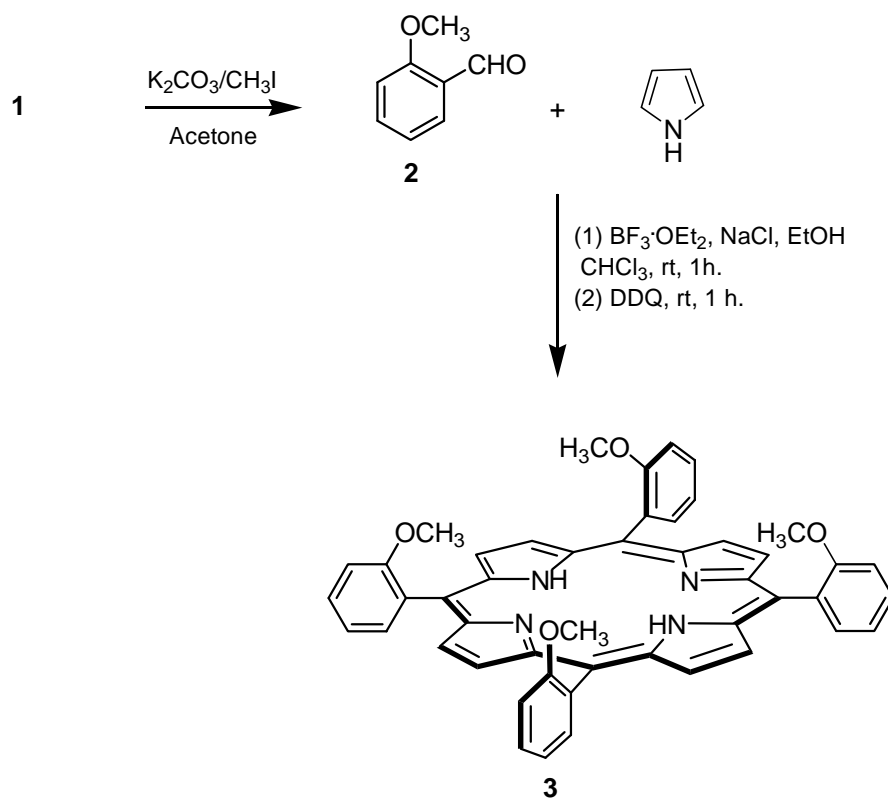
4.1 Porphyrin model

An attempt to synthesize of *meso*-tetrakis(2-hydroxyphenyl)porphyrin (**8**) was pursued by condensation of salicylaldehyde (**1**) with pyrrole in EtOH-containing CHCl₃ using BF₃·OEt₂ in the presence of NaCl, followed by oxidation with DDQ (Scheme 4-1). Reaction crude was found difficult to purify and, according to the UV-Vis absorption, minimal porphyrinic product was observed. This could be attributed to the partial oxidation of phenolic moieties of the porphyrin product **8** by reactive DDQ.



Scheme 4-1 Synthesis of *meso*-tetrakis(2-hydroxyphenyl)porphyrin.

To avoid the above problem the sensitive –OH group of **1** was protected as –OMe group by reacting **1** with K₂CO₃/CH₃I in acetone leading to compound **2**. Condensation of **2** with pyrrole in CHCl₃ (containing 0.13 M ethanol) using BF₃·OEt₂ in the presence of NaCl followed by oxidation with DDQ afforded porphyrin **2** in 40% yield (Scheme 4-2).

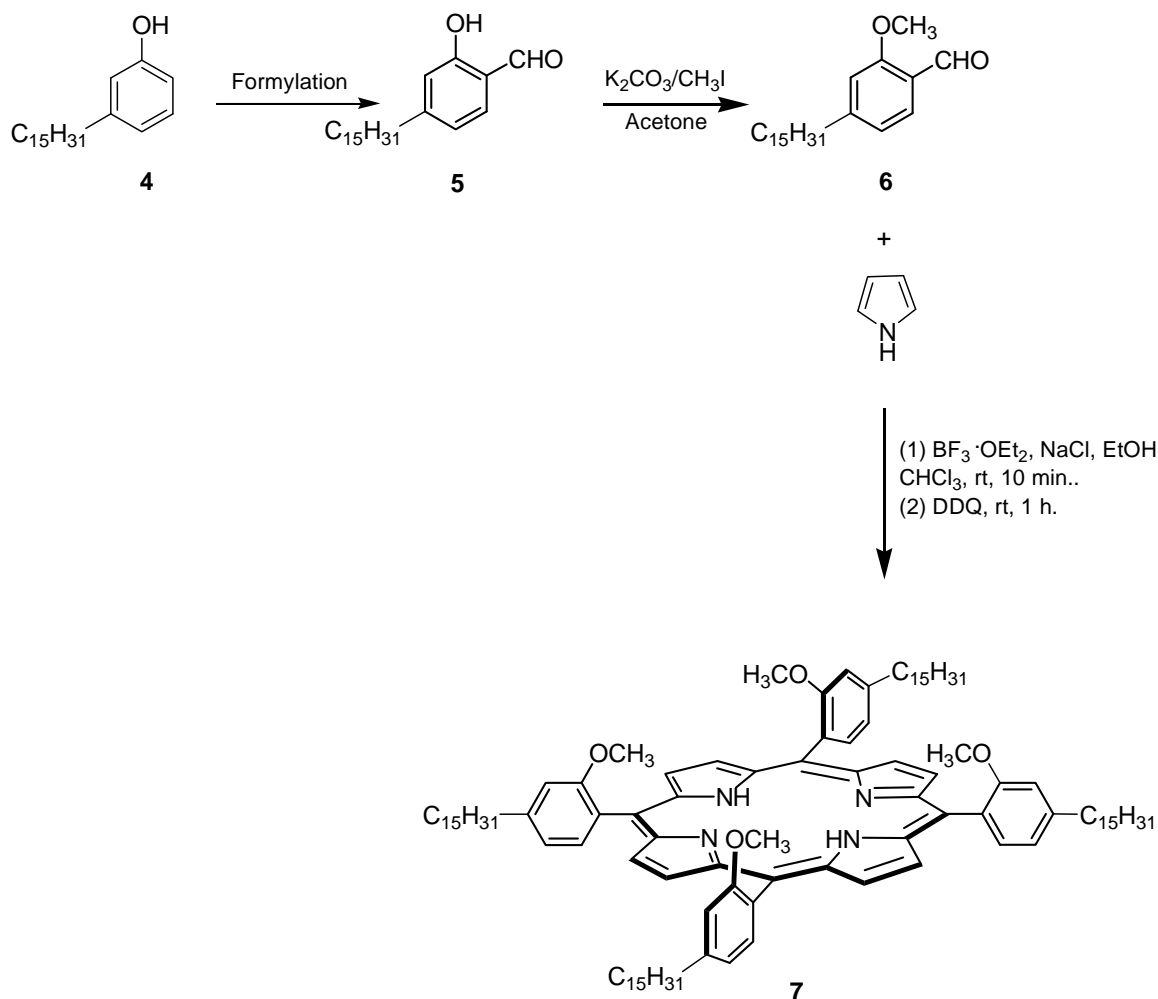


Scheme 4-2 The synthesis of *meso*-tetrakis(2-methoxyphenyl)porphyrin.

From 1H -NMR spectrum, a characteristic signal of inner protons of porphyrin **3** appears as a singlet at δ -2.63 ppm and the signal of aldehyde proton disappeared (**Figure A-5**). Regards the UV-Vis spectrum (**Figure B-1**), the porphyrin was confirmed by the presence of a typical strong Soret band at 419 nm arising from the transition of $a_{1u}(\pi) - e_g^*(\pi)$ and four Q bands at 514, 550, 589 and 643 nm corresponding to the $a_{2u}(\pi) - e_g^*(\pi)$ transition.

4.2 Porphyrinic derivatives **7** from hydrogenated cardanol

The synthesis started from formylation of hydrogenated cardanol **4** followed by protection of a hydroxyl group of the resulting aldehyde **5** (Scheme 4-3). Compound **6** was then condensed with pyrrole with the catalysis of $\text{BF}_3 \cdot \text{OEt}_2 / \text{NaCl} / \text{EtOH}$ and underwent subsequent DDQ-oxidation to give the desired porphyrin **7**. Preparation of precursors **5** and **6**, as well as the porphyrin product **7** was described in detail below.



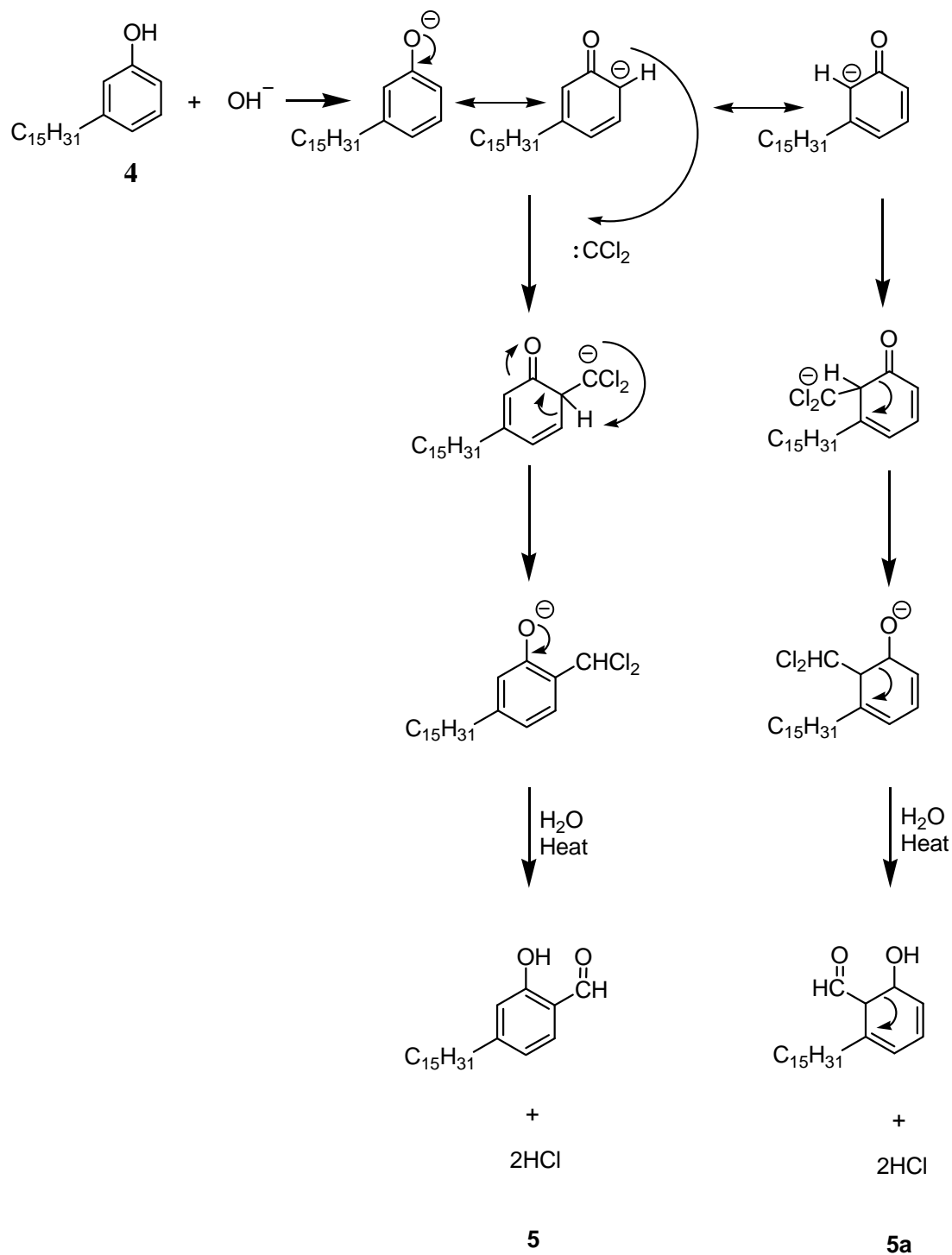
Scheme 4-3 The total synthesis of Compound **7**.

4.2.1 Synthesis of 2-hydroxy-4-pentadecylbenzaldehyde

Two methods were employed for the preparation of the aldehyde **5**: by the Reimer-Tiemann reaction [53] and adaptation from a formylation method [54].

4.2.1.1 Reimer-Tiemann reaction

In general formylation of hydrogenated cardanol using a Reimer-Tiemann process to produce 2-hydroxy-4-pentadecylbenzaldehyde was carried out by warming hydrogenated cardanol with CHCl_3 and aqueous alkali solution. The proposed mechanism is shown in Scheme 4-4.

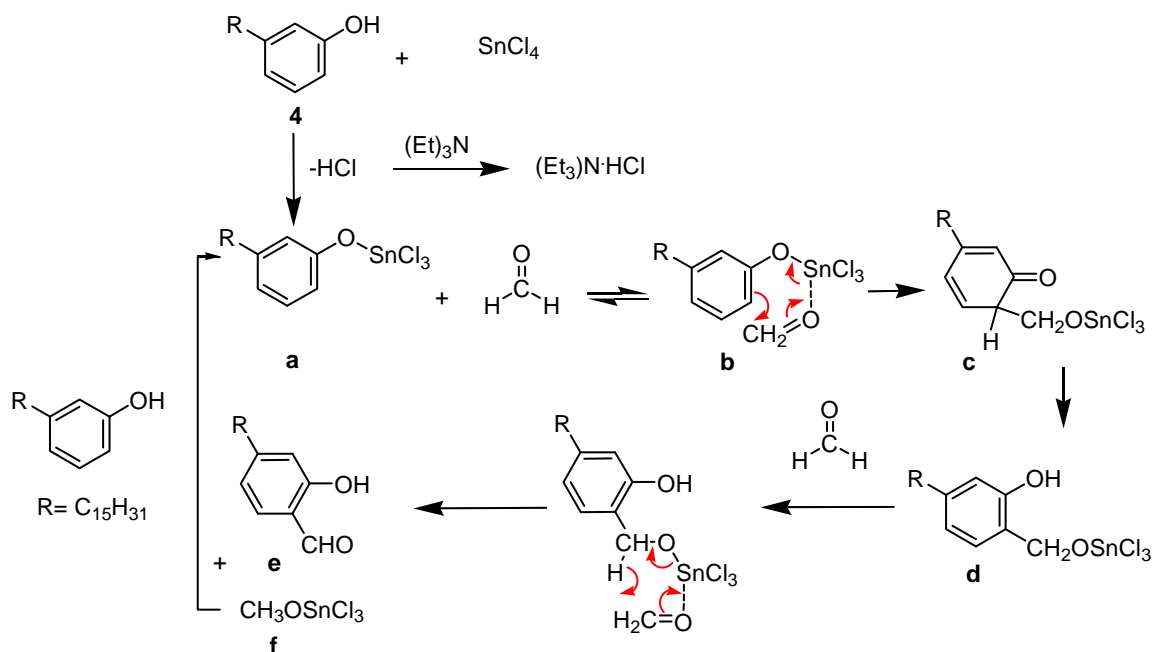


Scheme 4-4 Proposed mechanism of Reimer-Tiemann formylation.

The Reimer-Tiemann reaction generated two isomers of aldehyde: 2-hydroxy-4-pentadecylbenzaldehyde (**5**) as the major product and 2-hydroxy-6-pentadecylbenzaldehyde (**5a**) is formed as the minor product. This is explicable in terms of the two dienones believed to be intermediates, although steric hindrance restricts the formation of the minor product and this effect is magnified with longer chain alkyl group. Two isomers were always found as a mixture and their clear separation has not yet been achieved. The crude product showed 39.04% total yield. From $^1\text{H-NMR}$ spectral analysis, the signal of phenolic hydroxyl protons were appeared as 2 singlets at δ 9.82 and 11.04 ppm and the signal of carbonyl groups were appeared as 2 singlets at δ 10.23 and 11.93 ppm. From the integration of $^1\text{H-NMR}$, the ratio of major and minor product was 3:1. Thus the major **5** and minor **5a** product were about 30% and 10% yield respectively. However, both isomers of aldehyde could be used as starting materials for the synthesis of porphyrin derivatives but the major product **5** is likely to be more reactive than the minor product **5a** as having weaker steric effect.

4.2.1.2 *Ortho*-formylation of hydrogenated cardanol with paraformaldehyde

In this approach, cardanol **4** in toluene containing tri(*n*-butyl)amine and tin(IV)tetrachloride was allowed to react with paraformaldehyde [50]. The mechanism was shown in Scheme 4-5.



Scheme 4-5 The mechanism pathway of the tin(IV)tetrachloride+triethylamine-catalysed condensation of cardanol and paraformaldehyde.

Initially the cardanol **4** reacted with tin(IV)chloride giving the phenoxide intermediate. The resulting hydrogen chloride which could bring about uncontrolled acid catalyzed cardanol-formaldehyde condensation is trapped by the triethylamine. The second stage is the interaction between **a** and formaldehyde giving an active oriented complex **b**, in which the metal atom serves as a link between the reaction partners. Such interaction has probably two main consequences: (i) simultaneous activation of both reaction partners (formaldehyde by co-ordination with the metal atom and cardanol by enhancing nucleophilicity of the nucleus itself) and (ii) orientation and close contact of partners enabling the formaldehyde to enter easily into the *ortho*-position of the phenolic ring. The subsequent intramolecular collapse of **b** leads to **d** probably *via* the dienone **c**. The next stage apparently involve a redox process between the cardanol and formaldehyde to cardanol derivative **e** and tin(IV) methoxide **f**. The last stage of the proposed catalytic cycle is considered to be the alcoholysis of **f** with **4** leading to methanol with re-formation of the active species **b**.

From this reaction, compound **5** was produced in the yield up to 89%. Regards ^1H -NMR spectral analysis, the signal of phenolic hydroxyl proton of **5** appeared as a singlet at δ 11.04 ppm (lit. 10.94 ppm [54], **Figure A-9** in Appendix A) indicating that the molecule bears intramolecular hydrogen bond between hydroxyl hydrogen and formyl oxygen atom.

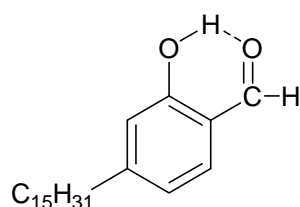


Figure 4-1 Intramolecular hydrogen bond of Compound **5**

4.2.2 Synthesis of 2-methoxy-4-pentadecylbenzaldehyde (**6**)

Compound **5** was methylated by using potassium carbonate and iodomethane in basic condition to provide **6** in 65% yield. From ^1H -NMR spectral analysis, the signal of intramolecular hydrogen bond with carbonyl group was absent and a singlet signal of methoxy group proton at δ 3.90 ppm showed up instead (**Figure A-13** in Appendix A).

4.2.3 Synthesis of *meso*-tetrakis(2-methoxy-4-pentadecylphenyl)porphyrin (7)

The synthesis of **7** was successfully performed by using 2-methoxy-4-pentadecylbenzaldehyde (**6**) as aldehyde precursor with pyrrole in CHCl₃ (containing 0.13 M ethanol) using BF₃·OEt₂ in the presence of NaCl followed by oxidation with DDQ, affording porphyrin **7** in 15% yield.

4.2.3.1 Optimization of reaction condensation for porphyrin formylation.

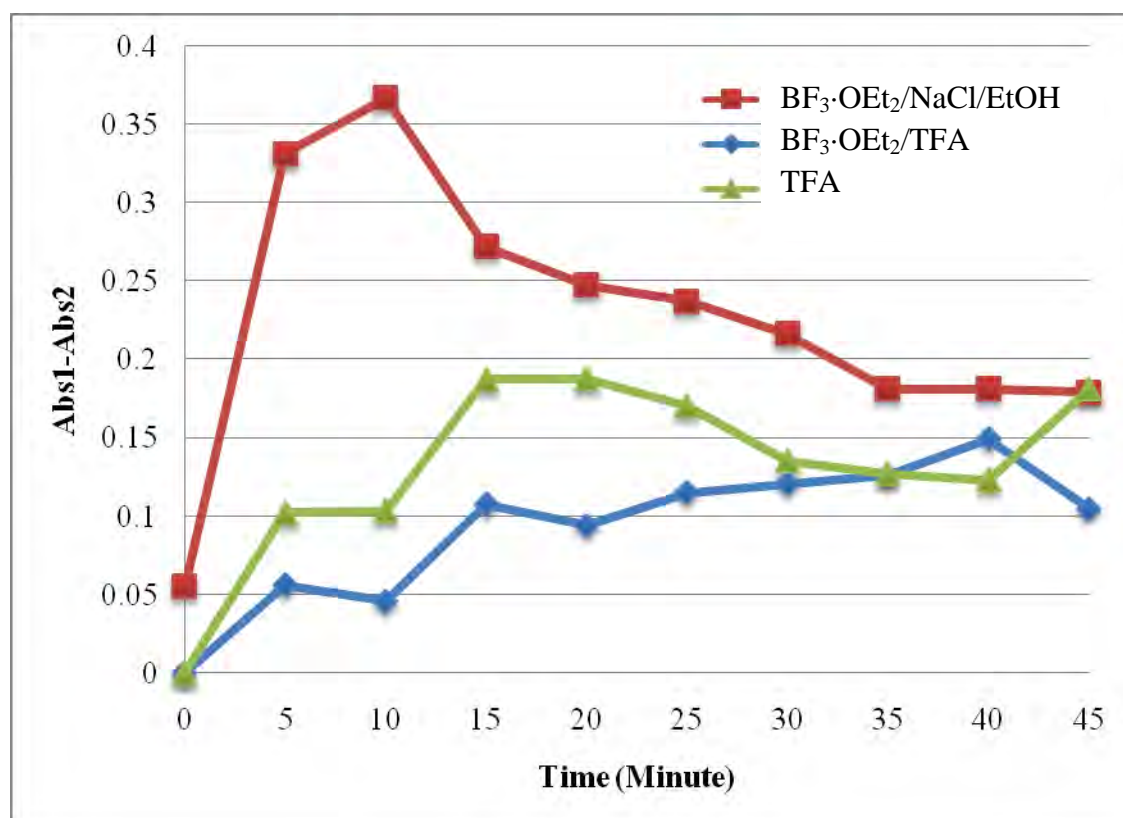
The overall rate of reaction and ultimate yield of porphyrin is dependent on the concentration of the reactants, the nature of the acid catalyst, and on the concentration of the acid [66]. Obtaining a maximum yield of porphyrin required careful monitoring of the reaction “trajectory” so that oxidation, the second step of the porphyrin-forming process (which terminate all condensation processes), could be initiated at the appropriate time [66].

To monitor the progress of the reaction, aliquots were periodically removed from reaction mixture by syringe and injected into an oxidizing solution. The oxidation of porphyrinogen to porphyrin occurs almost instantaneously. The yield of porphyrinogen at any point in the condensation is taken to be equal to the yield of porphyrin form upon oxidation. Absorbance were recorded by UV-visible spectrometer and the yield of this condition were compared spectroscopically [67].

The conditions described in Table 4-1 were used for synthesis of porphyrin bearing branched alkyl groups at the *meso* positions [62]. Acid screening experiments were performed using the following acid catalysts and yields of each experiment are summarized as follows:

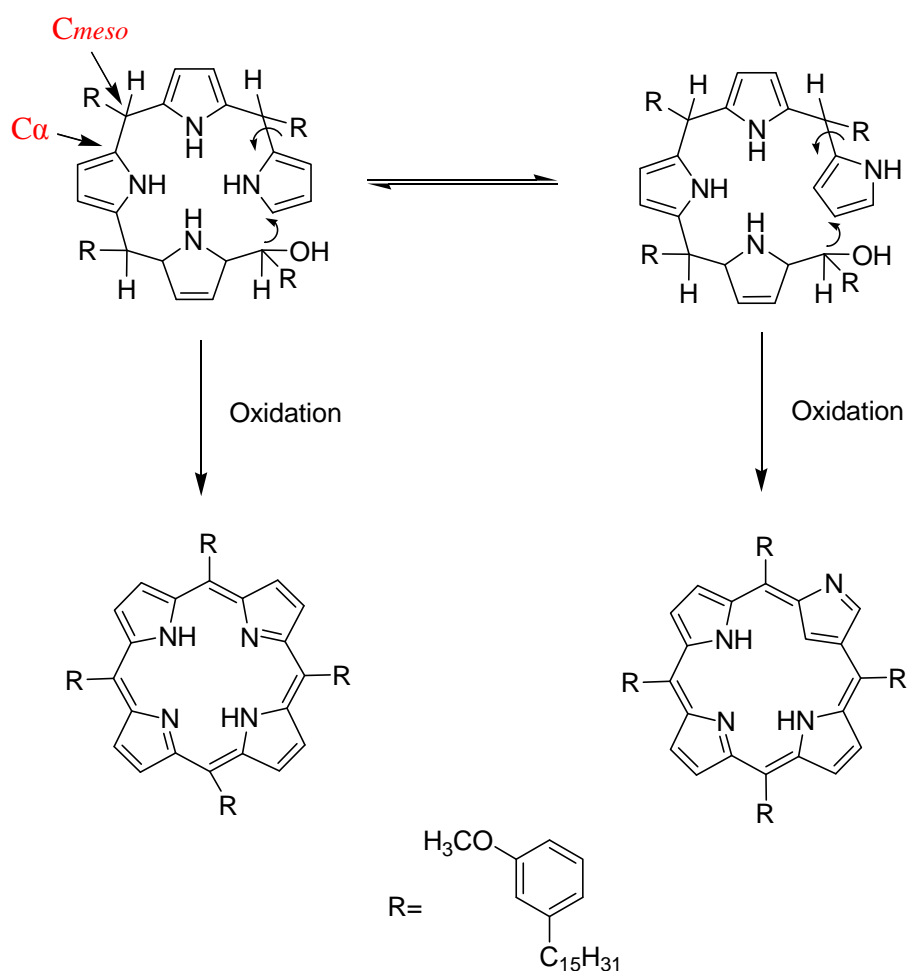
Table 4-1 Condition for the synthesis of Compound 7

Entry	catalyst	concentration (mM)	Reaction time (min)	% yield
1	BF ₃ ·OEt ₂ /NaCl/EtOH	1.0/250	10	35
2	BF ₃ ·OEt ₂ /TFA	0.32/15	40	6
3	TFA	10	55	28

**Figure 4-2** Effect of acid catalyst on the time-course of porphyrin 7 formation

These results showed that the rate of formation of the porphyrinogen is dependent on type of acid catalyst. From Figure 4-2, the condition was found optimal for BF₃·OEt₂/NaCl/EtOH with the reaction time of 10 min. In this condition, BF₃·OEt₂ serves as Lewis acid catalyst which coordinated with carbonyl group to increase reactivity of aldehyde of methoxy cardanol (electrophile). According to the previous study [25], NaCl was used as metal template to perform porphyrinogen because size of Na⁺ is fitted to the cavity of porphyrinogen so the substrates are induced to react to desired product by Na⁺. Moreover, NaCl can absorb water which is byproduct of this reaction. This function of

NaCl drives the equilibrium to product increasing as well [67]. The use of EtOH as co-solvent has been reported to increase polarity of system, leading to the partial dispersion of Na^+ into organic phase in condensation process [68]. It should be noted that the yield of the $\text{BF}_3 \cdot \text{OEt}_2/\text{NaCl}/\text{EtOH}$ catalytic condition was dropped after 10 min, this possibly results from the formation of N-Confused porphyrin as byproduct of the routine preparation of the structurally isomeric meso-substituted porphyrins. Those were unusual in that one of the macrocycle's pyrrole rings has been inverted so that what was once a central nitrogen atom has now become an external [69]. The mechanism for formation of porphyrin has been reported that two helical conformations of tetrapyrromethane differ only by the rotation of the terminal pyrrole moiety with respect to the $\text{C}_\alpha\text{-C}_{\text{meso}}$ bond during the porphyrinogen ring closure (Scheme 4-5).



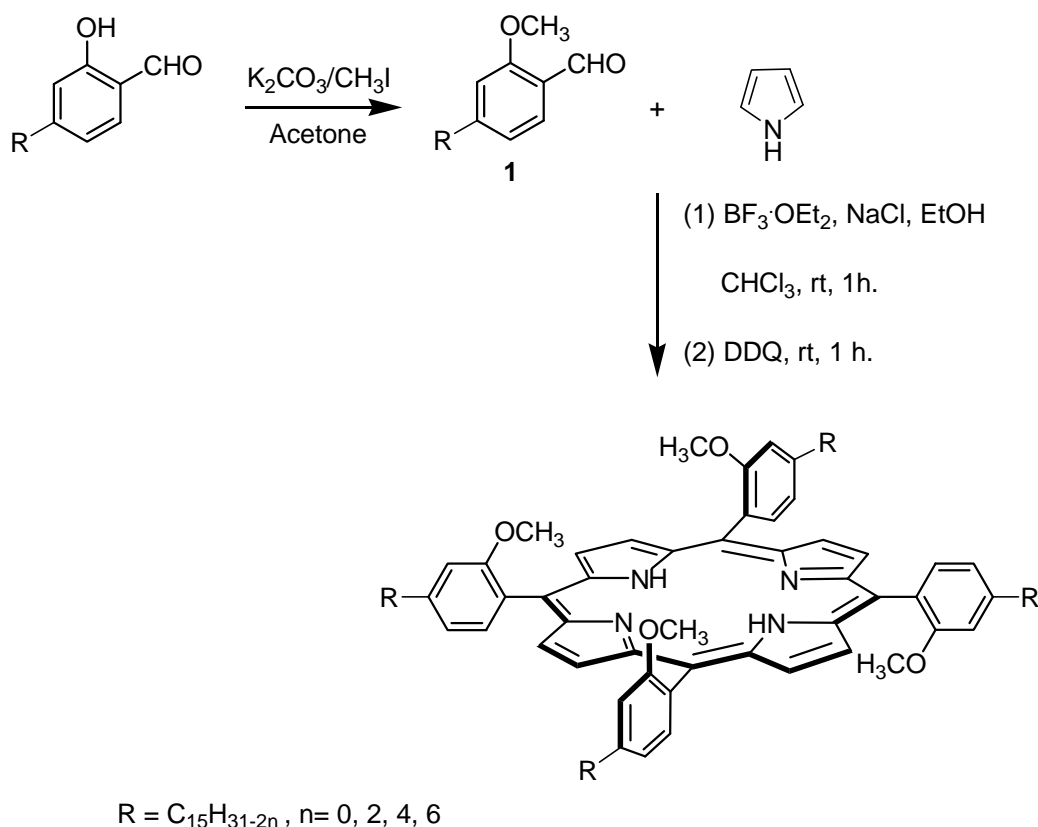
Scheme 4-6 Proposed the mechanism of the porphyrin and N-confused formation.

Compound **7** was synthesized under the optimized condition gave the improved yield up to 35%. From $^1\text{H-NMR}$ spectrum, the characteristic signal of inner protons of porphyrin **7** appears as a singlet at δ -2.63 ppm (**Figure A-18**). In addition, the presence

of porphyrin was confirmed by the presence of a typical strong Soret band at 420 nm and four Q bands at 515, 548, 591 and 644 nm in UV-Vis spectrum (**Figure B-2**).

4.3 Porphyrinic derivatives from non-hydrogenated cardanol

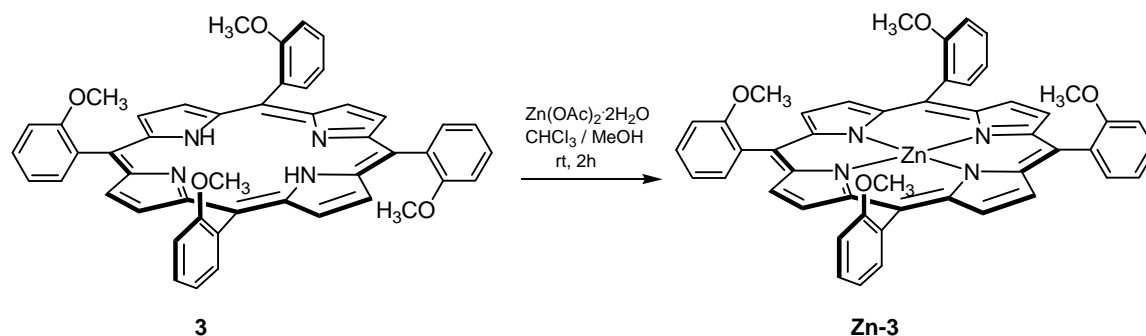
The cardanol can be used to synthesized porphyrinic derivatives in a similar manner as the hydrogenated cardanol, the pathway of the synthesis shown in Scheme 4-5.



Scheme 4-6 The total synthesis of meso-tetrakis(2-methoxy-4-alkenylphenyl)porphyrin.

The crude product of porphyrinic derivatives which were obtained as mixture of isomers was separated by repeated column chromatography. It was found that the mixture could not be separated into pure form of each isomer. UV-Vis spectrum of product mixture exhibits absorption at 420 nm of Soret band and four Q band at 512, 540, 590 and 650 nm respectively, while its fluorescent spectrum shows emission at $\lambda_{(em)}$ at 650 nm and 720 nm, which are consistent with those of porphyrinic derivative **7**, which was obtained from hydrogenated cardanol.

4.4 Synthesis of *meso*-tetrakis(2-methoxyphenyl)porphinatozinc(II) (**Zn-3**)



Reaction of **3** with $\text{Zn(OAc)}_2 \cdot 2\text{H}_2\text{O}$ in $\text{CHCl}_3/\text{MeOH}$ at room temperature for 2 h afforded porphyrin **Zn-3** in 93% yield. ¹H-NMR spectrum shows the absence of the signal of inner protons at -2 to -3 ppm due to the coordination of metal ion with the N atoms (**Figure A-22**). In addition, the **Zn-3** structure was confirmed by UV-Vis spectroscopy.

In general, the central part of the metalloporphyrin ring is occupied by a metal ion linked to a pyrrole ring. The metal ion accepts the lone-pair-electrons of the N atoms of the pyrrole ring, while electrons of the metal ion are donated to the porphyrin molecule, forming delocalized π bonds, which permit the easy flow of electrons within the delocalized π system. It can be seen in **Figure B-3** that the UV-Vis spectra of the metalloporphyrin exhibited one Soret band at 419 nm and two Q band at 545 and 590 nm; the small number of Q bands is typical of metalloporphyrins. When the metal ion coordinates with the N atoms, the symmetry of the molecule increases and the number of Q bands therefore decreases [70].

The objective in this research was the synthesis fluorescent marker to be used in diesel, therefore metalloporphyrin was not emphasized. However, the metalloporphyrin model (**Zn-3**) in this study was made available for applications in the future.

4.5 Fluorescent properties of porphyrin model and porphyrinic derivative

Fluorescent properties of porphyrin model and porphyrinic derivative were studied by using dichloromethane as solvent and the measuring parameters for fluorescent measurement were set as the followings:

- The wavelength of the excitation monochromator (λ_{ex}) was set at 420, 512, 550 590 or 645 nm.
- The response was set for one second.
- The photomultiplier tube voltage level (PMT Grain) was set at a medium level.
- The spectrum bandwidth of the emission monochromator (EM SBW) was set at 5.
- The spectrum bandwidth of the excitation monochromator (EM SBW) was set at 5.

Ideally, the fluorescent marker useful in the practice should have adequate solubility in diesel fuel, and strong intensity of fluorescent in the 400-800 nm, and the emission wavelength of fluorescent marker should be not interfered with the emission wavelength of diesel fuel. The detectable of this marker can be responded the emission level when added to diesel fuel at extremely low levels, e.g. 1 ppm or less [54].

Fluorescent properties of porphyrin model and porphyrinic derivative were shown in Table 4-2.

Table 4-2. The summarized excitation wavelength (λ_{ex} ; nm) and emission wavelength (λ_{em} ; nm) of porphyrin model and porphyrinic derivative **7** in dichloromethane.

Compound	Excitation wavelength (nm)	Emission wavelength (nm)
Porphyrin model (Compound 2)	420	652, 719
	512	652, 719
	550	652, 719
	590	652, 719
	645	719
Porphyrinic derivative (Compound 7)	420	652, 719
	512	652, 719
	550	652, 719
	590	652, 719
	645	719
Diesel fuel	420	443
	512	-
	550	-
	590	-
	645	-

The excitation wavelength (λ_{ex}) and emission wavelength (λ_{em}) of porphyrin model (**2**), porphyrin **7** and unmarked diesel fuel in dichloromethane are shown in **Figure B-5**, **B-6** and **B-7** respectively. These spectra indicate that the emission of **2** and **7** are not interfered by the emission of diesel fuel. Therefore, it was possible that the Compound **7** could be used as a marker in diesel fuel.

4.5.1 Quantitative determination of fluorescent marker in diesel

The standard calibration curve of fluorescent marker in diesel was prepared by adding fluorescent marker into diesel at different concentrations. The standard calibration curve was a plot between intensity of λ_{em} at 652 nm and concentration of fluorescent marker in diesel (**Figure B-15**).

The standard calibration equation of fluorescent marker in diesel is $Y = 58.35X$ with the correlation coefficient equal to 0.9984. This equation is used to evaluate the stability of the marker **7** in diesel fuel as described in the following part.

4.5.2 Stability Test of fluorescent marker in diesel

Generally, diesel is consumed within 3 months after released to the market. Therefore in this study, the stability test of the fluorescent marker **7** in diesel was designed to be performed in a period of 3 months. The test was carried out with a solution of compound **7** in diesel at 2 and 5 ppm using a spectrofluorometer.

Table 4-3 The stability of Compound **7** (2 and 5 ppm) in diesel

Month	Concentration in diesel (ppm)					
	2 ppm		Average	5 ppm		Average
	1 st	2 nd		1 st	2 nd	
1	2.04±0.02	2.01±0.02	2.02±0.02	4.96±0.01	4.98±0.01	4.97±0.01
2	2.02±0.01	2.01±0.01	2.02±0.01	4.96±0.01	4.97±0.01	4.97±0.01
3	2.02±0.01	2.01±0.01	2.02±0.01	4.96±0.01	4.98±0.01	4.97±0.01

The fluorescence intensity at 652 nm was converted into the marker concentration by the above-mentioned calibration equation. The result show in Table 4-3 indicated that the fluorescent marker has the stability for at least 3 months and hence it was possible that the compound **7** could be used as a marker in diesel fuel.

4.5.3 Effect of fluorescent marker on physical properties of fluorescent diesel

The fluorescent marker **7** was high soluble in diesel fuel and common organic solvents, such as CH₂Cl₂, CHCl₃, hexane because of the long alkyl side-chain of cardanol moiety.

PTT diesel containing 5 ppm of fluorescent marker **7** was tested for physical properties using the ASTM methods. The physical properties of marked and unmarked diesel were compared. The results are shown in Table 4-4.

Table 4-4 Physical properties of marked and unmarked diesel

Test items	ASTM	Limit	Result	
			Marked	Unmarked
API gravity @ 60°C	D 1298	Report	39.25	39.25
Specific gravity @ 15.6/15.6 °C	D 1298	0.81-0.87	0.82869	0.82868
Calculate cetane index	D 976	47-50	55.86	55.95
Kinematic viscosity @40oC,cst	D 445	1.8-4.1	2.884	2.876
Pour point, °C	D 97	10 max	1	1
Flash point, °C	D 93	52 min	70	72
Sulfur content, %wt	D 4294	0.035 max	0.0317	0.0313
Distillation (Correct Temp.)	D 86			
IBP, °C		Report	175.3	177.3
10% rec, °C		Report	208.5	210.1
50% rec, °C		Report	272.6	273.3
90% rec, °C		357 max	349.8	349.2
Color	D 1500	2.0 max	0.7	0.6

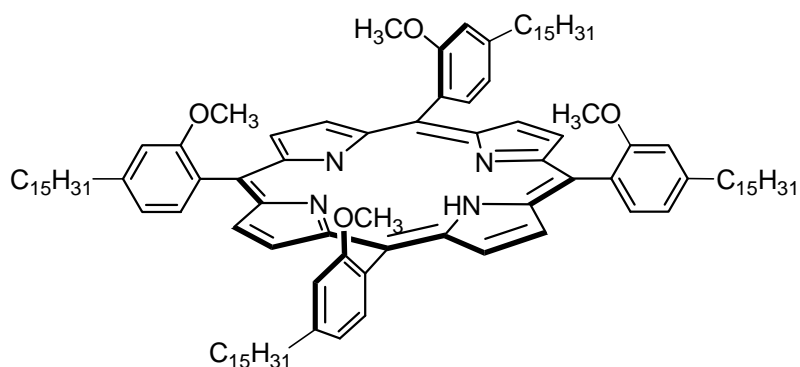
The physical properties of marked diesel were not significantly different from those of unmarked diesel. The results revealed that marker **7** do not have any significant effect on the physical properties of diesel. Therefore, it is possible to use this fluorescent marker as the marker in diesel.

CHAPTER V

CONCLUSION

The synthesis of porphyrin model has been successfully performed by using salicylaldehyde as starting material reacted with pyrrole in EtOH-containing CHCl_3 using $\text{BF}_3 \cdot \text{OEt}_2$ in the presence of NaCl, followed by oxidation with DDQ. The desired *meso*-tetrakis(2-methoxyphenyl)porphyrin was performed as a model synthetic pathway in the synthesis of porphyrin from cardanol. In addition the synthesis of metalloporphyrin model (Zn II) has been successfully performed by using $\text{Zn}(\text{OAc})_2 \cdot 2\text{H}_2\text{O}$ in methanol.

This research involved the synthesis of a novel porphyrinic derivative from cardanol for use as fluorescent marker in diesel fuels. The synthesis starts from the formylation of hydrogenated cardanol and subsequent protection of hydroxyl group. *meso*-Tetrakis(2-methoxy-4-pentadecylphenyl)porphyrin (**7**) was successfully prepared from the condensation of the resulting aldehyde precursor and pyrrole under catalysis of $\text{BF}_3 \cdot \text{OEt}_2/\text{NaCl}/\text{EtOH}$ in 35 % yield.



As expected, the cardanol-based porphyrin **7** shows high solubility in diesel fuels and common organic solvents due to the presence of long alkyl chain. The color of the fluorescent marker **7** is indistinguishable in diesel fuels when added at the concentration of 2-5 ppm. At this concentration, marker **7** exhibited an obvious fluorescence (652 nm and 719 nm) in separated range from where diesel fuels fluoresces (443 nm) upon excitation at 512 nm. The physical properties of diesel fuels, which were tested according to ASTM methods, are unaffected by the marker.

Moreover, marker **7** was found to be stable in diesel fuels for at least three months. According to above properties, it can be concluded that marker **7** was suitable for being a fluorescent marker in diesel fuels.

REFERENCES

- [1] Morisaki, M.; Ito, T.; Hayvali, M.; Tabata, I.; Hisada, K.; Hori, T. "Preparation of skinless polymer foam with supercritical carbon dioxide" *Polymer*. **2008**, *49* 1611–1619.
- [2] Ochiai, T.; Asaoka, T.; Kato, T.; Osaka, S.; Dewa, T.; Yamashita, K.; Hashimoto, H.; Nango, M. "Molecular assembly of Zn porphyrin complexes onto a gold electrode using synthetic light-harvesting model polypeptides" *Tetrahedron Lett.* **2007**, *48*, 8468–8471.
- [3] Tohru Shiga, T.; Motohiro, T. "Photosensitization of nanoporous TiO₂ film with porphyrin-linked fullerene" *Thin Solid Films* **2008**, *516*, 1204–1208.
- [4] Maeda, C.; Kamada, T.; Aratani, N.; Osuka, A. "Chiral self-discriminative self-assembling of *meso-meso* linked diporphyrins" *Coordin. Chem. Rev.* **2007**, *251*, 2743–2752.
- [5] Lakowicz, J.R. Principles of fluorescence spectroscopy. 3rd ed. New York: Springer Science + Business Media, **2006**, 1–25.
- [6] Bartrop, J.A.; Coyle J.D. Principles of Photochemistry. New York: Wiley, **1998**, 78–83.
- [7] Wayne, C.E.; Wayne, R. P. Photochemistry. USA: Oxford chemistry primer, **1996**, 43–47.
- [8] Olympus Microscopy Resource Center: Specialized Microscopy Techniques - Fluorescence - Basic Concepts in Fluorescence [Online]. Available from: www.olympusmicro.com/proimer/technique/tecniques/fluorescence/fluorescenceintro.html. [2007; Dec 7].
- [9] Photosynthesis, [Online]. Available from: www.steve.gb.com/science/photosynthesis.html [2005; Jan 12].
- [10] Battersby, A. R., Fookes, C. J. R., Matcham, G. W. J., McDonald, E. "Biosynthesis of the pigments of life: formation of the macromolecule" *Nature* **1980**, *285*, 17–20.
- [11] Falk, J. E. "Porphyrins and metalloporphyrins; their general, physical and coordination chemistry, and laboratory methods" Elsevier: Amsterdam, **1964**.

- [12] Chaundry, I. A.; Clezy, P. S.; Mizra, A. H. "Chemistry of pyrrolic compounds. XLVI. Benzyl β -keto propionate porphyrins: a new synthesis of deoxophylloerythroaetioporphyrin and harderoporphyrin" *Aust. J. Chem.* **1980**, *33*, 1095–1104.
- [13] Rothmund, P. "New porphyrin synthesis. The synthesis of porphin 1" *J. Am. Chem. Soc.* **1936**, *58*, 625–627.
- [14] Alder, A.D.; Longo, F.R.; Finarelli, J.D.; Goldmacher, J.; Assour, J.; Korsakoff, L. "A simplified synthesis for *meso*-tetraphenylporphin" *J. Org. Chem.* **1967**, *32*, 476–476.
- [15] Reddy, D.; Chandrashekar, T.K. "Short-Chain basket handle porphyrins: Synthesis and characterisation" *J. Chem. Soc., Dalton Trans.* **1992**, 619–625.
- [16] Czuchajowski, L.; Habdas, J.; Niedbala, H.; Wandrekar, V. "Porphyrinyl-uridines as the first water soluble porphyrinyl-nucleosides" *Tetrahedron Lett.* **1991**, *32*, 7511–7512.
- [17] Kaelin, A. C.; Zanelli, G. D.; "Synthesis and radioiodination of a *meso*-tetra (hydroxynaphthyl) porphyrin and its sulphonated derivative as potential tumour localizers" *J. Labelled Compd. Radiopharm.* 1990, *28*, 343–354.
- [18] Lindsey, J.S.; Schreiman, I.C.; Hsu, H.C.; Kearney, P.C.; Marguerettaz, A.M. "Rothmund and Adler-Longo reactions revisited: synthesis of tetraphenylporphyrins under equilibrium conditions" *J. Org. Chem.* **1987**, *52*, 827–836.
- [19] Lindsey, J.S.; Wagner, R. W. "Investigation of the synthesis of *Ortho*-substituted tetraphenylporphyrins" *J. Org. Chem.* **1989**, *54*, 828–836.
- [20] Barkigia, K. M.; Chantranupong, L.; Smith, K. M.; Fajer, J. "Structural and theoretical models of photosynthetic chromophores. Implications for redox, light absorption properties and vectorial electron flow" *J. Am. Chem. Soc.* **1983**, *105*, 7566–7567.
- [21] Groves, J. T.; Nemo, T.E. "Aliphatic hydroxylation catalyzed by iron porphyrin complexes" *J. Am. Chem. Soc.* 1983, *105*, 6243–6248.
- [22] Medforth, C. J.; Smith, K. M. "*meso*-paracyclophanyltriphenylporphyrin: electronic consequences of linking paracyclophane to porphyrin" *Tetrahedron Lett.* **1990**, *31*, 5583–5583.

- [23] Wagner, R. W.; Ruffing, J.; Breakwell, B. V.; Lindsey, J. S. "Synthesis of facially-encumbered porphyrins. An approach to light-harvesting antenna complexes" *Tetrahedron Lett.* **1991**, 32, 1703–1706.
- [24] Lindsey, J. S.; Prathapan, S.; Jonhson, T.E.; Wagner, R.W. "Porphyrin building blocks for modular construction of bioorganic model system" *Tetrahedron* **1994**, 50, 8941–8968.
- [25] Li, F.; Yang, K.; Tyhonas, J.S.; MacCrum, K.A.; and Lindsey, J.S. "Beneficial effects of salts on an acid-catalyzed condensation leading to porphyrin formation" *Tetrahedron* **1997**, 53(37), 12339–12360.
- [26] Cady, S. S.; Pinnavaia, T. J. "Porphyrin intercalation in mica-type silicates" *Inorg. Chem.* **1978**, 17, 1501–1507.
- [27] Onaka, M.; Shinodo, T.; Izumi, Y.; Nolen, E. "Porphyrin synthesis in clay nanopspaces" *Chem. Lett.* **1993**, 117–120.
- [28] Gradillas, A.; Del Campo, C.; Sinisterra, J. V.; Llama, E. F. "Novel synthesis of 5,10,15,20-tetraarylporphyrins using high-valent transition metal salts" *J. Chem. Soc., Perkin Trans. 1* **1995**, 2611–2613.
- [29] Arsenault, G. P.; Bullock, E.; MacDonald, S. F. "Pyrromethanes and porphyrins therefrom" *J. Am. Chem. Soc.* **1960**, 82, 4238–4389.
- [30] Honeybourne, C. L.; Jackson, J. T.; Simmonds, D.J.; Jones, O. T. G. "The Synthesis and solution confirmation of dodecylphenylporphyrin" *Tetrahedron* **1980**, 36, 1833–1838.
- [31] Lee, C. -H., Li, F.; Iwamoto, K.; Dadok, J.; Bothner-By, A.A.; Lindsey, J. S. "Synthetic approaches to regioisomerically pure porphyrins bearing four different meso-substituents" *Tetrahedron* **1995**, 51, 11 645–11673.
- [32] Boudif, A.; Momenteau, M. "Synthesis of a porphyrin-2,3-diacrylic acid using a new '3+1' type procedure" *J. Chem. Soc., Chem. Commun.* **1994**, 2069–2077.
- [33] Clezy, P. S.; Van, Thuc, L. "The chemistry of pyrrolic compounds. LVII. The oxidative cyclization of derivatives of 1,19-dideoxybilanes-b" *Aust. J. Chem.* **1984**, 37, 2085–2092.
- [34] Wijesekera, T. P.; Dolphin, D. "1-Bromo-19-methylbiladienes-ac; useful precursors to porphyrins" *Synlett* **1990**, 235–244.
- [35] Dogutan, D. K.; Zaidi, S. H.; Tham Yongkit, P.; Lindsey, J. S. "New route to ABCD-porphyrin via bilanes" *J. Org. Chem.* 2007, 72, 7701–7714.

- [36] Poporich, M.; and Carl, H. “Fuel and lubricants”, New York : Jonh Wiley & sons, **1959**, 135–136.
- [37] Holmes, R. T. “Diesel fuel composition” *US Patent 4678479*, **1987**.
- [38] ประกาศกรมธุรกิจพลังงาน เรื่อง กำหนดลักษณะและคุณภาพของน้ำมันดีเซล (ฉบับที่ 3), ราชกิจจานุเบกษา เล่ม 122 ตอนพิเศษ 70 ง หน้า 14, 24 สิงหาคม 2548.
- [39] Orelup, R. B. “Colored petroleum markers” *US Patent 4735631*, **1988**.
- [40] Blazdell, P. “The mighty cashew” *Interdisciplinary Sci. Rev.*, **2000**, 25, 7–12.
- [41] Tyman, J. H. P.; Johnson R. A.; Muir M.; Rekhgar R.; “The extraction of natural cashew nut shell liquid from the cashew nut (*Anarcadium occodentate*)” *Journal Am. Oil Chem. Soc.*, **1989**, 66(4), 553–557.
- [42] Menon, A. R. R.; Pillai, C. K. S.; Sudha, J. D.; Mathew, A.G.; “Cashew nut shell liquids – its polymeric and other industrial products” *J. Sci. Ind. Res.*, **1985**, 44, 324–338 .
- [43] Chemical composition of CNSL, Sanoor Cashew (Importer & Exporters), India [Online]. Available from: www.adarshsanoor.com [2001; March 13].
- [44] Aggarwal, L. K.; Thapliyal, P. C.; Karade, S. R. “Anticorrosive properties of the epoxy–cardanol resin based paints” *Prog. Org. Coat.*, **2007** 59, 76–80.
- [45] Li, X.; Lope G. Tabil, L.G.; Panigrahi, S. “Chemical treatments of natural fiber for use in natural fiber-reinforced composites: a review” *J. Polym. Environ.* **2007**, 15, 25–33.
- [46] Ganguly, A.; George, R. “Asbestos free friction composition for brake linings” *Bull. Mater. Sci.*, 2008, 31, 19–22.
- [47] Maffezzoli, A.; Calo, E.; Zurloa, S.; Mele, G. Antonella Tarziab, A.; Stifani, C. “Cardanol based matrix biocomposites reinforced with natural fibres” *Compos. Sci. Technol.*, **2004**, 64, 839–845.
- [48] Leerawan Khaokhum, L.; Sawasdipuksa, N.; Kumthong, N.; Tummatorn, J.; Roengsumran, S. “Cardanol polysulfide as a vulcanizing agent for natural rubber” *J. Sci. Res. Chula. Univ.*, **2005**, 30, 23–30.
- [49] Prabhakaran, K.; Narayanan, A.; Pavithran, C. “Cardanol as a dispersant plasticizer for an alumina/toluene tape casting slip” *J. Europ. Ceram. Soc.*, **2001**, 21, 2873–2878.
- [50] Rodrigues, F. H. A.; Feitosa, J. P. A.; Nágila M. P. S.; Ricardo, N. M. P. S.

- de França, F. C. F.; Carioca, J. O. B. "Antioxidant activity of cashew nut shell liquid (CNSL) derivatives on the thermal oxidation of synthetic *cis*-1,4-polyisoprene" *J. Braz. Chem. Soc.* **2006**, 1–7.
- [51] Friswell, M.R.; and Zimin, A. "Silent fluorescent petroleum markers" *US Patent 5980593*, **1999**.
- [52] Halissy, M. J. "Base extractable petroleum markers" *US Patent 5252106*, **1993**.
- [53] Smith, M. J.; and Desai, B. "Colorless petroleum markers" *US patent 6002056*, **1988**.
- [54] Smith, M. J. "Fluorescent petroleum markers" *US Patent 5498808*, **1996**.
- [55] Friswell, M. R., and Hinton, M. P. "Marker for petroleum, method of tagging, and method of detection" *US Patent 5205840*, **1993**.
- [56] Mele, G.; Sole, R. D.; Vasapollo, G.; Garcìa-Lo`pez, E.; Palmisano, L.; Mazzetto, S. E.; Attanasi, O. A.; Filippone, P. "Polycrystalline TiO₂ impregnated with cardanol-based porphyrins for the photocatalytic degradation of 4-nitrophenol" *Green Chem.* **2004**, 6, 604–608.
- [57] Attanasi, O.A.; Ciccarella, G.; Filippone, P.; Mazzetto, S. E.; Mele, G., Spadavecchia, J.; and Vasapollo, G. "Novel phthalocyanines containing cardanol derivatives" *J. Porphyrins Phthalocyanines.* **2003**, 7, 52–57.
- [58] Attanasi, O.A.; Del Sole, R.; Filippone, P.; Mazzetto, S. E.; Mele, G.J.; Vasapollo, G. "Synthesis of novel lipophilic porphyrin-cardanol derivatives" *J. Porphyrins Phthalocyanines.* **2004**, 8, 1276–1284.
- [59] Guo, Y. C.; Xiao, W.J.; Mele, G.; Martina, F.; Margapoti, E.; Mazzetto, S. E.; and Vasapollo, G. "Synthesis of new meso-tetraarylporphyrins bearing cardanol and further transformation of the unsaturated chains" *J. Porphyrins Phthalocyanines.* **2006**, 10, 1071–1079.
- [60] Guo, Y. C.; Mele, G.; Martina, F.; Margapoti, E.; Vasapollo, G.; Xiao, W. J. "An efficient route to biscardanol derivatives and cardanol-based porphyrins via olefin metathesis" *J.organomet. Chem.* **2006**, 691, 5358–5390.
- [61] Svelle, S.; Stein Kolboe, S.; Olsbye, U.; Swang, O. "A Theoretical investigation of the methylation of methylbenzenes and alkenes by halomethanes over acidic zeolites" *J. Phys. Chem. B* **2003**, 107, 5251–5260.
- [62] Thamyongkit, P.; Speckbacher, M.; Diers, J. R.; Kee, H. L.; Kirmaier, C.; Holten, D., Bocian, D. F.; Lindsey, J. S. "Swallowtail porphyrins: synthesis,

- characterization and incorporation into porphyrin dyads” *J. Org. Chem.* **2004**, *69*, 3700–3710.
- [63] Seidl, P. R.; Pinto, A. D. C.; Menzel, A. R.; Couto, R. O. “Process for preparation of oximes and resulting products” *US Patent 6673969 B2*, **2004**.
- [64] Payne, P.; Tyman, J. H. P.; Mehet, S. K.; Ninagawa, A. “The synthesis of 2-hydroxymethyl derivatives of phenols” *J. Chem. Res.*, **2006**, 402–405.
- [65] Lindsey, J. S.; Schreiman, I. C.; Hsu, H. C., Kearney P. C.; Marguerettaz, A. M. “Rothemund and Adler-Longo Reactions Revisited: synthesis of tetraphenylporphyrins under equilibrium conditions” *J. Org. Chem.* **1987**, *52*, 827–836.
- [66] Geier, G.R.; Lindsey, J.S. “Effects of aldehyde or dipyrromethane substituents on the reaction course leading to *meso*-substituted porphyrins” *Tetrahedron.* **2004**, *60*, 11435–11444.
- [67] Thomson, M. C.; Busch, D. H. “Reaction of coordinated ligands. ix. utilization of the template hypothesis to synthesize macrocyclic ligands *in Situ*” *J. Am. Chem. Soc.* **1964**, 3651–3656.
- [68] Sharghi, H.; Nejad, A. H. “Phosphorus pentachloride (PCl₅) mediated synthesis of tetraarylporphyrins” *Helv. Chim. Acta.* **2003**, *86*, 408–414.
- [69] Pushpan, S. K.; Venkatraman, S.; Anand, V. G.; Sankar, J.; Rath, H.; Chandrashekar, T. K. “Inverted porphyrins and expanded porphyrins: an overview” *Proc. Indian Acad. Sci.* **2002**, *114*, 311–338.
- [70] Zheng, W.; Shan, N.; Yu, L.; Wang, X. “UV-visible, fluorescence and EPR properties of porphyrins and metalloporphyrins” *Dyes Pigm.* **2008**, *77*, 153–157.

APPENDICES

APPENDIX A

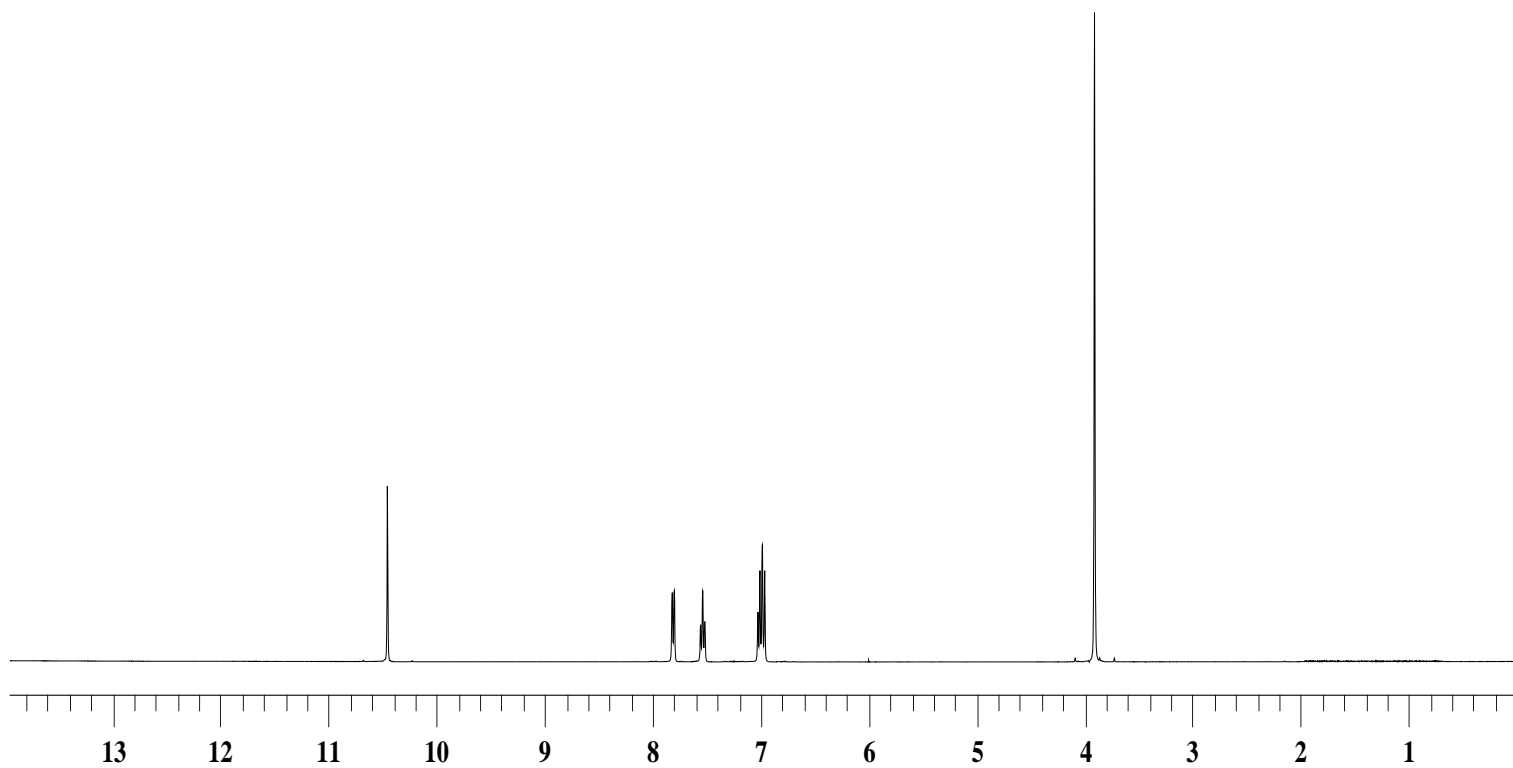


Figure A-1 $^1\text{H-NMR}$ spectrum of 2-methoxybenzaldehyde (Compound 2)

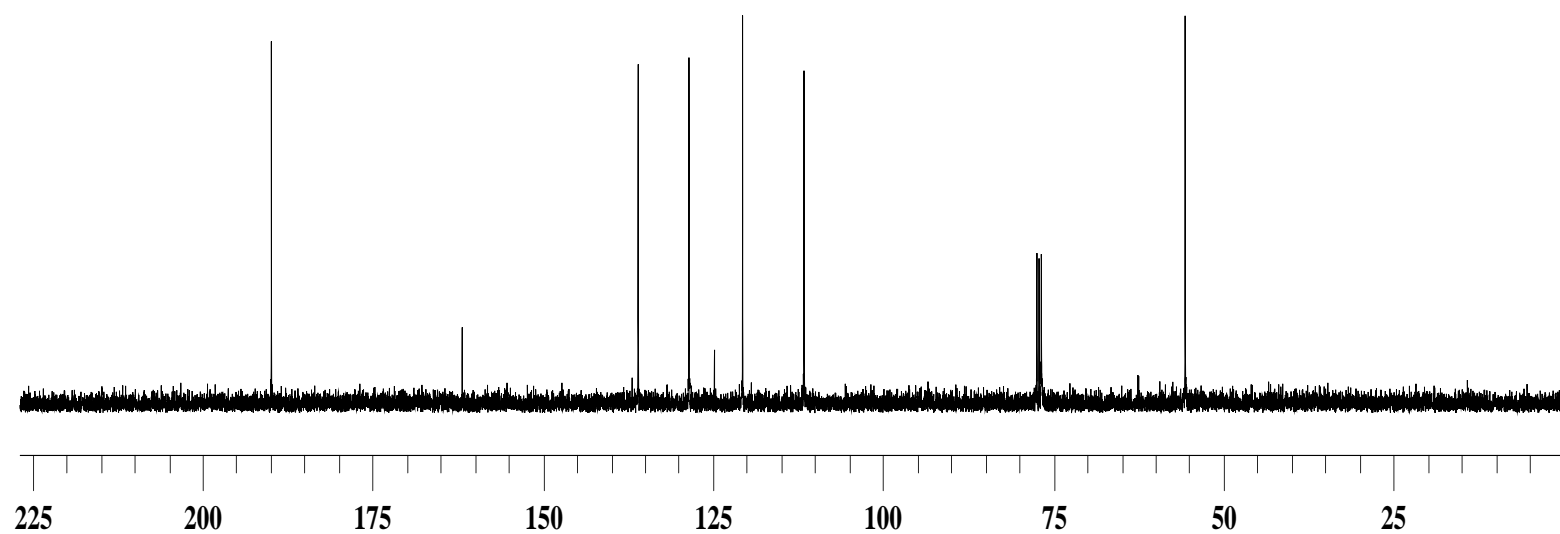


Figure A-2 ^{13}C -NMR spectrum of 2-methoxybenzaldehyde (Compound 2)

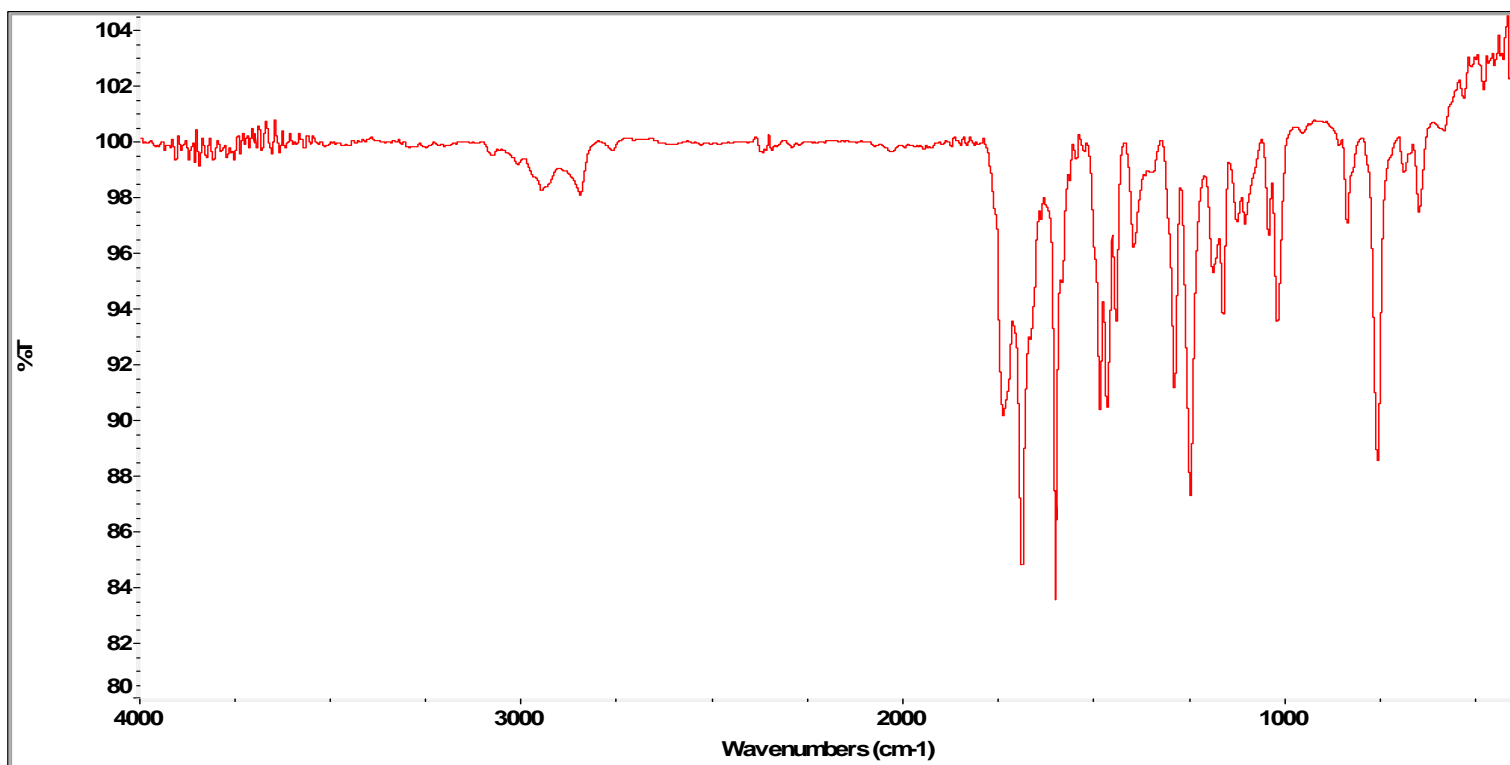


Figure A-3 IR spectrum of 2-methoxybenzaldehyde (Compound 2)

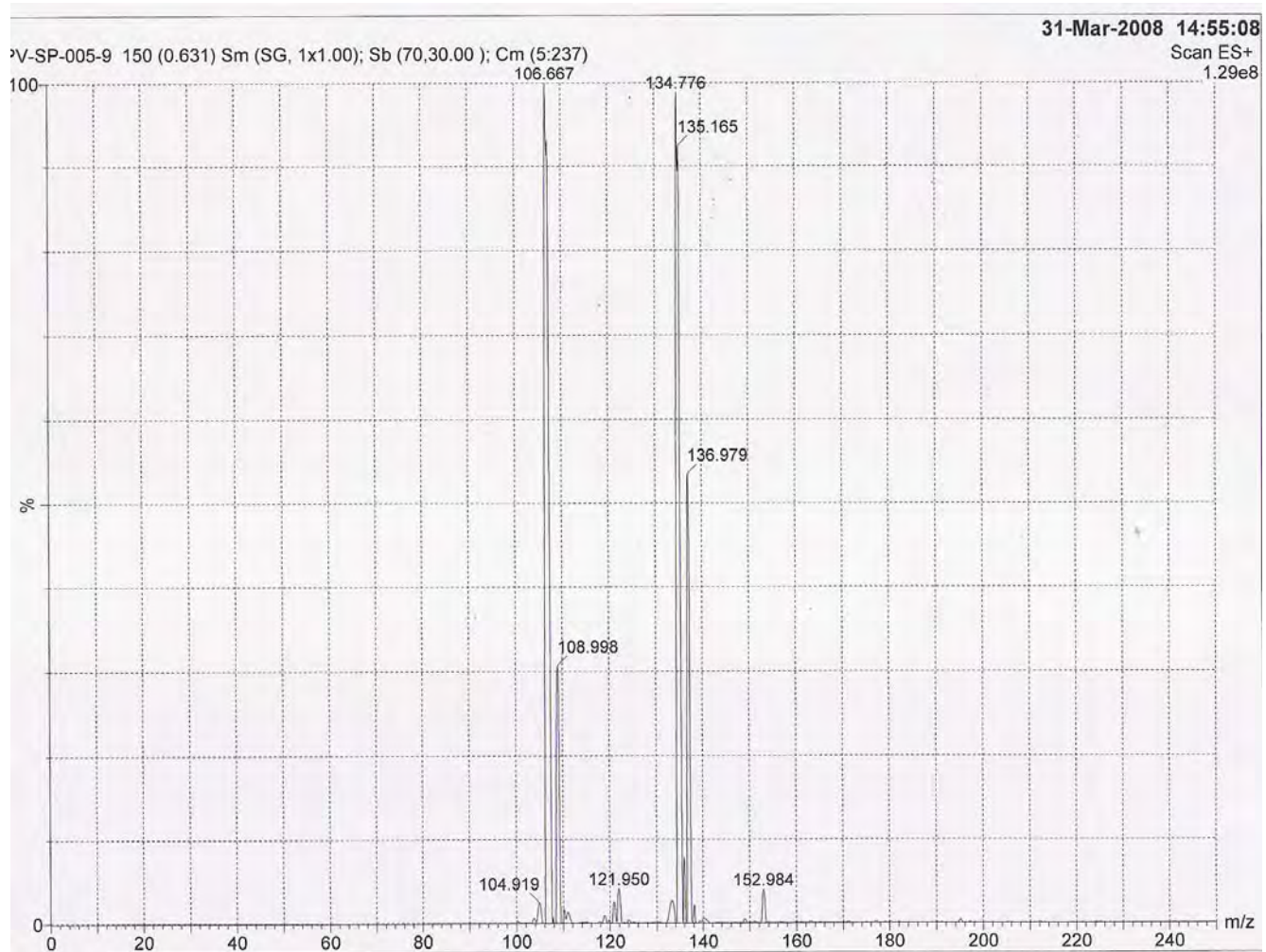


Figure A-4 Mass spectrum of 2-methoxybenzaldehyde (Compound 2)

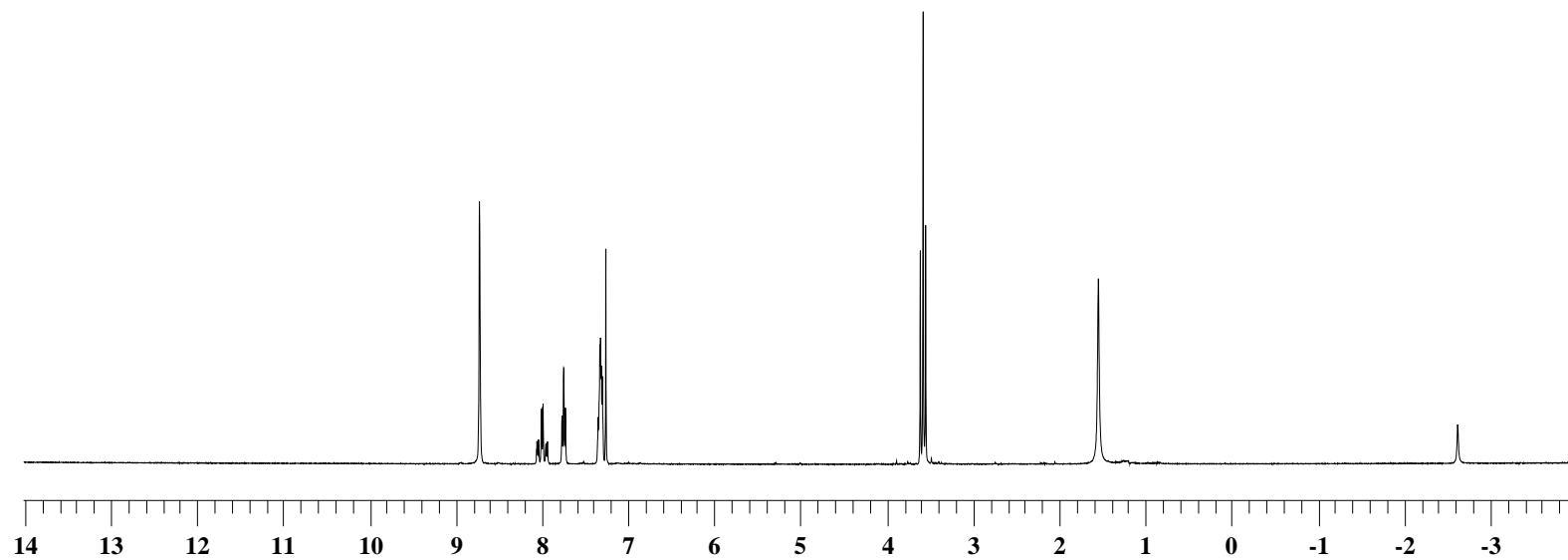


Figure A-5 $^1\text{H-NMR}$ spectrum of porphyrin model (Compound **3**)

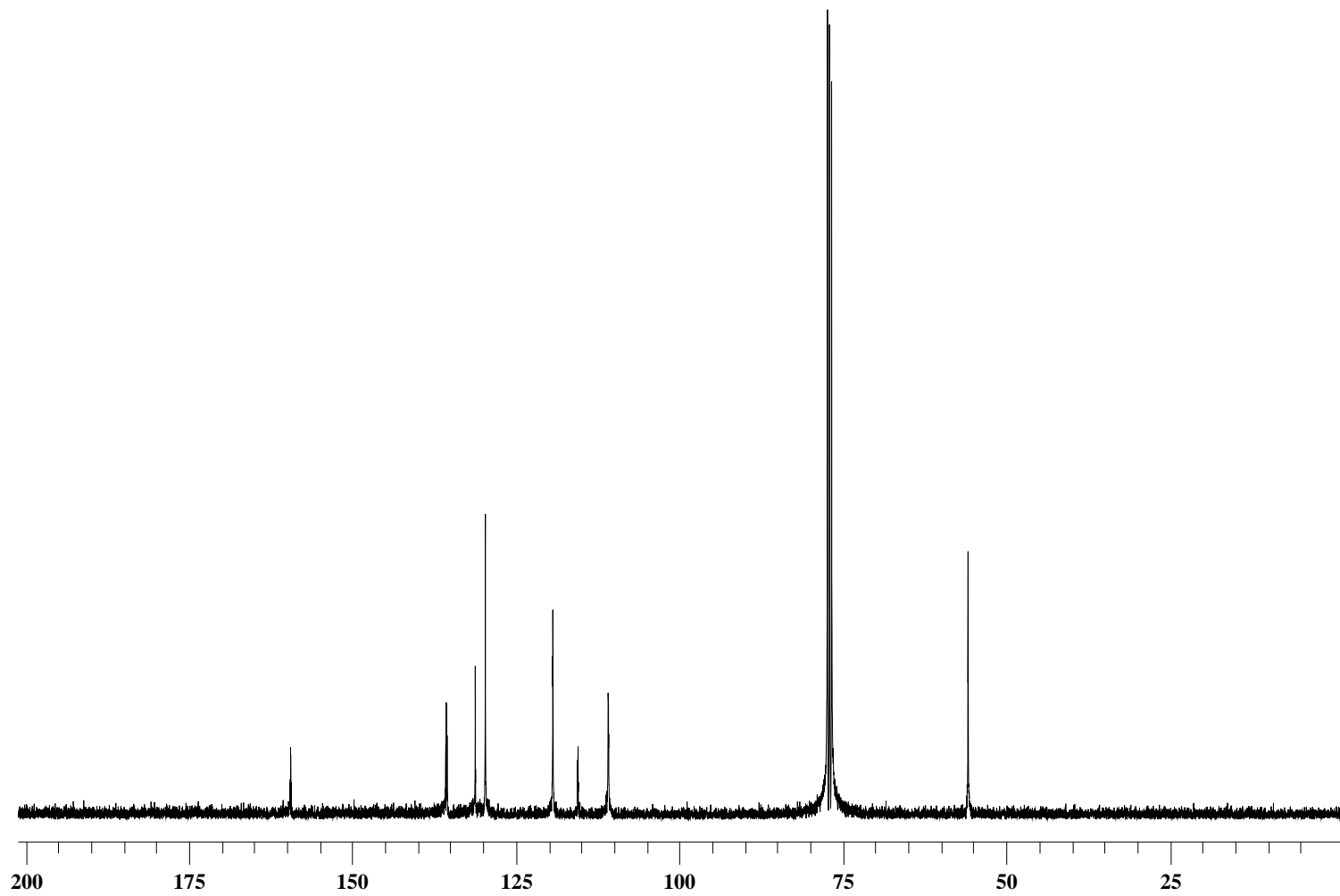


Figure A-6 ^{13}C -NMR spectrum of porphyrin model (Compound 3)

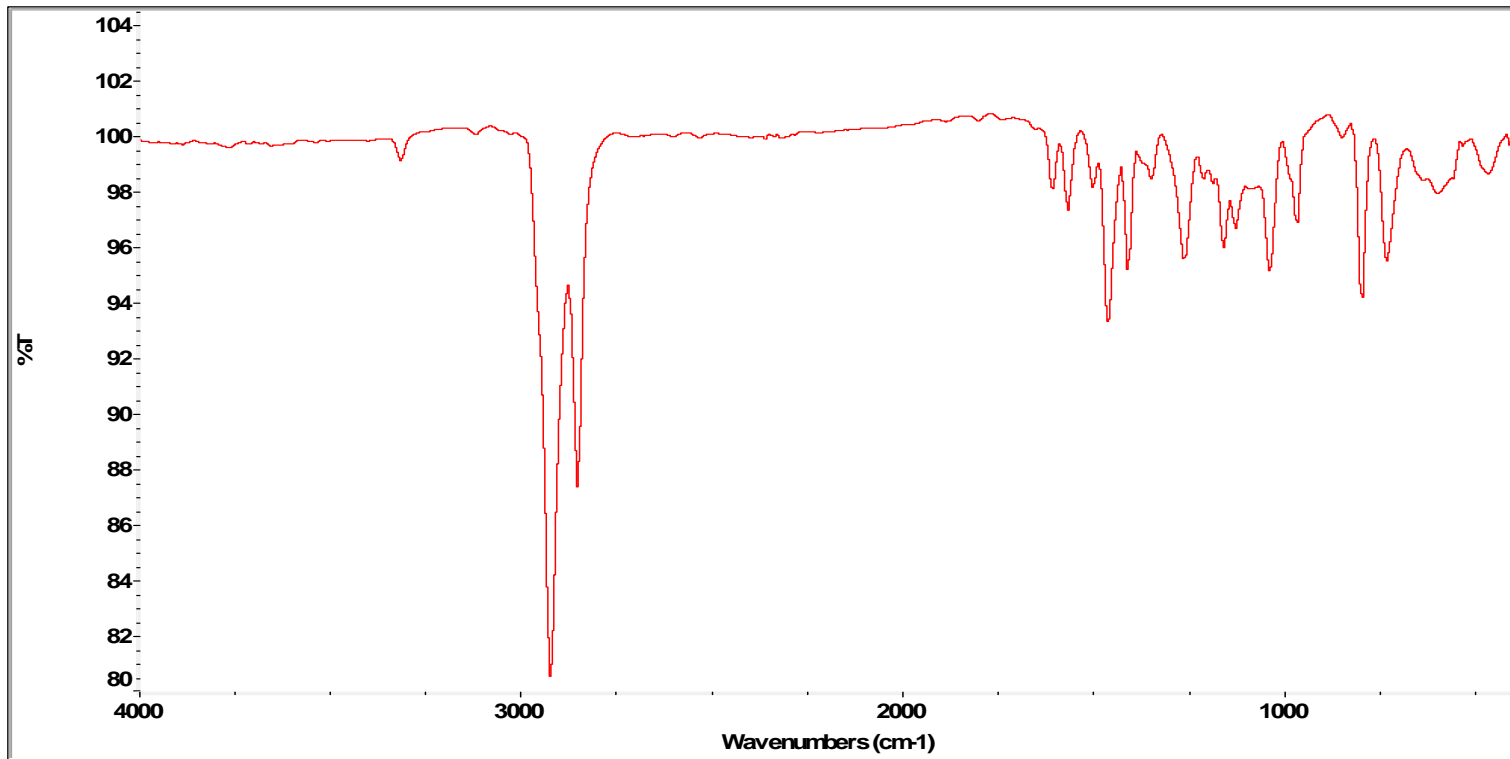


Figure A-7 IR spectrum of porphyrin model (Compound 3)

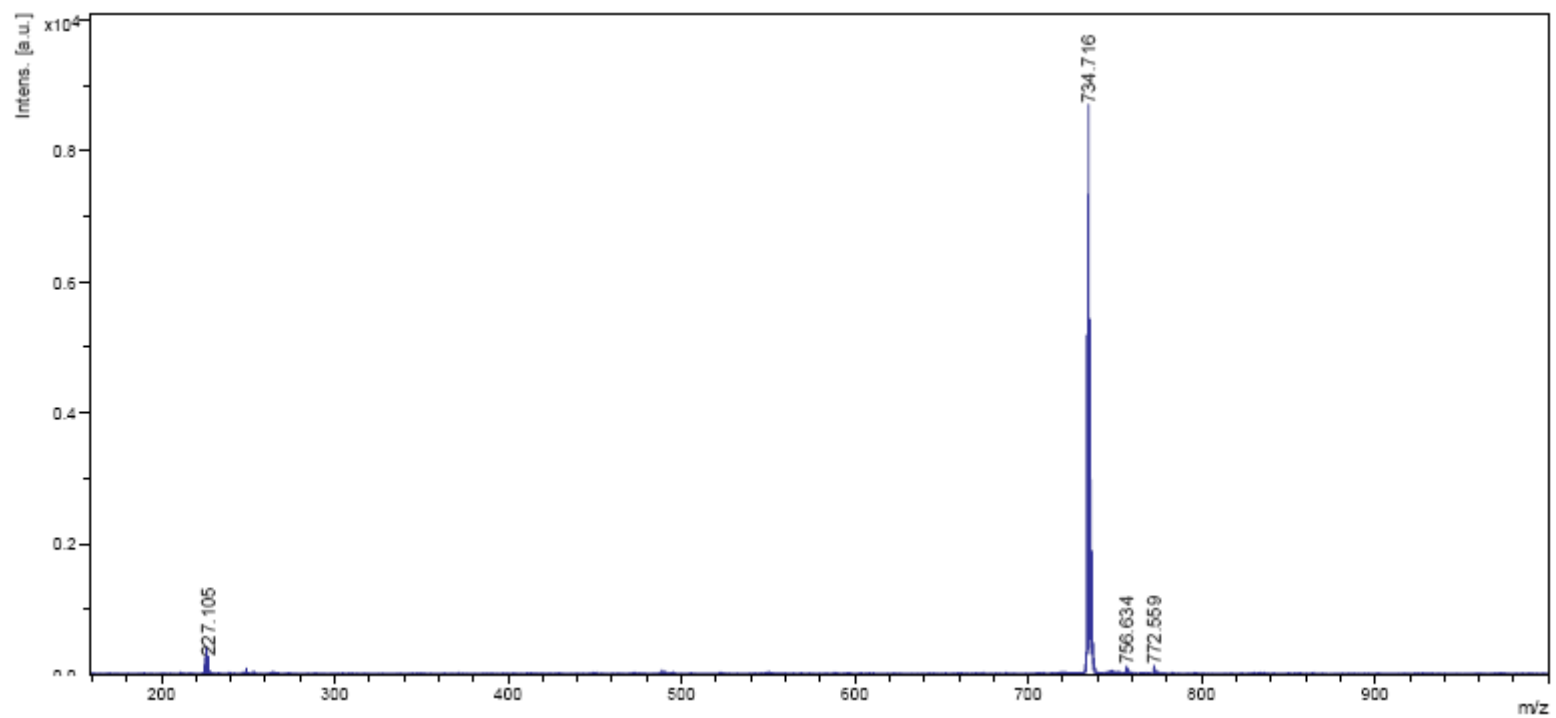


Figure A-8 Mass spectrum of porphyrin model (Compound **3**)

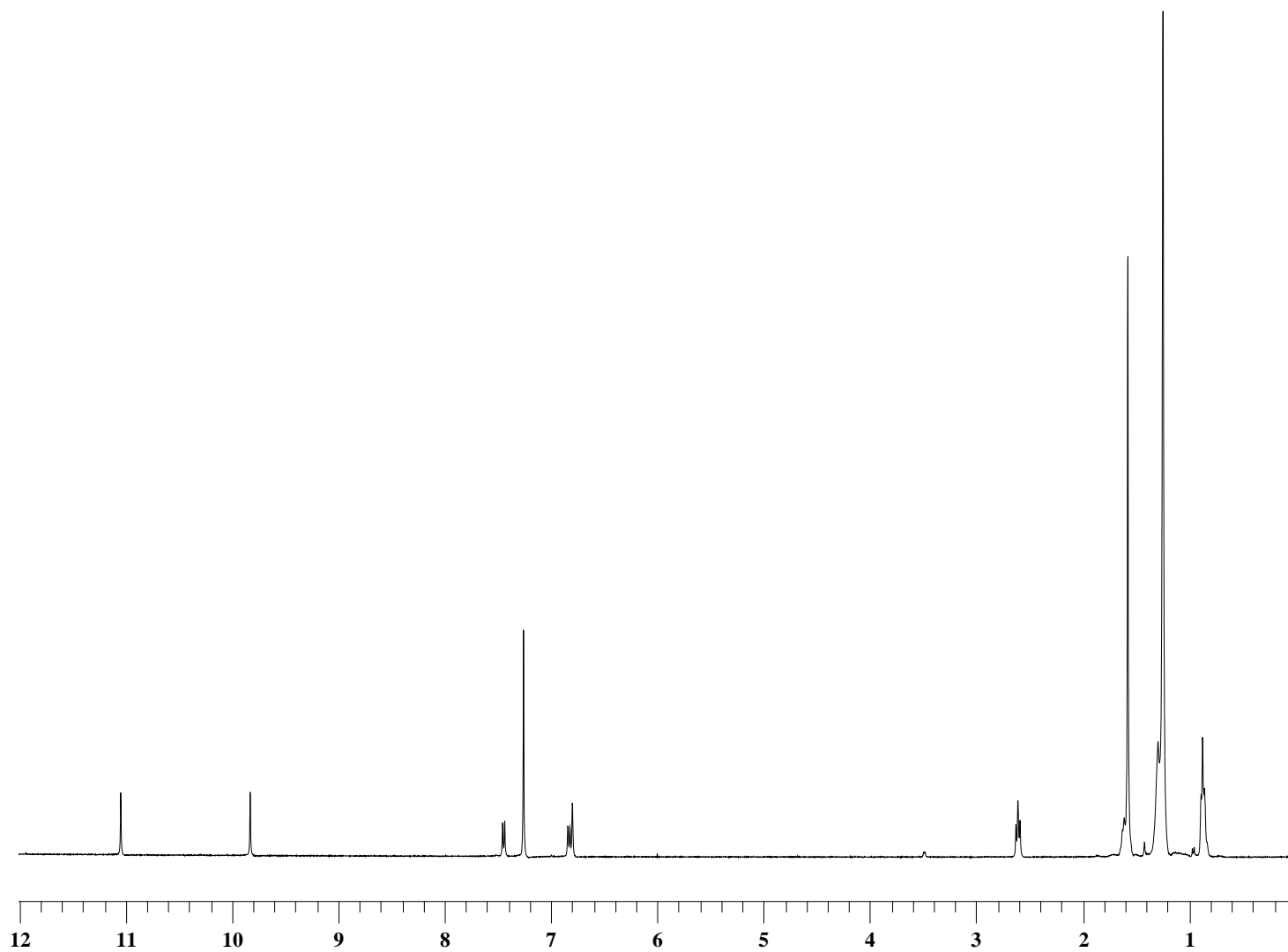


Figure A-9 $^1\text{H-NMR}$ spectrum of 2-hydroxy-4-pentadecylbenzaldehyde (Compound **5**)

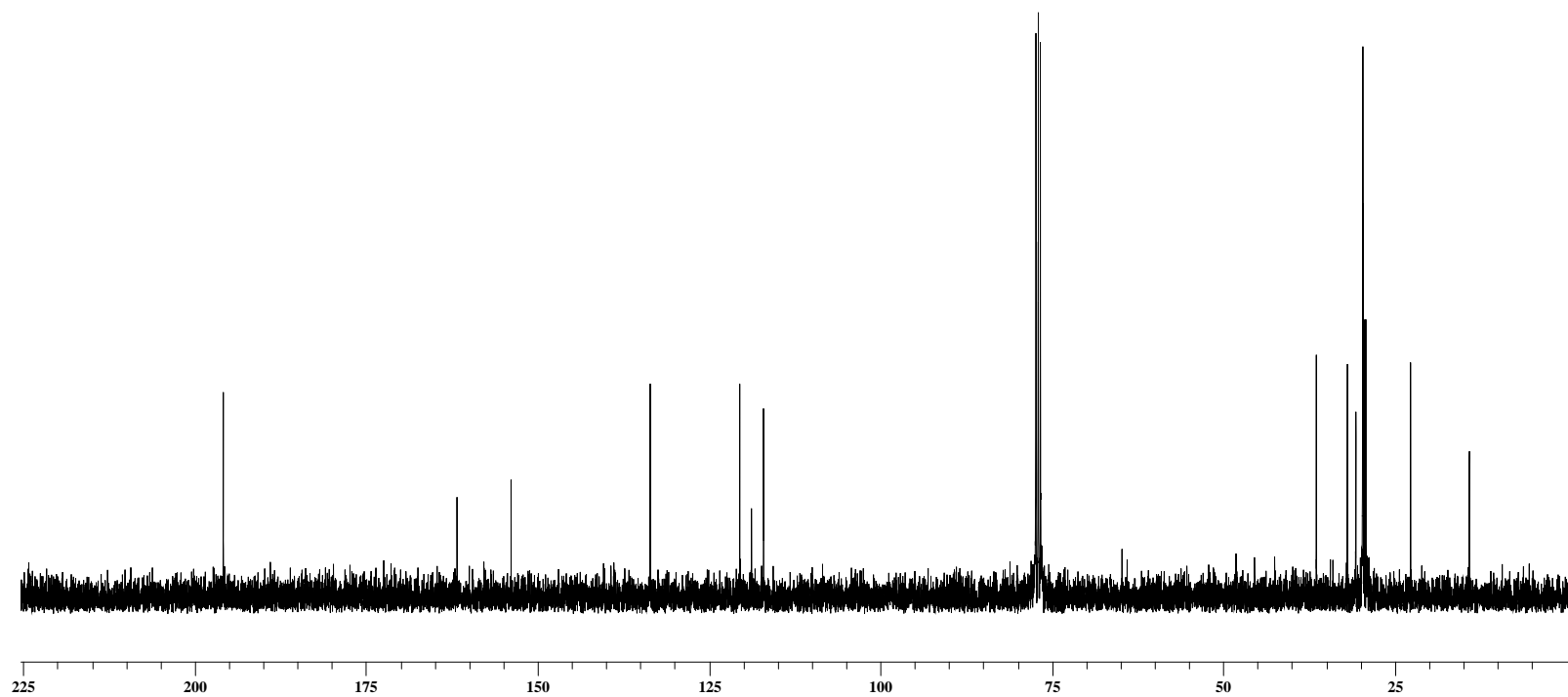


Figure A-10 ^{13}C -NMR spectrum of 2-hydroxy-4-pentadecylbenzaldehyde (Compound 5)

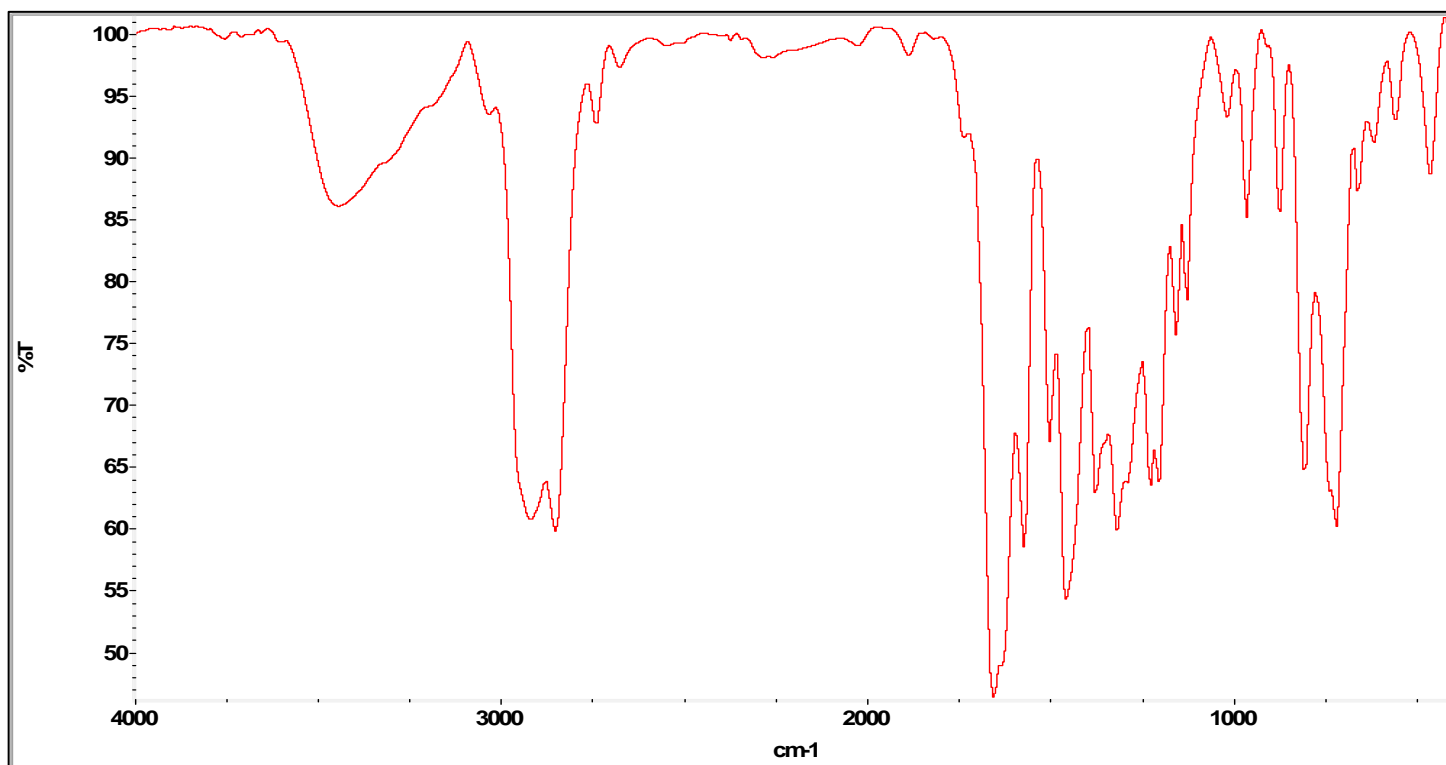


Figure A-11 IR spectrum of 2-hydroxy-4-pentadecylbenzaldehyde (Compound 5)

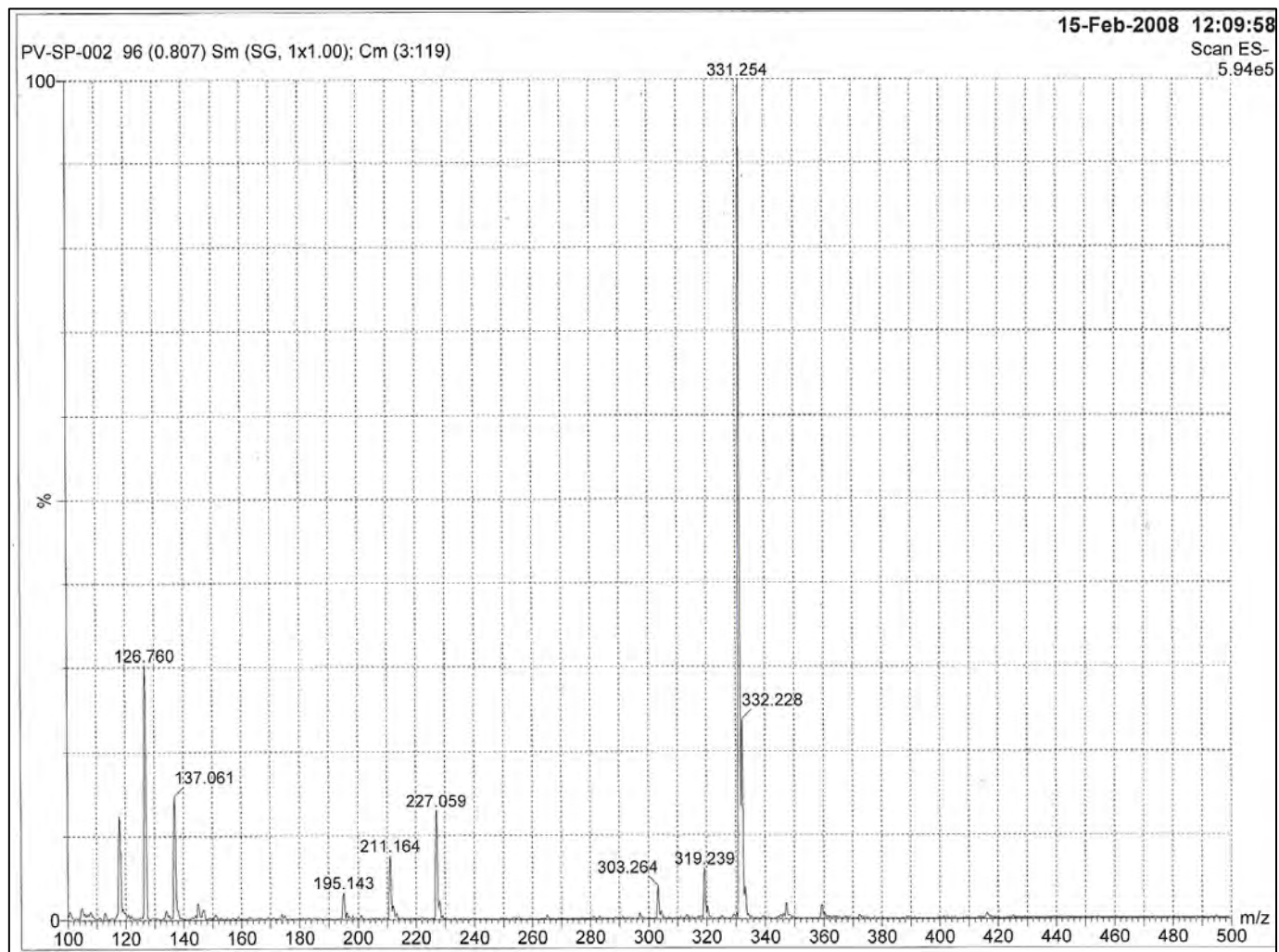


Figure A-12 Mass spectrum of 2-hydroxy-4-pentadecylbenzaldehyde (Compound 5)

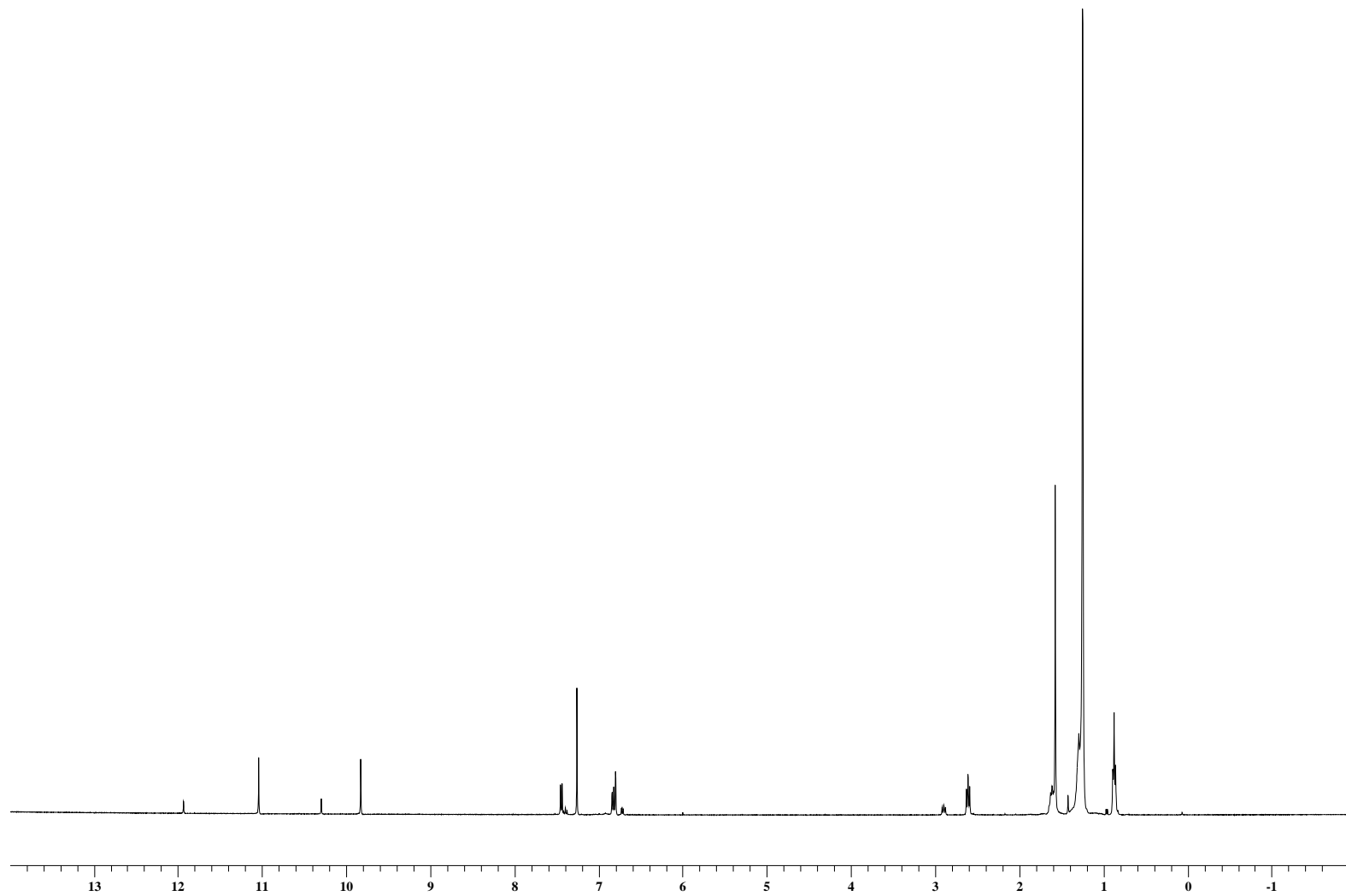


Figure A-13 ^1H -NMR spectrum of 2-hydroxy-6-pentadecylbenzaldehyde (Compound **5a**)

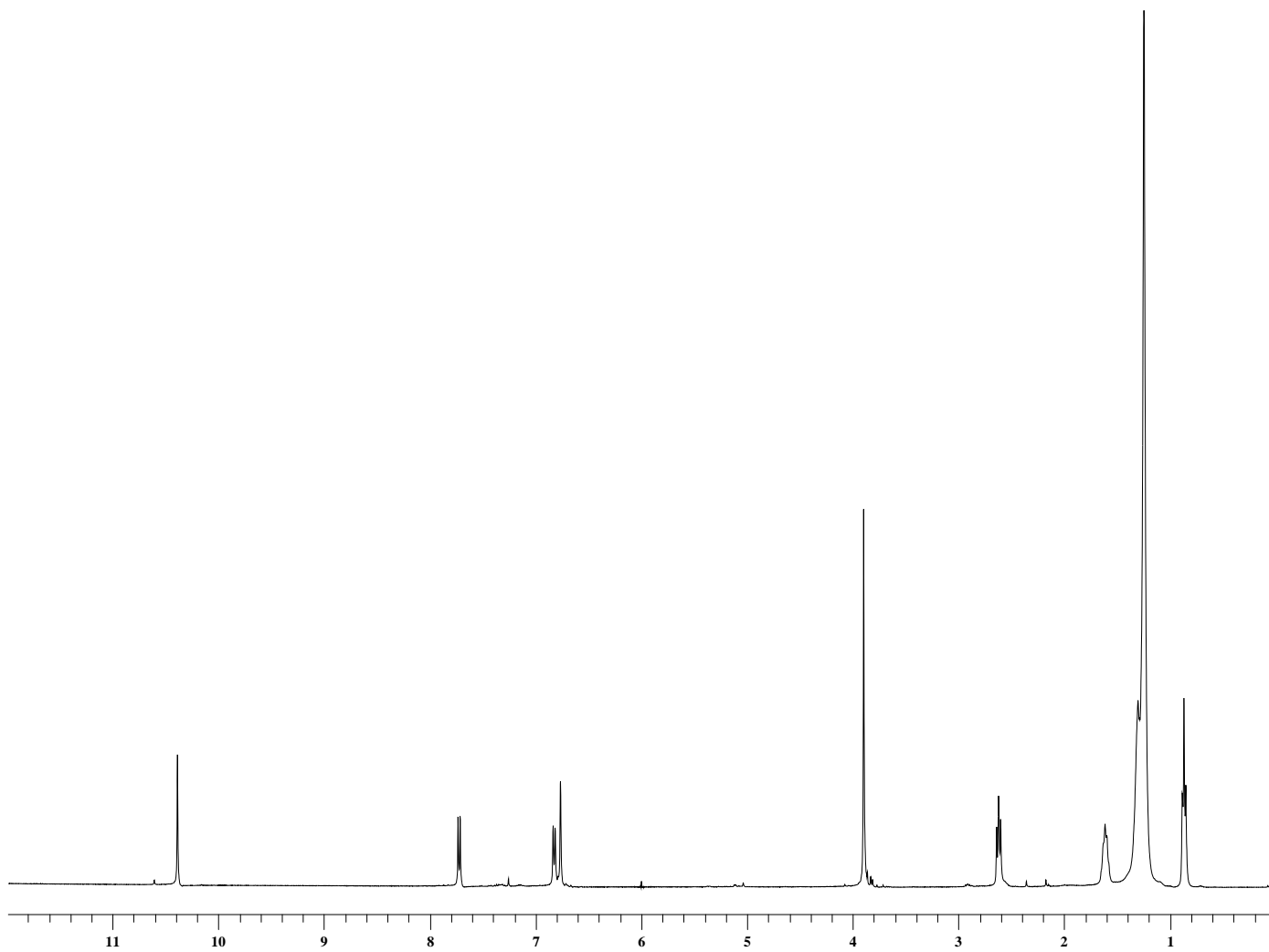


Figure A-14 ^1H -NMR spectrum of 2-methoxy-4-pentadecylbenzaldehyde (Compound **6**)

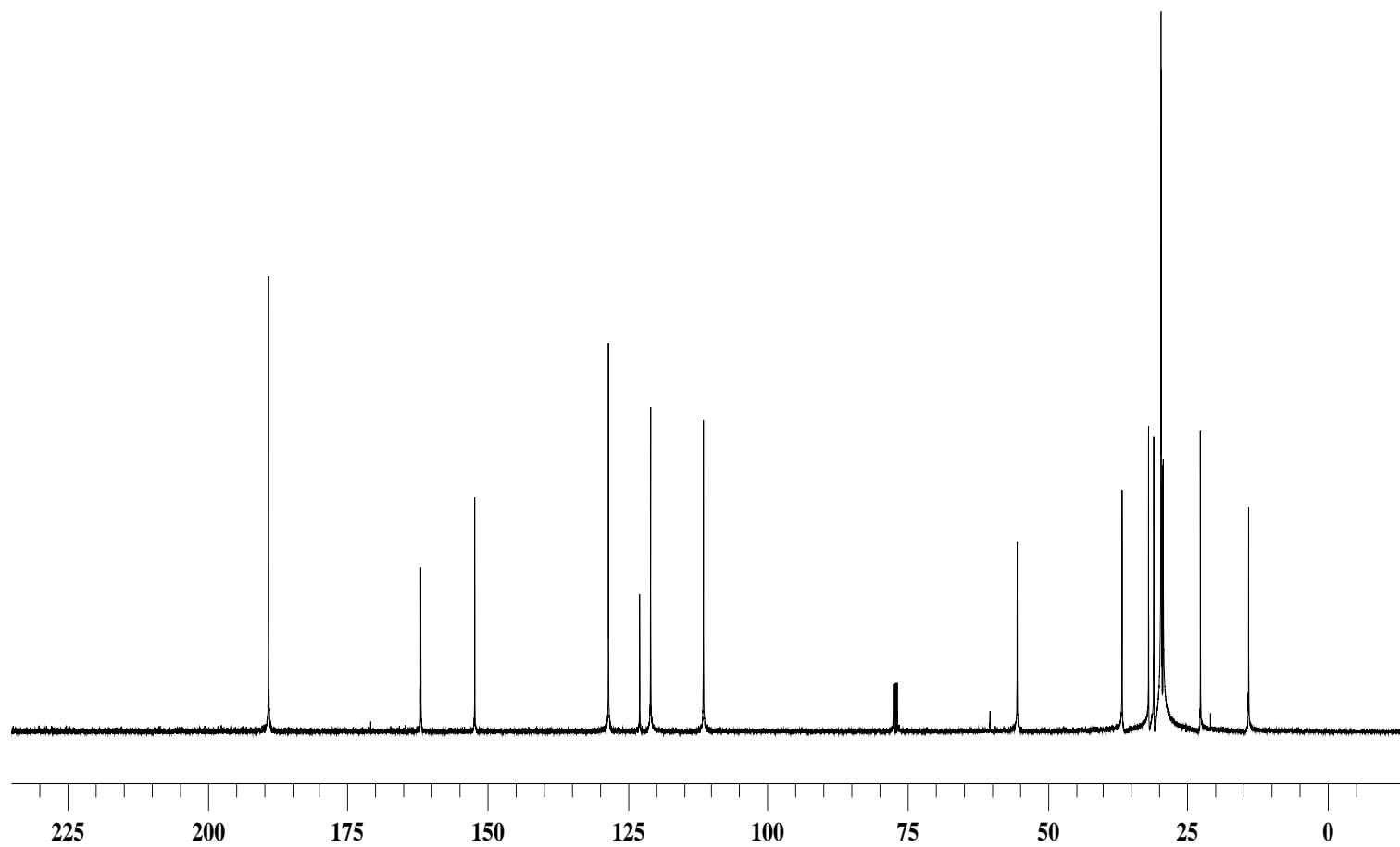


Figure A-15 ^{13}C -NMR spectrum of 2-methoxy-4-pentadecylbenzaldehyde (Compound **6**)

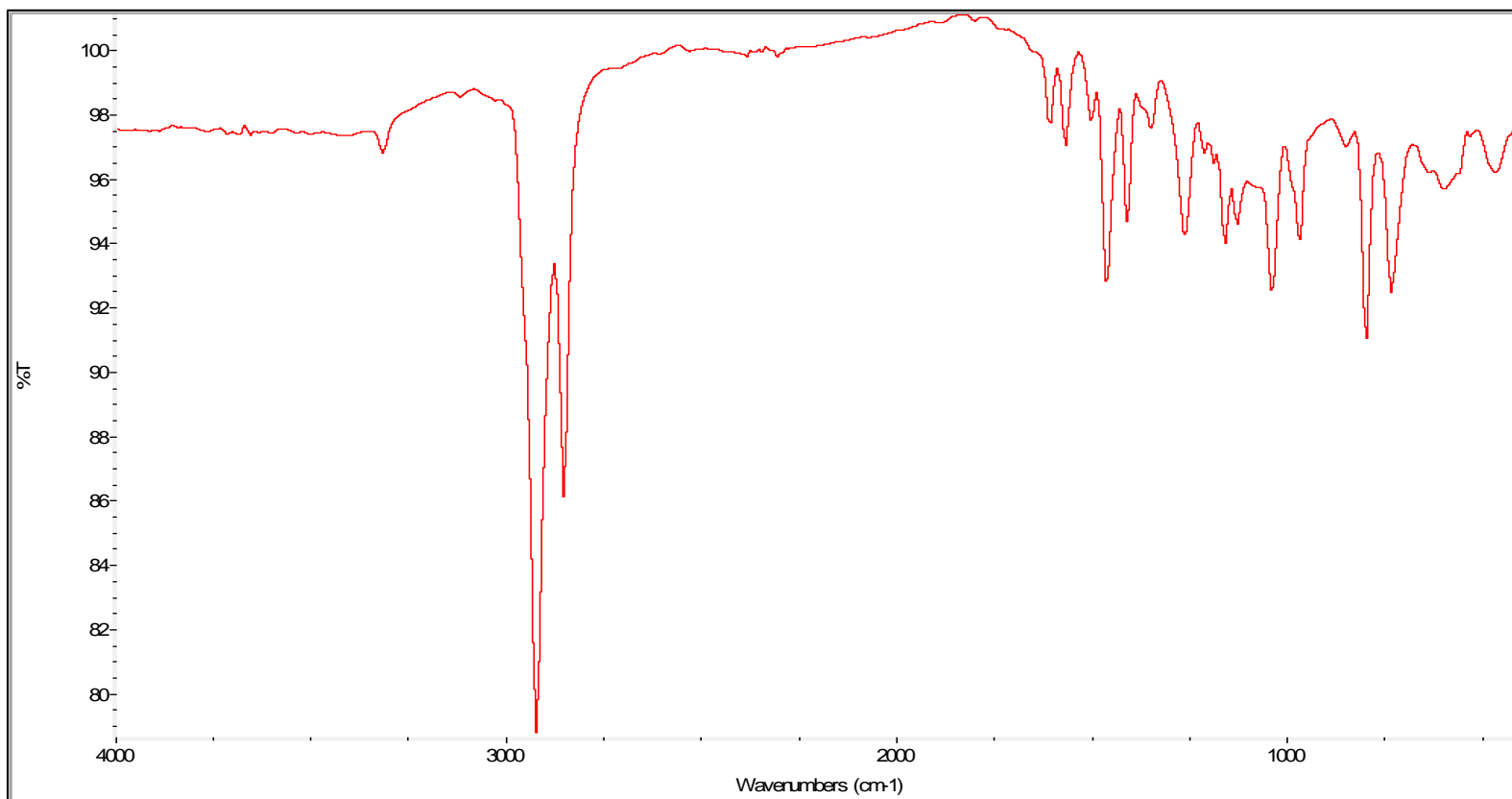


Figure A-16 IR spectrum of 2-methoxy-4-pentadecylbenzaldehyde (Compound 6)

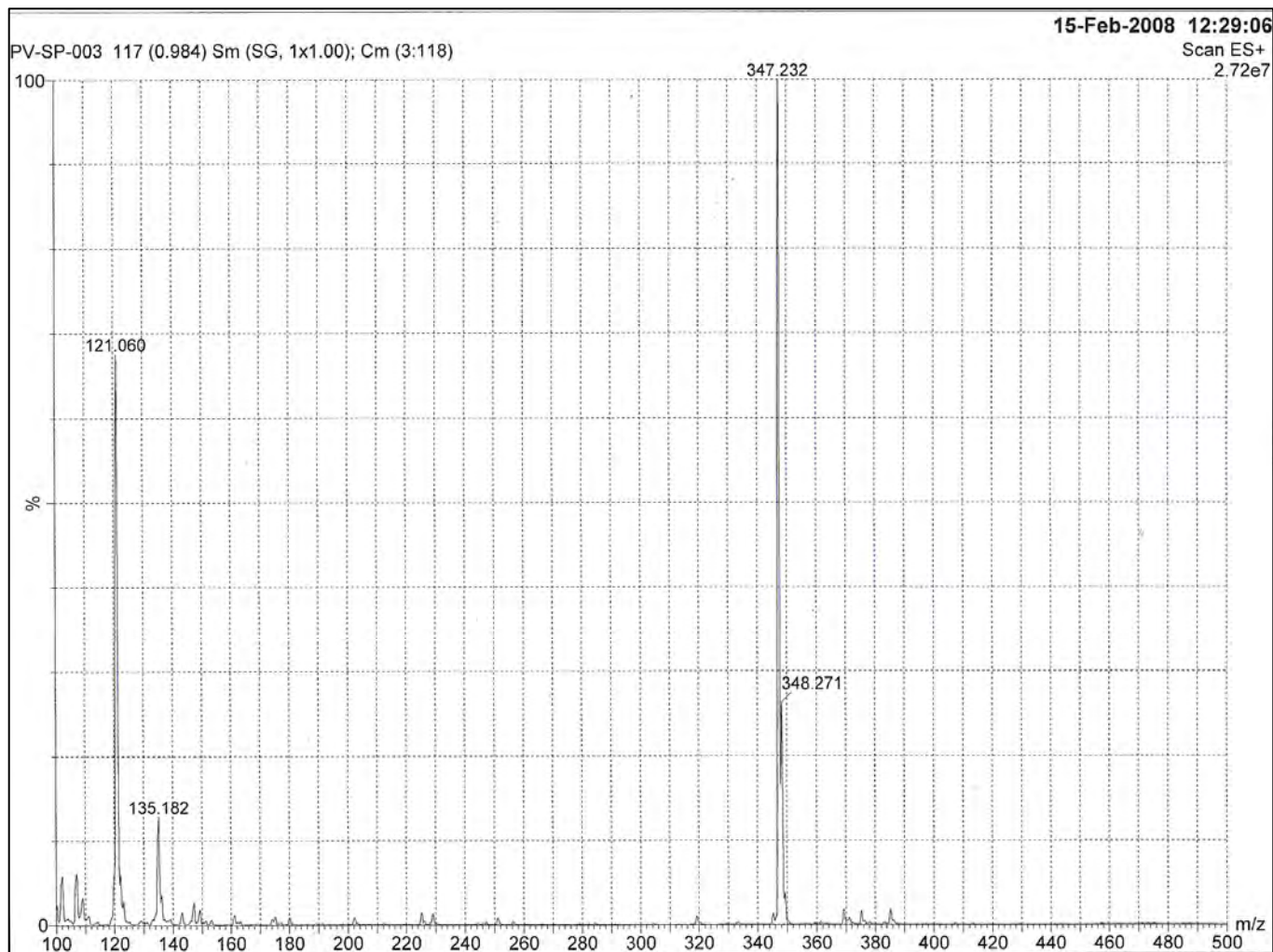


Figure A-17 Mass spectrum of 2-methoxy-4-pentadecylbenzaldehyde (Compound **6**)

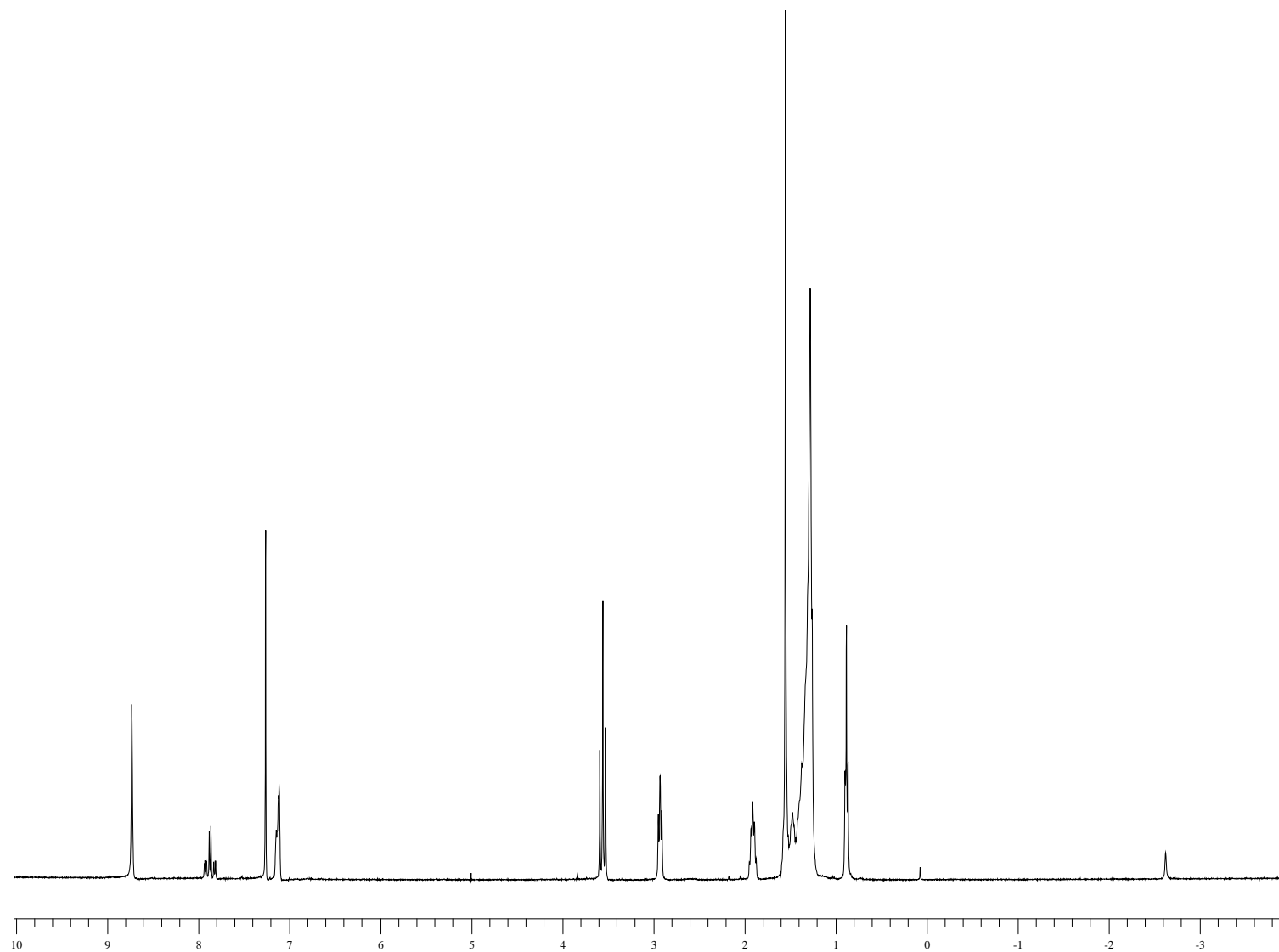


Figure A-18 $^1\text{H-NMR}$ spectrum of porphyrinic derivative (Compound 7)

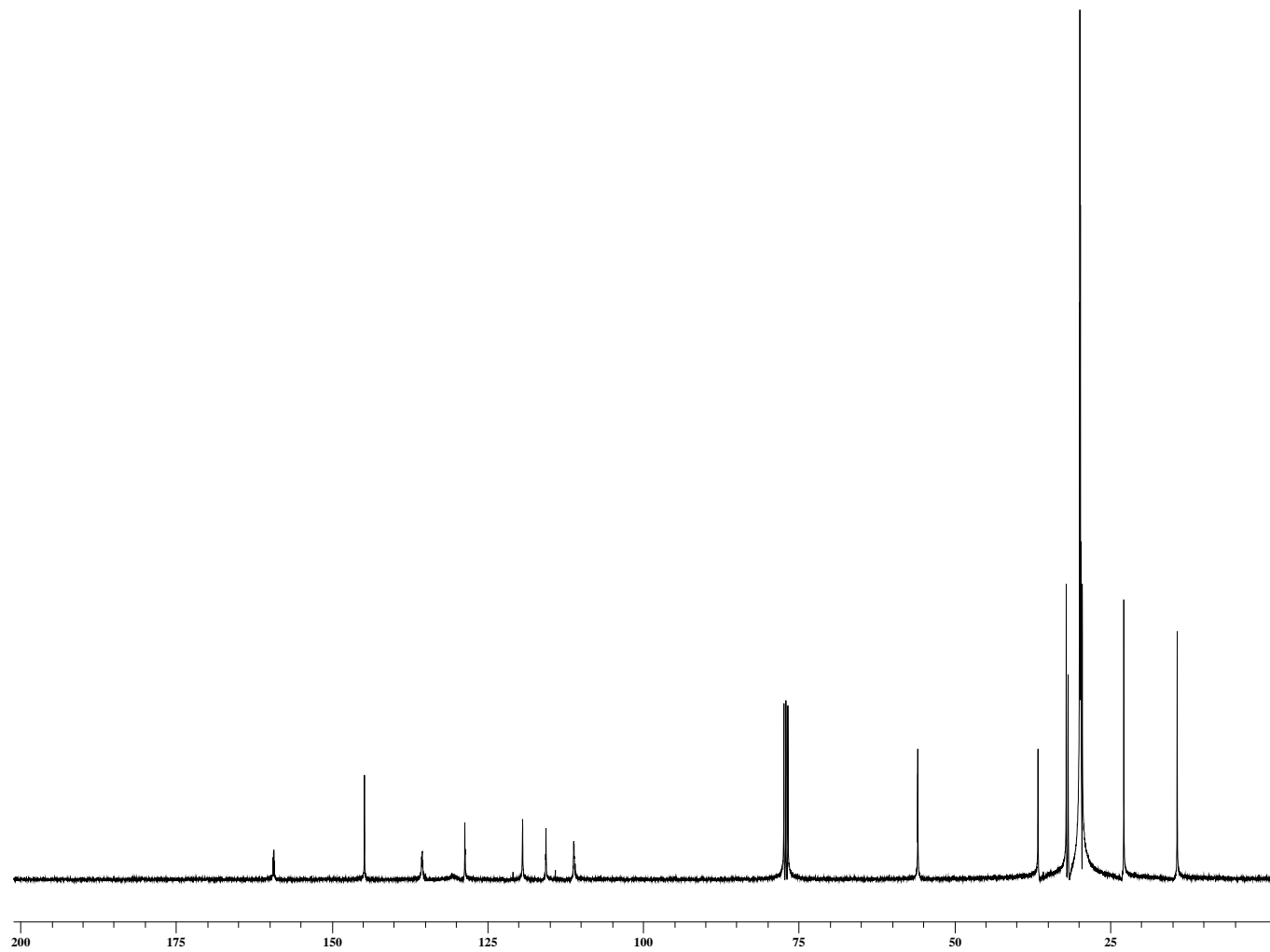


Figure A-19 ^{13}C -NMR spectrum of porphyrinic derivative (Compound 7)

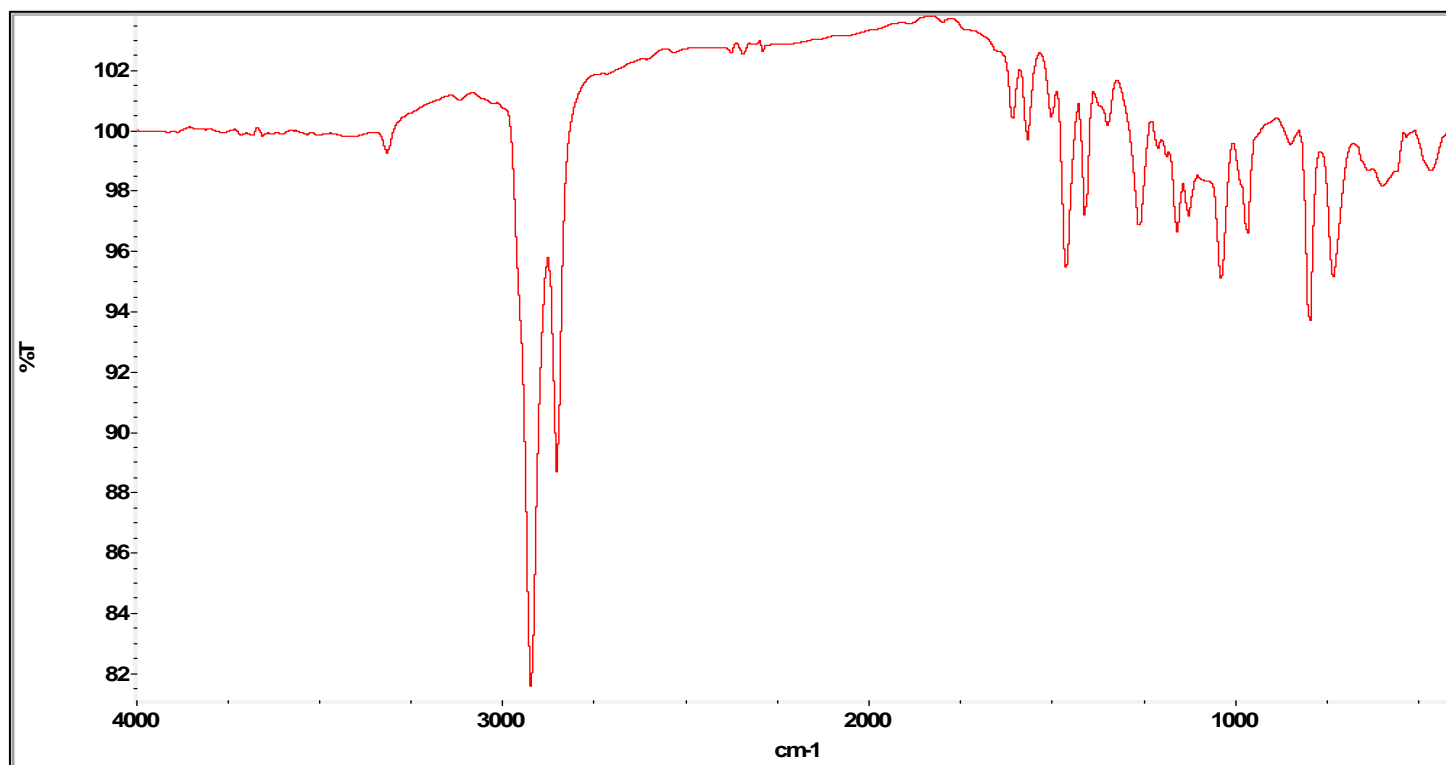


Figure A-20 Infrared spectrum of porphyrinic derivative (Compound 7)

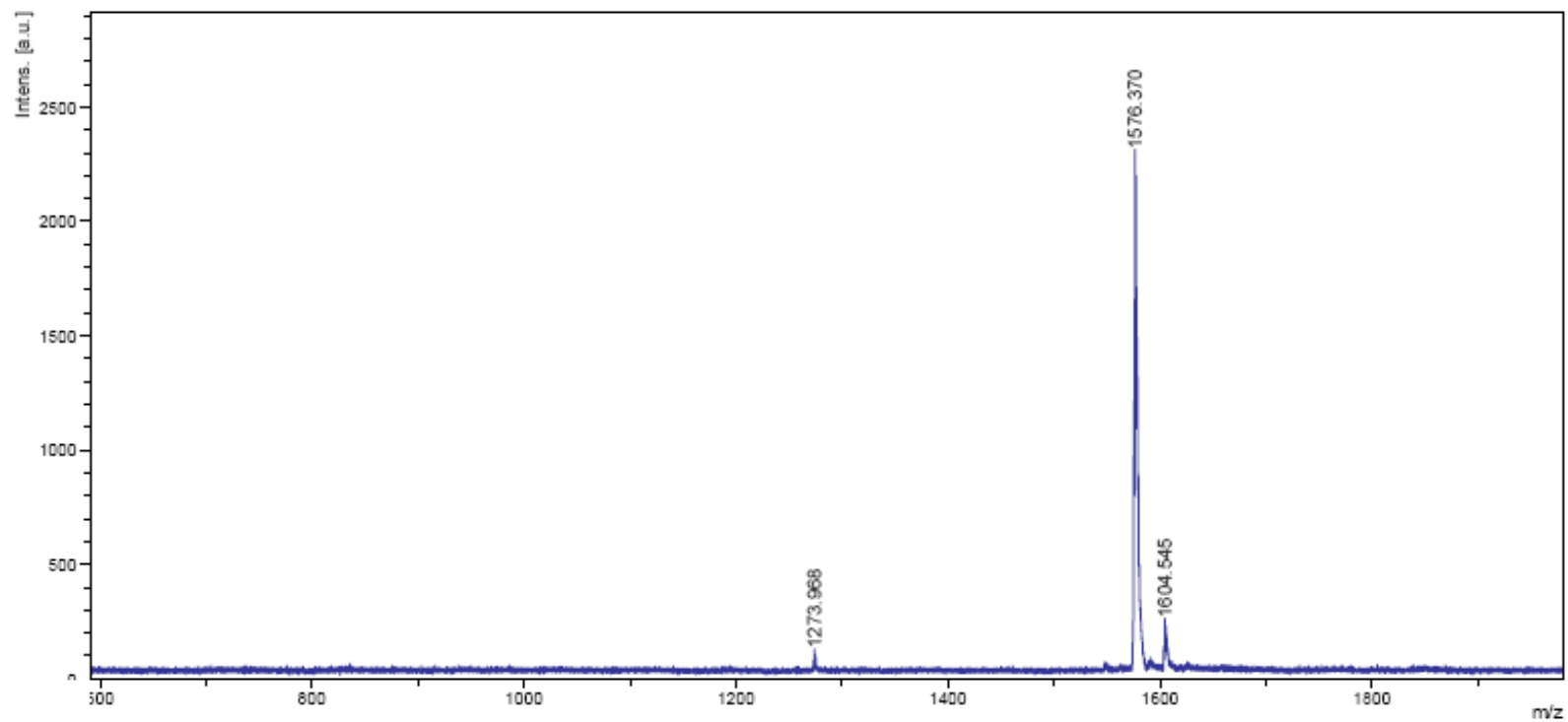


Figure A-21 Mass spectrum of porphyrinic derivative (Compound 7)

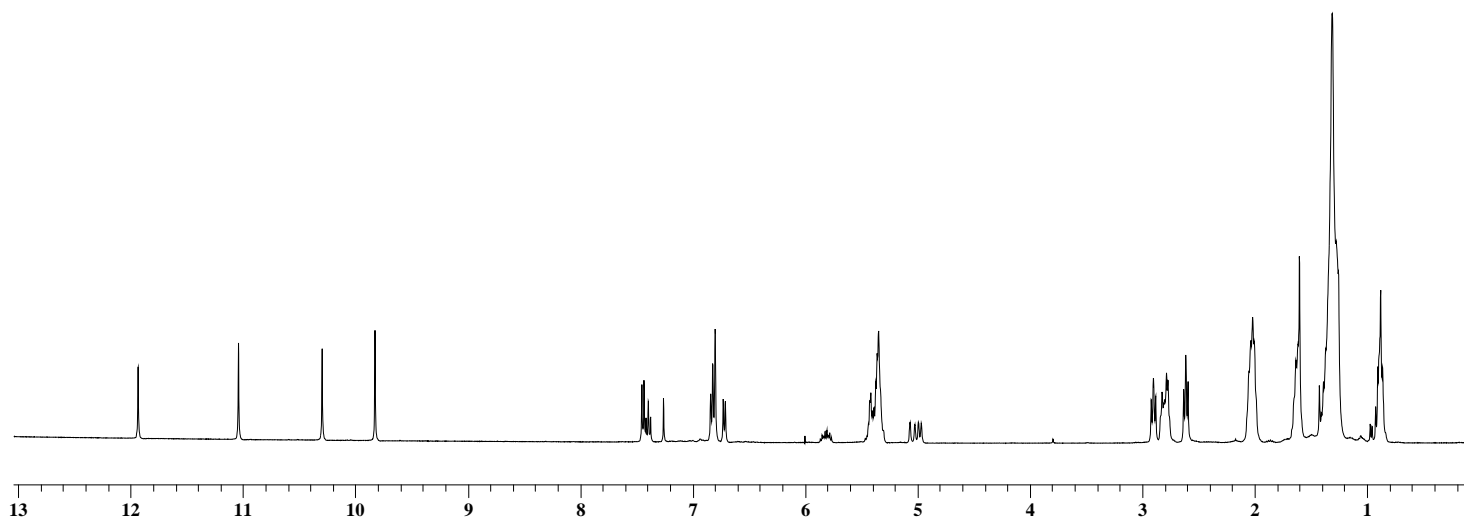


Figure A-22 $^1\text{H-NMR}$ spectrum of 2-hydroxy-4-alkenylbenzaldehyde and 2-hydroxy-6-alkenylbenzaldehyde

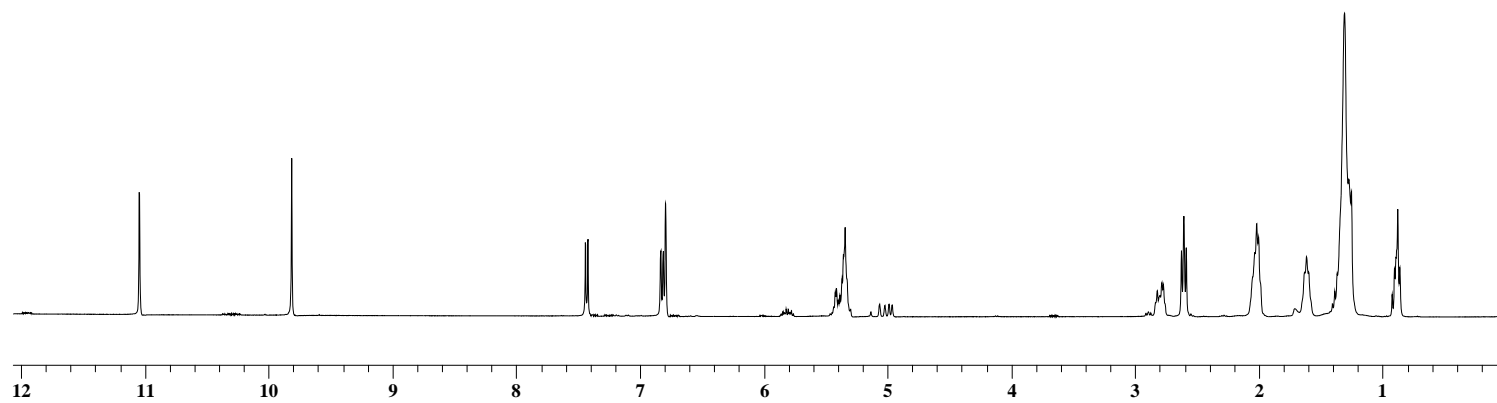


Figure A-23 ^1H -NMR spectrum of 2-hydroxy-4-alkenylbenzaldehyde

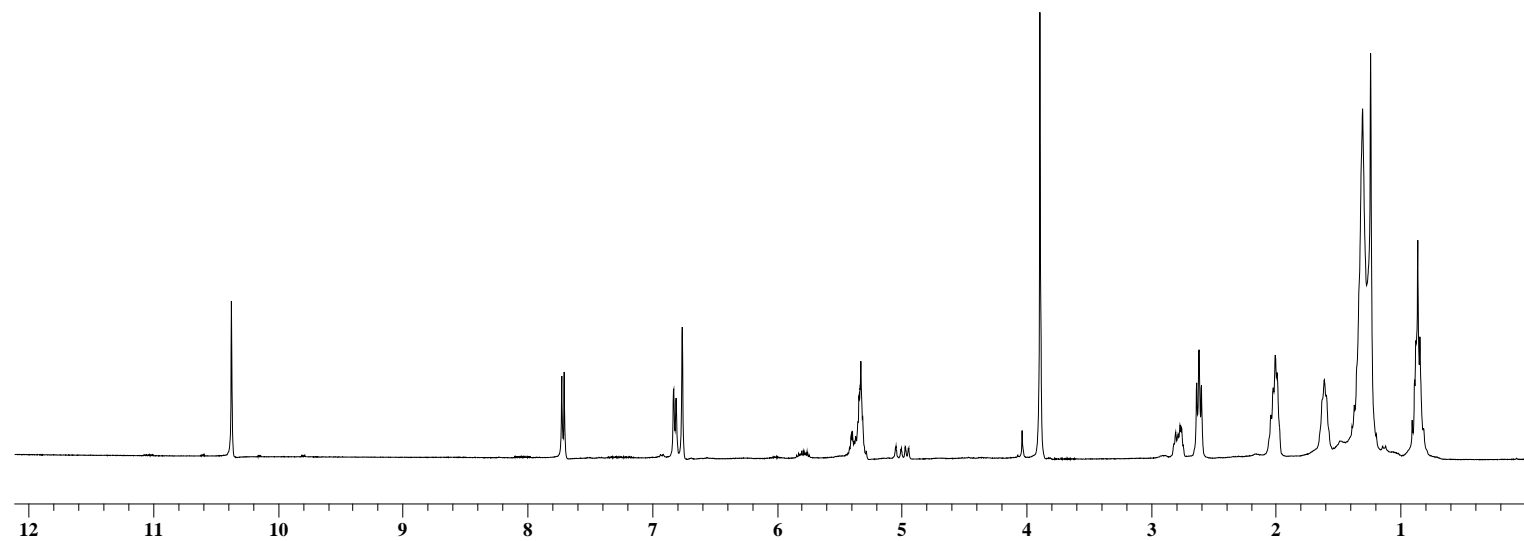


Figure A-24 $^1\text{H-NMR}$ spectrum of 2-methoxy-4-alkenylbenzaldehyde

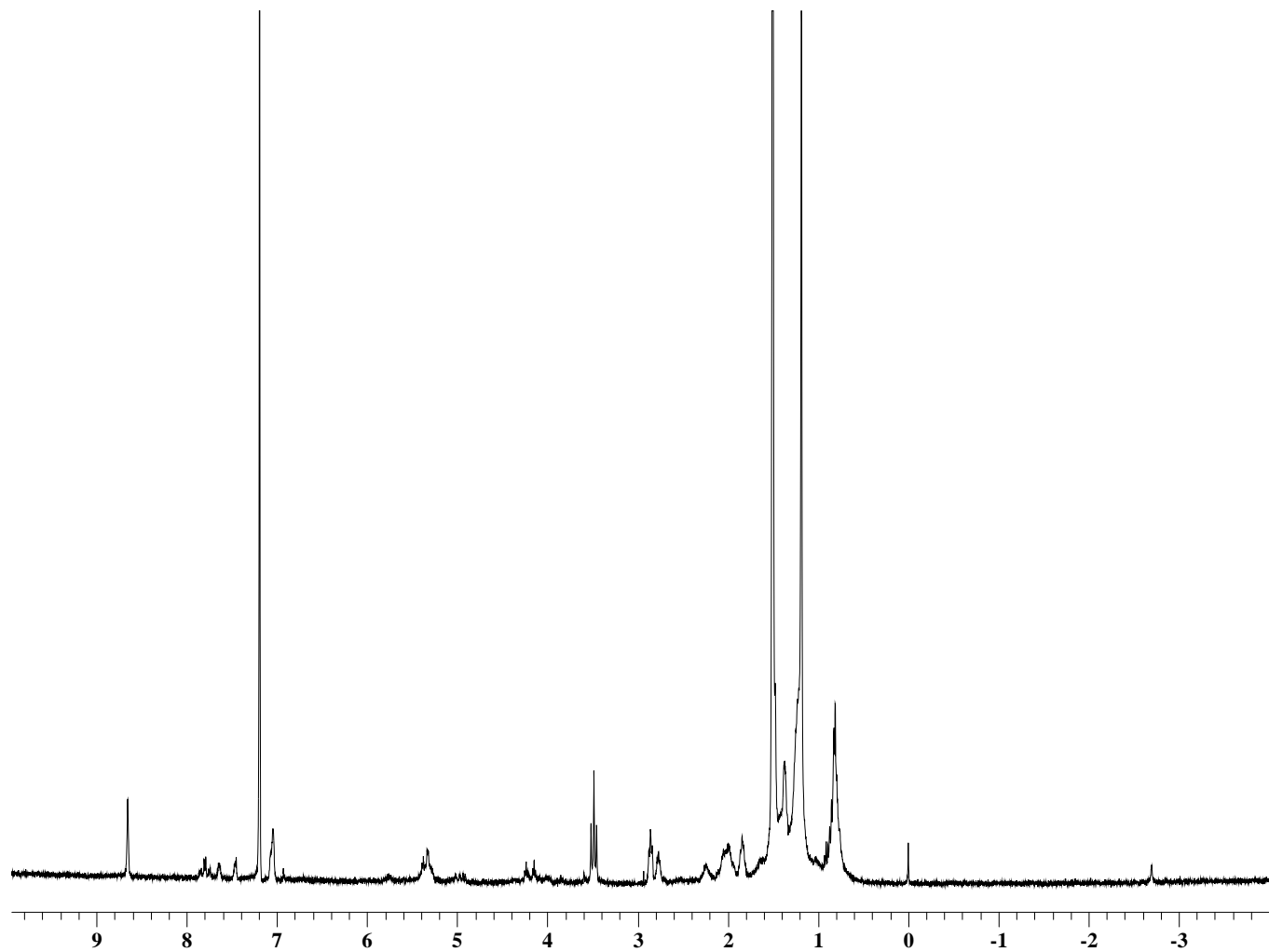


Figure A-25 $^1\text{H-NMR}$ spectrum of porphyrin derivatives from cardanol

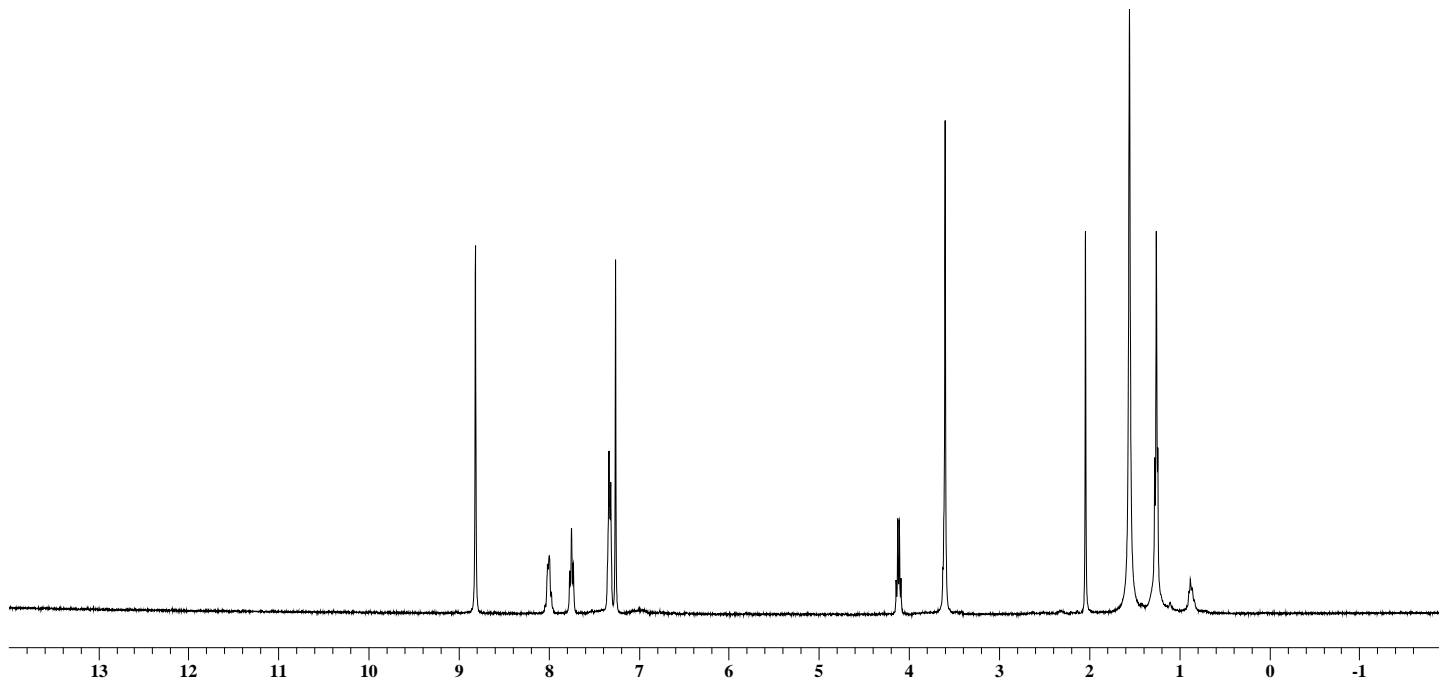


Figure A-26 ^1H -NMR spectrum of Zn(II) porphyrin model (Compound **Zn-3**)

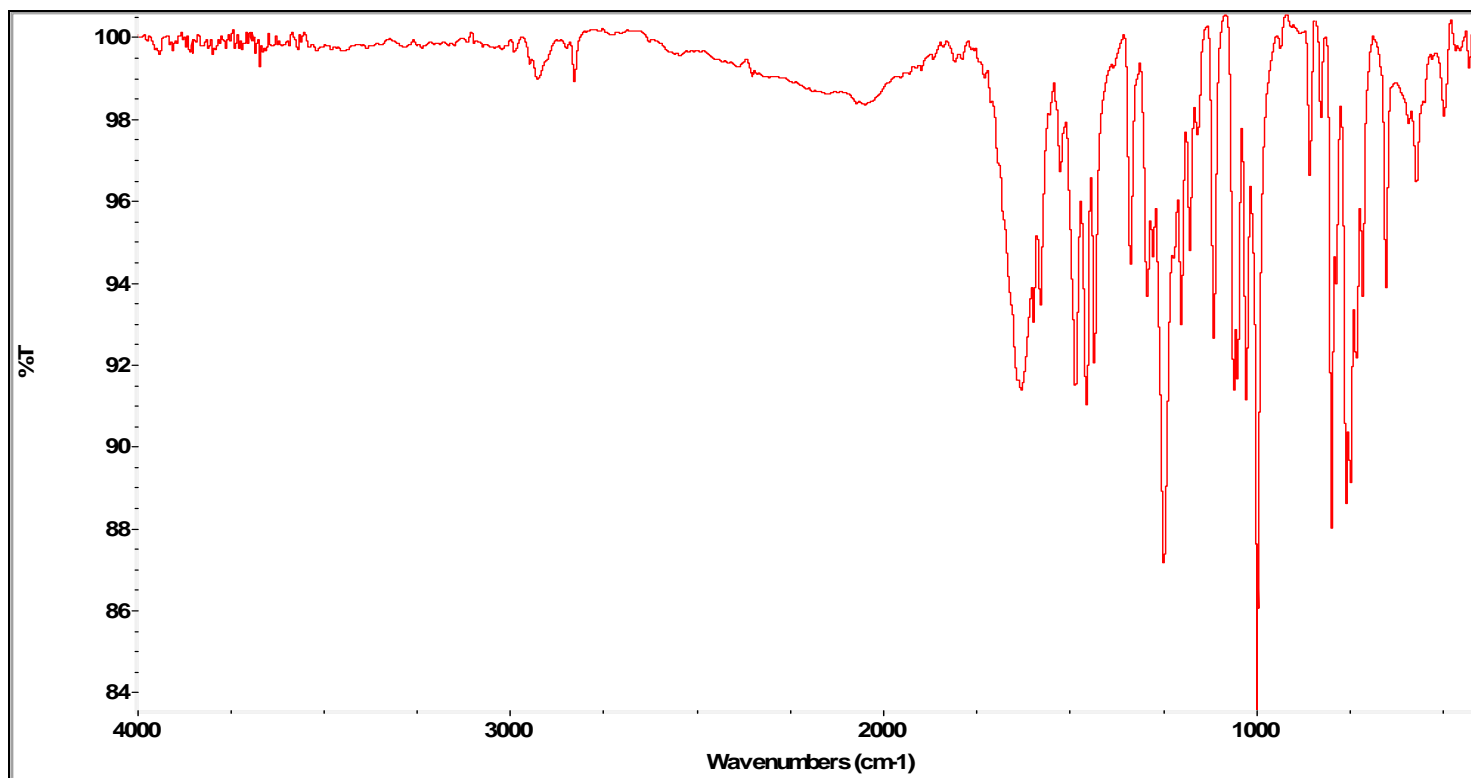


Figure A-27 IR spectrum of Zn(II) porphyrin model (Compound **Zn-3**)

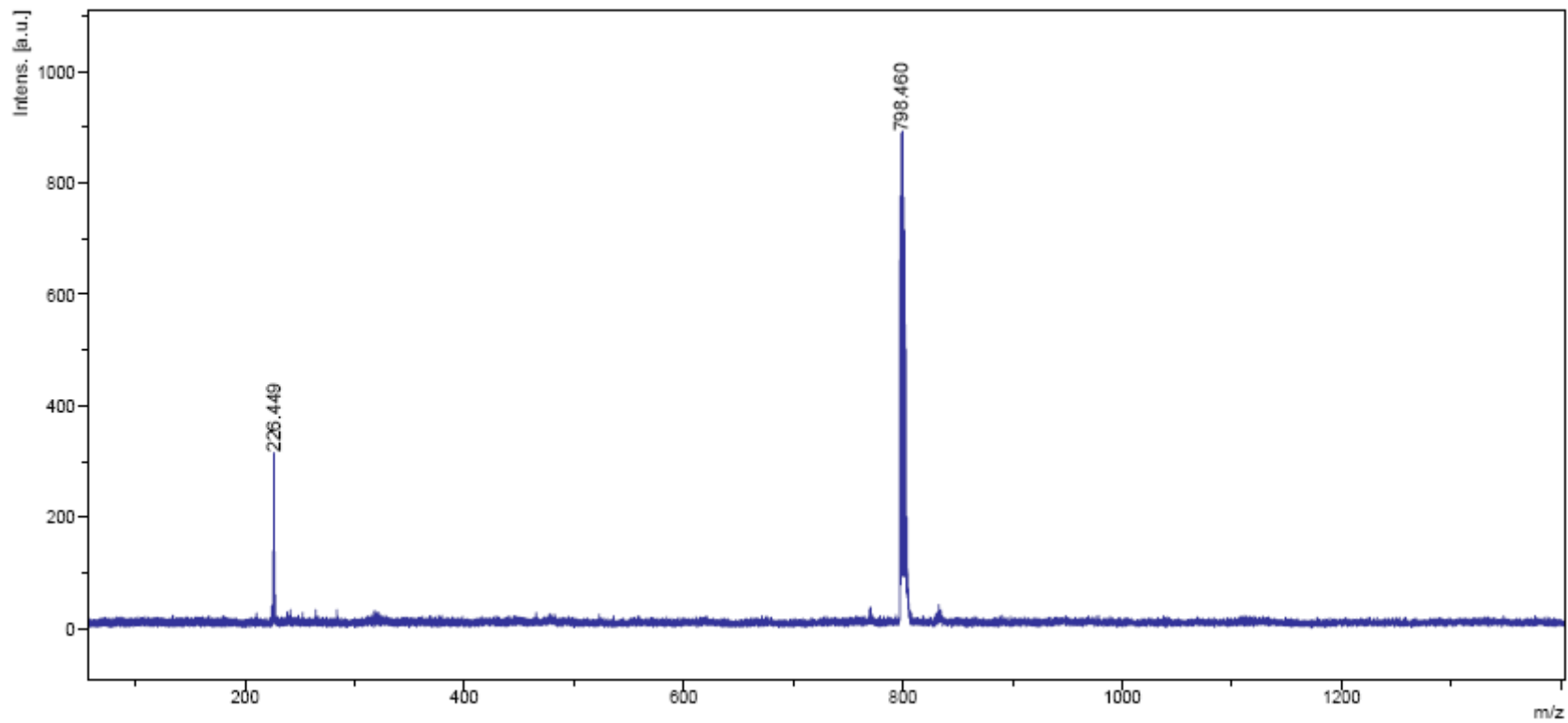


Figure A-28 Mass spectrum of Zn(II) porphyrin model (Compound **Zn-3**)

APPENDIX B

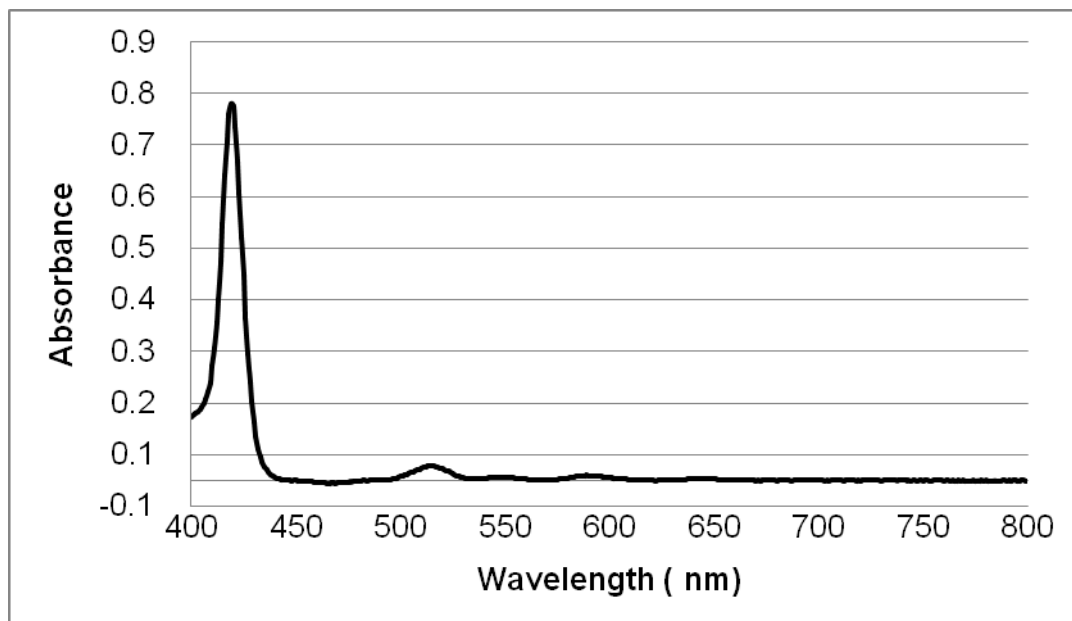


Figure B-1 Absorption spectrum of Compound **3** in CH₂Cl₂

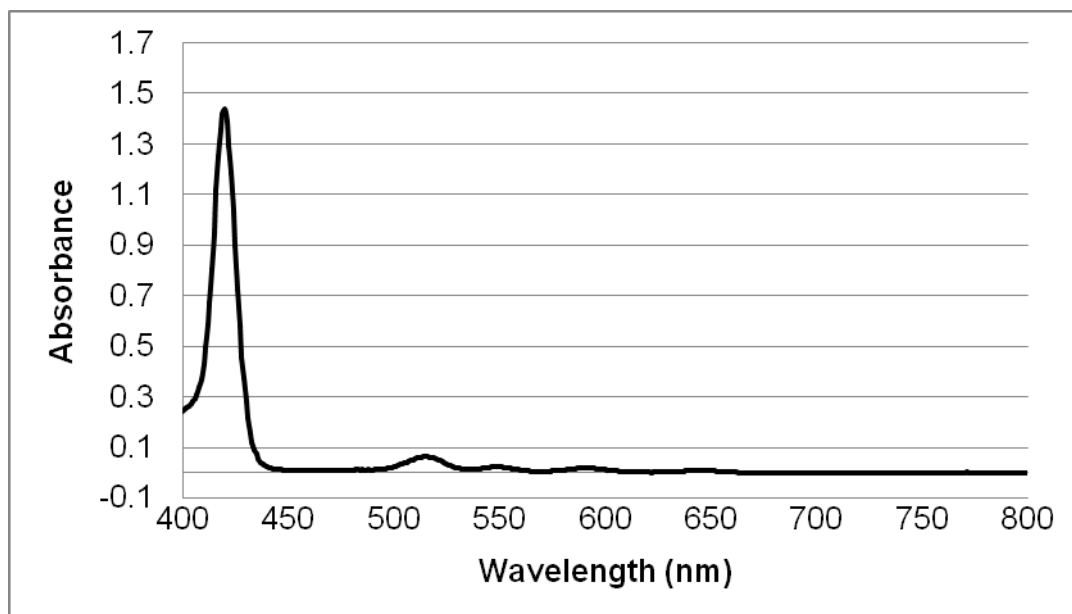


Figure B-2 Absorption spectrum of Compound **7** in CH₂Cl₂

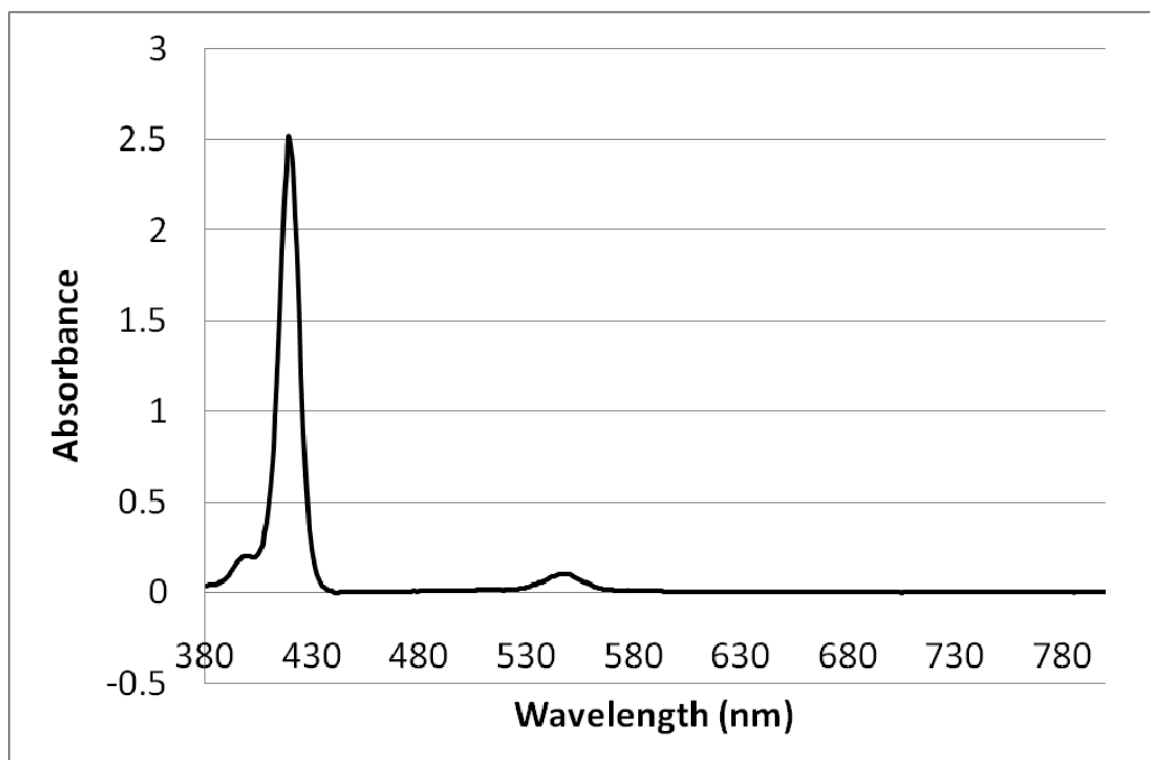


Figure B-3 Absorption spectrum of **Zn-3**

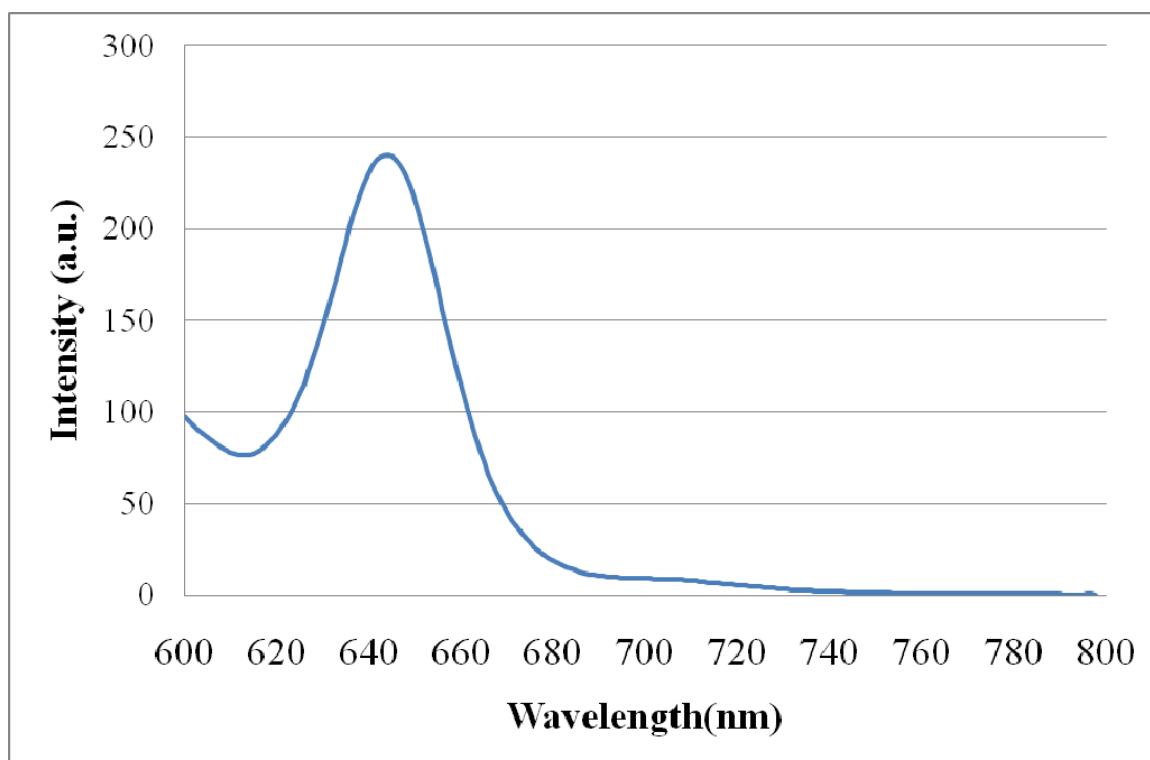


Figure B-4 Fluorescent spectrum spectra of **Zn-3**

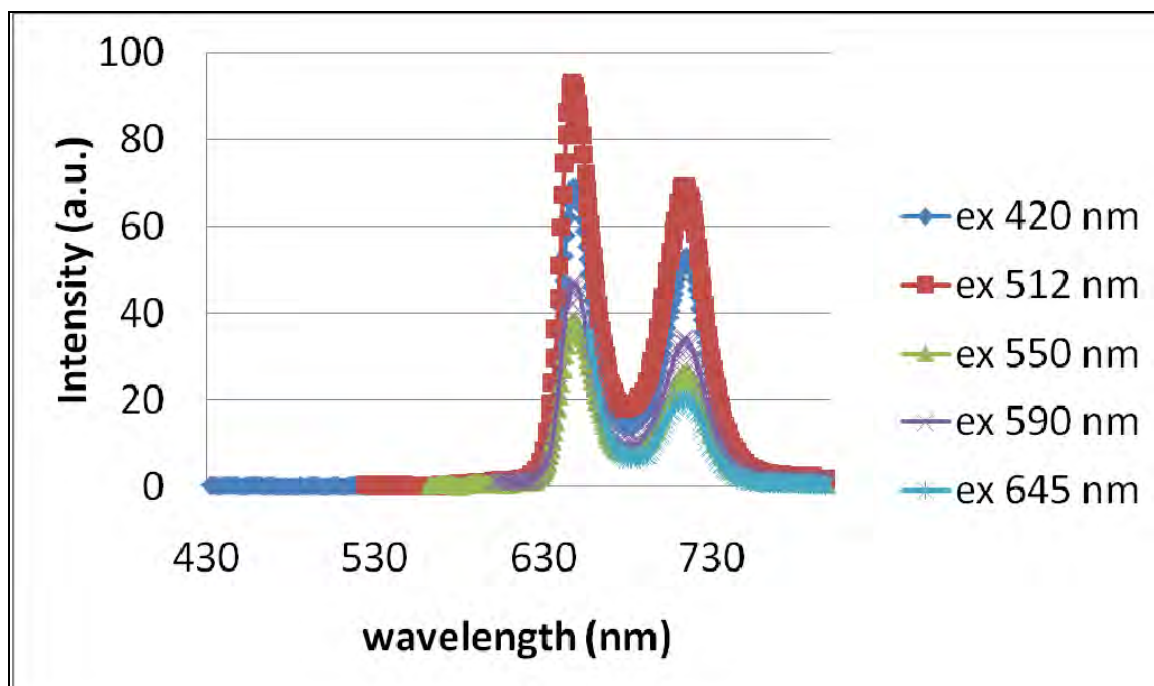


Figure B-5 Fluorescent spectra of Compound 3 in CH₂Cl₂

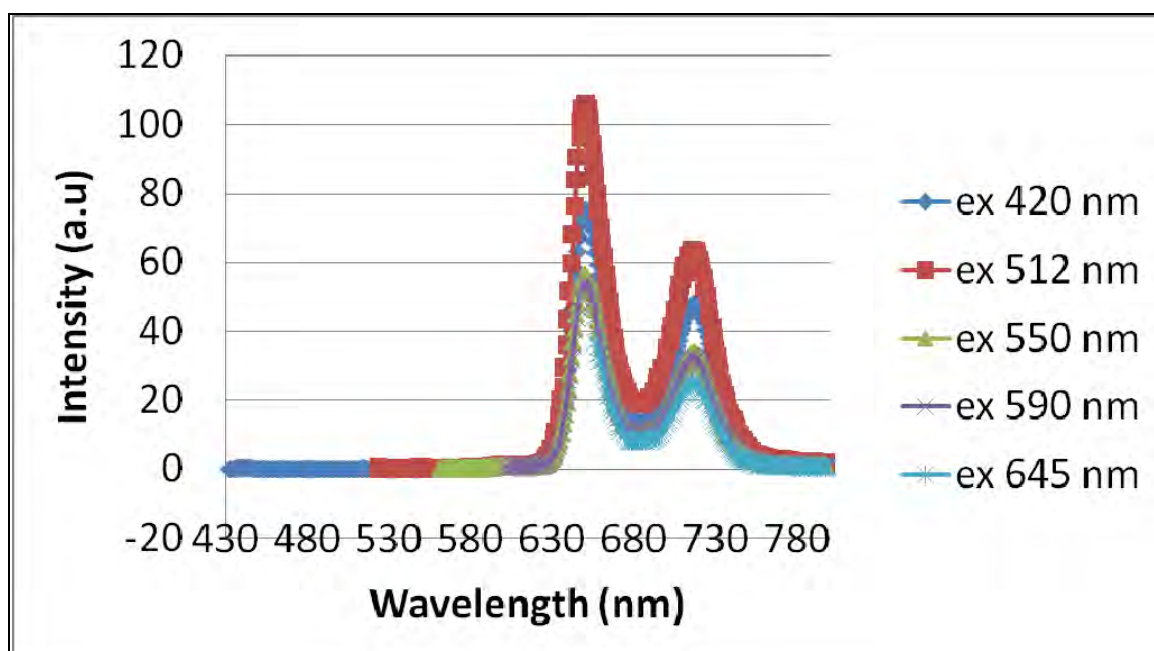


Figure B-6 Fluorescent spectra of Compound 7 in CH₂Cl₂

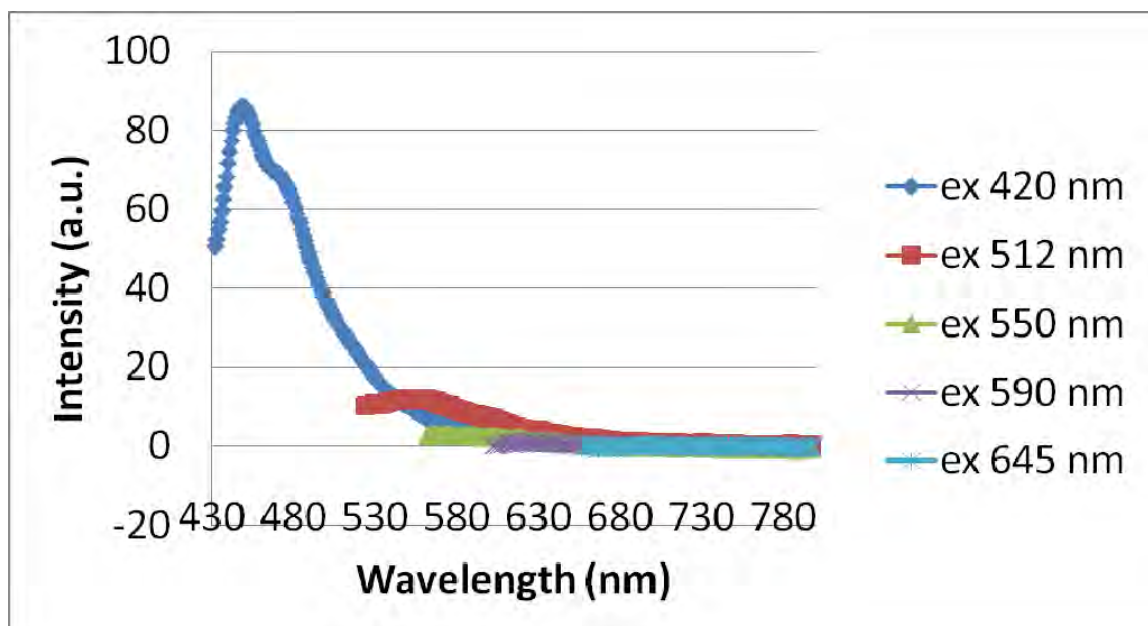


Figure B-7 Fluorescent spectra of diesel fuel in CH_2Cl_2

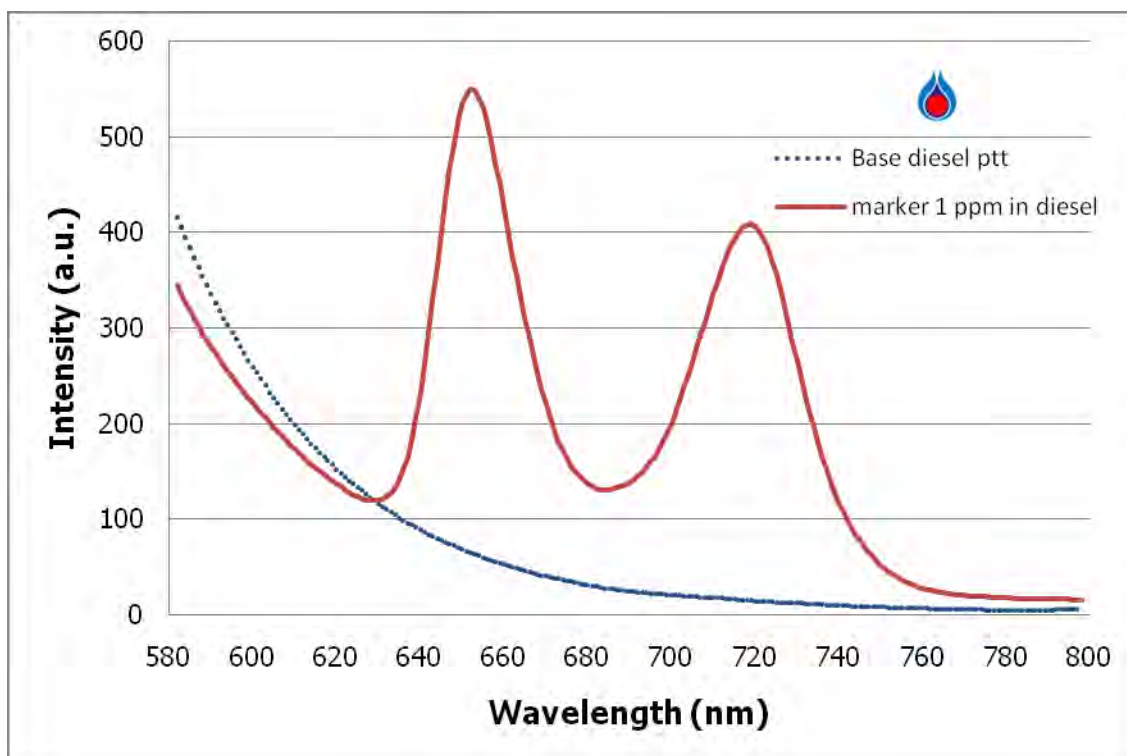


Figure B-8 The excitation wavelength ($\lambda_{\text{ex}} = 420 \text{ nm}$) and emission wavelength ($\lambda_{\text{em}} = 652 \text{ nm}$ and 719 nm) of Compound **7** (1 ppm) in diesel oil (PTT Public Co., Ltd.)

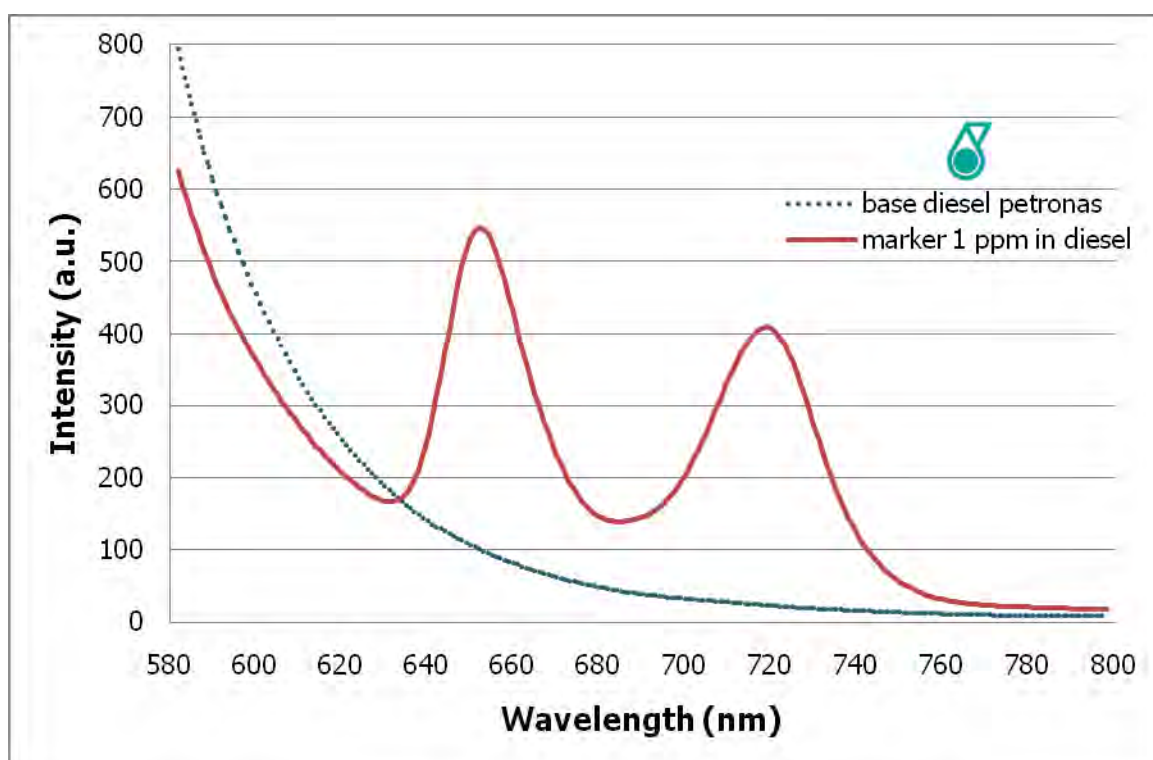


Figure B-9 The excitation wavelength ($\lambda_{\text{ex}} = 420 \text{ nm}$) and emission wavelength ($\lambda_{\text{em}} = 652 \text{ nm}$ and 719 nm) of Compound **7** (1 ppm) in diesel oil (Petronas)

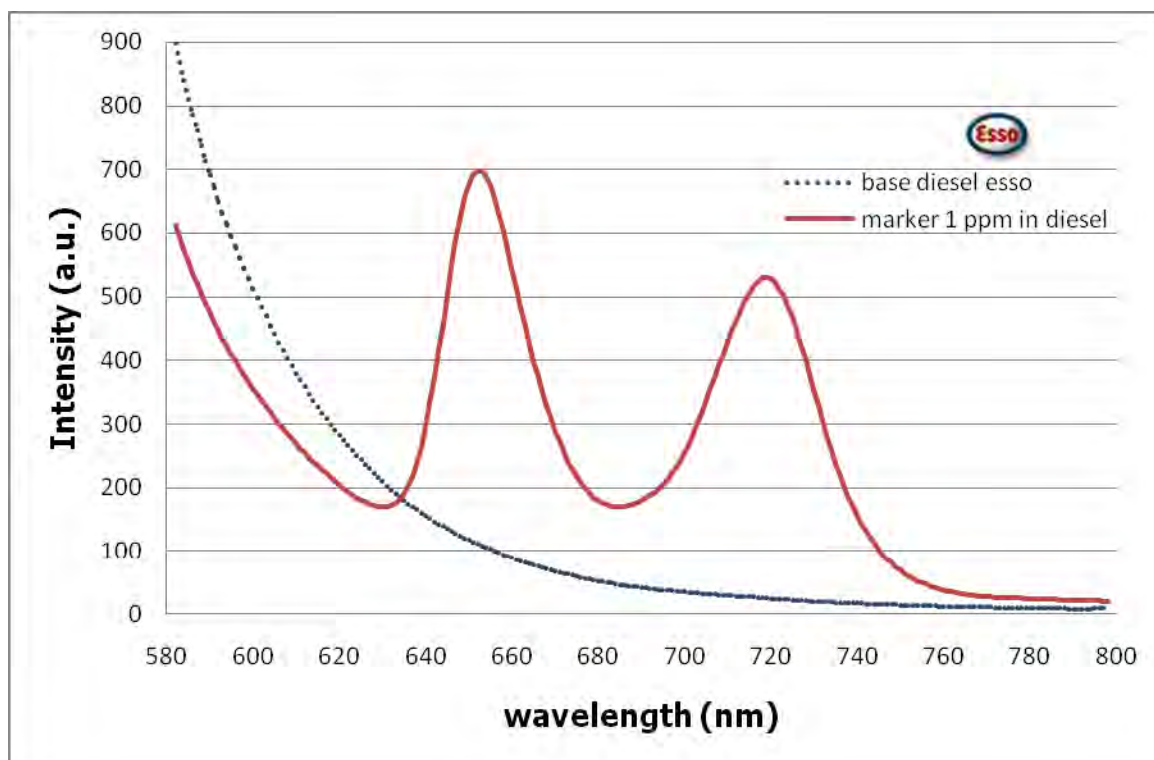


Figure B-10 The excitation wavelength ($\lambda_{\text{ex}} = 420 \text{ nm}$) and emission wavelength ($\lambda_{\text{em}} = 652 \text{ nm}$ and 719 nm) of Compound **7** (1 ppm) in diesel oil (Esso)

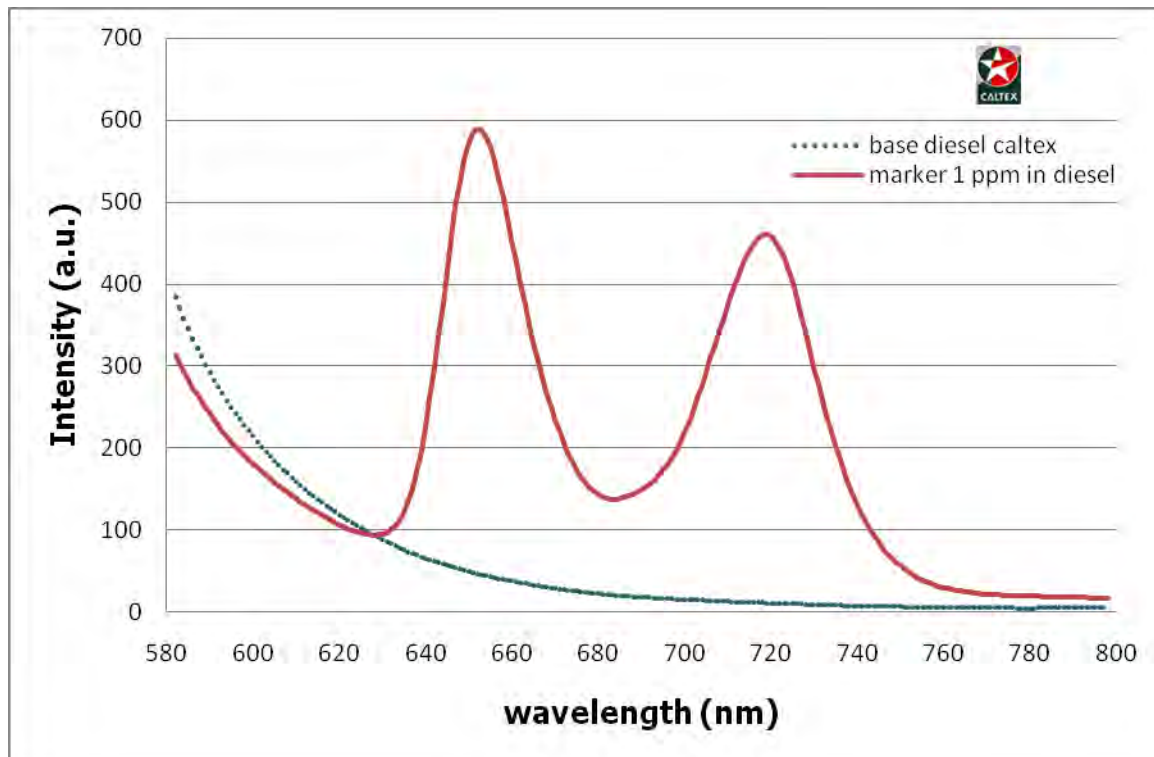


Figure B-11 The excitation wavelength ($\lambda_{\text{ex}} = 420 \text{ nm}$) and emission wavelength ($\lambda_{\text{em}} = 652 \text{ nm}$ and 719 nm) of Compound **7** (1 ppm) in diesel oil (Caltex)

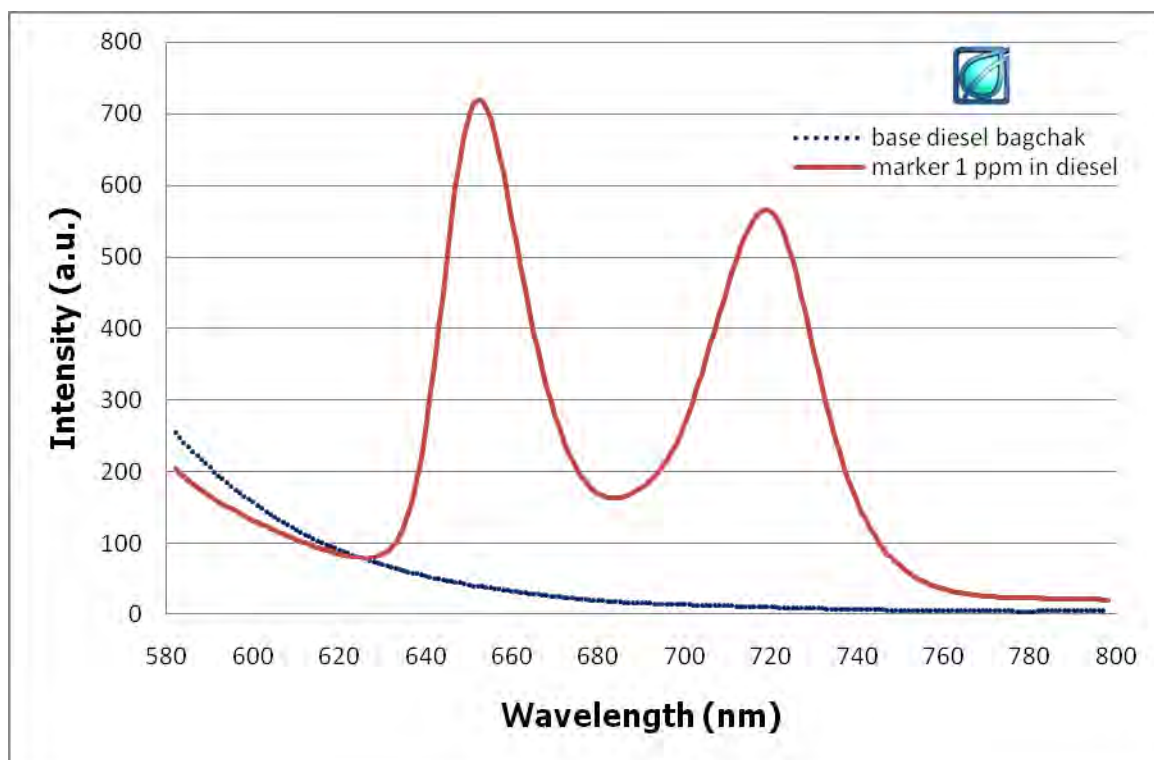


Figure B-12 The excitation wavelength ($\lambda_{\text{ex}} = 420 \text{ nm}$) and emission wavelength ($\lambda_{\text{em}} = 652 \text{ nm}$ and 719 nm) of Compound **7** (1 ppm) in diesel oil (Bangchak)

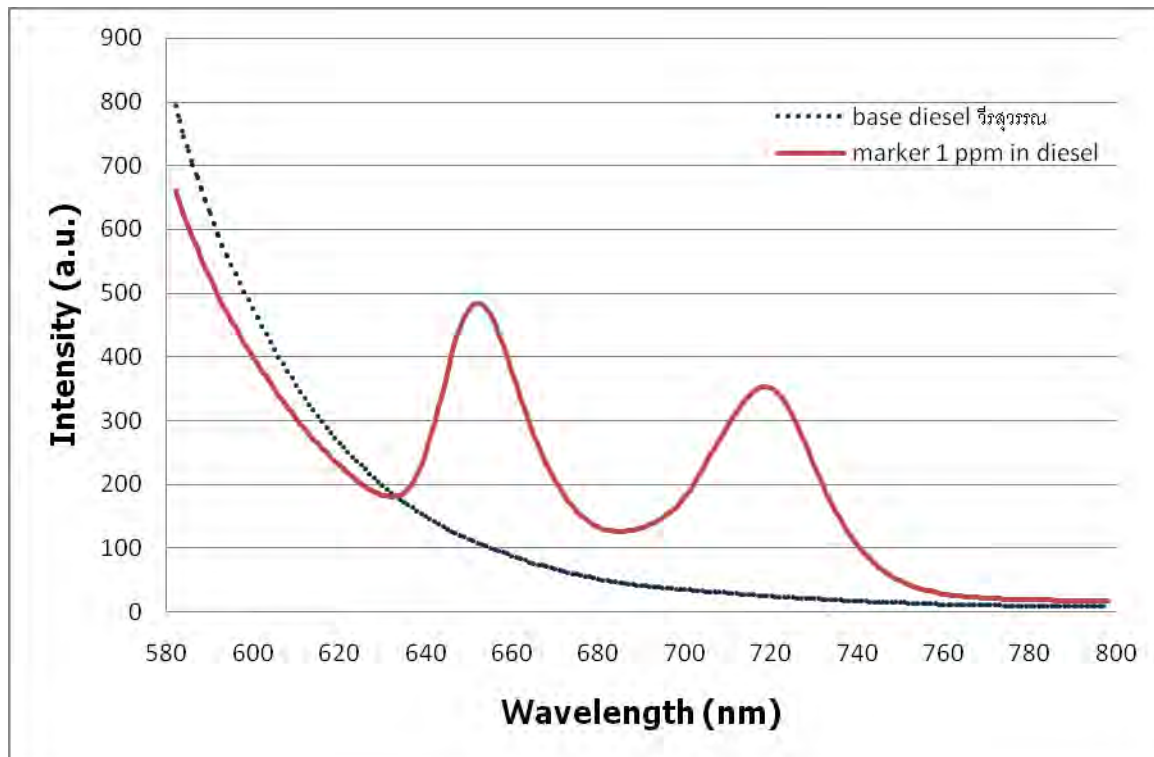


Figure B-13 The excitation wavelength ($\lambda_{\text{ex}} = 420 \text{ nm}$) and emission wavelength ($\lambda_{\text{em}} = 652 \text{ nm}$ and 719 nm) of Compound **7** (1 ppm) in diesel oil (veerasuwan)

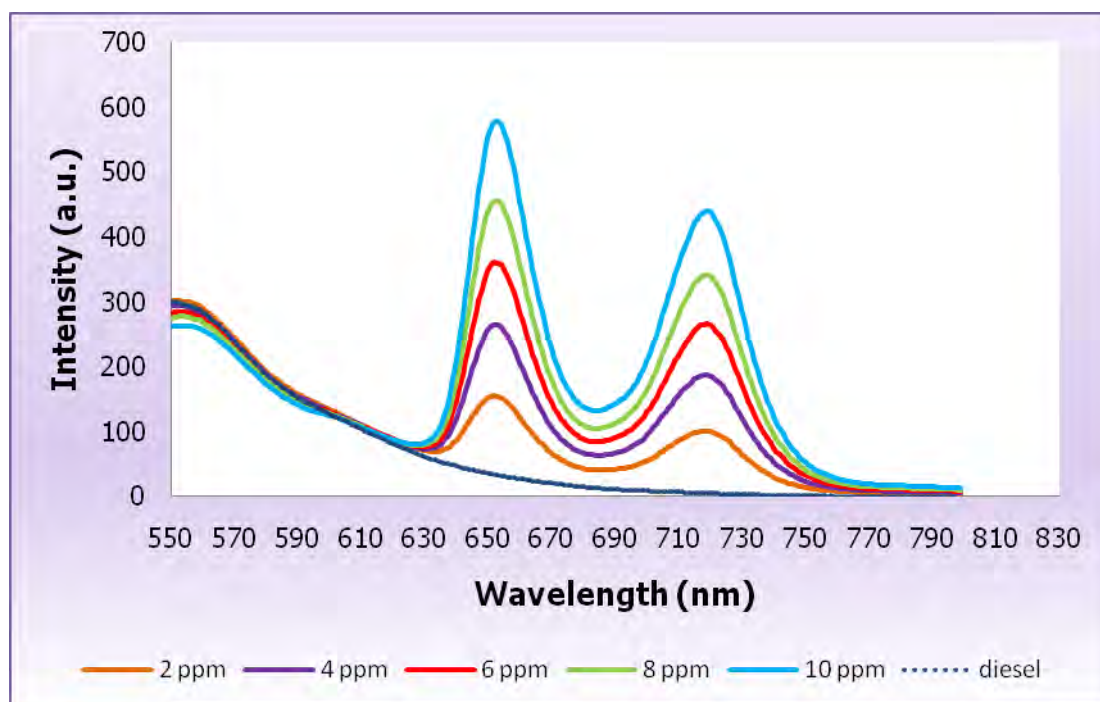


Figure B-14 The fluorescent spectrum of Compound 7 in diesel oil at 2, 4, 6, 8 and 10 ppm. ($\lambda_{\text{ex}} = 512 \text{ nm}$ and $\lambda_{\text{em}} = 652 \text{ nm}$ and 719 nm)

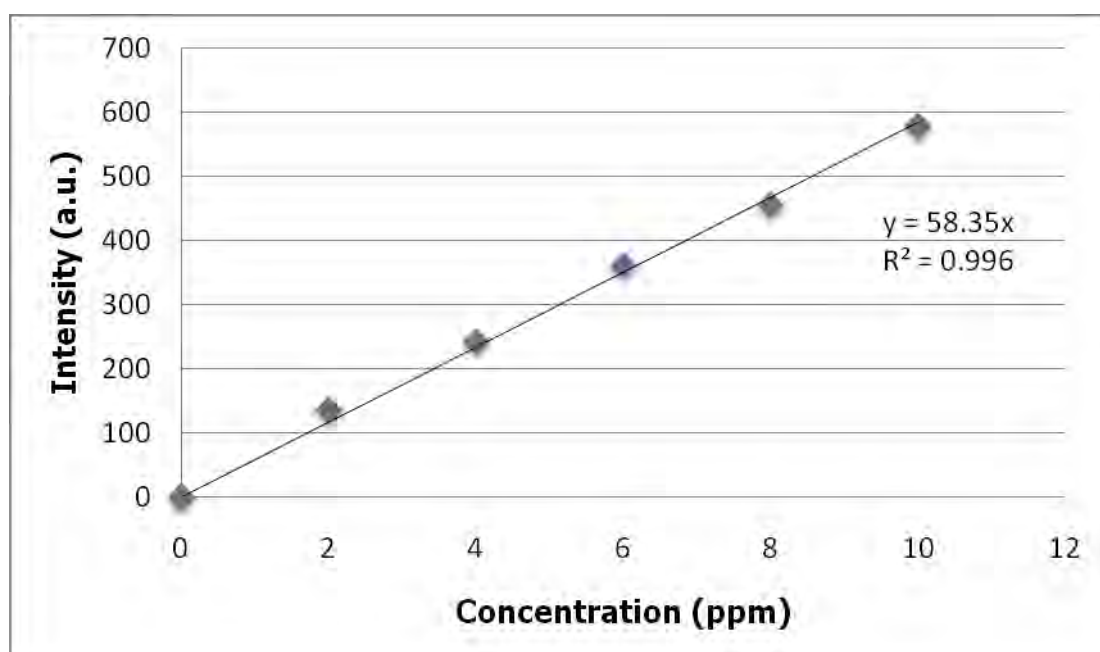


Figure B-15 The Calibration curve for the quantitative determinations of Compound 7 in diesel oil ($\lambda_{\text{ex}} = 512 \text{ nm}$ and $\lambda_{\text{em}} = 652 \text{ nm}$)

VITA

Miss Siriorn Puangmalee was born on November 8, 1981 in Suphanburi province, Thailand. She got a Bachelor's Degree of Applied Science in Industrial Chemistry from King Mongkut's University of Technology North Bangkok in 2004. After that, she started work in business development officer at THAI POWER OPERATION Co.,Ltd. (Double A Alliance Network) for 13 months. Then, she was admitted into a Master Degree program in Petrochemistry and Polymer Science, Chulalongkorn University in 2005 and completed the program in 2007.